AD-A080 367 AIR FORCE INST OF TECH WRIGHT-PATTERSON AFB OH SCHOO--ETC F/G 17/9
PREDICTED MICROWAVE ELECTRO-MAGNETIC BACKSCATTERING RETURNS FOR--ETC(U)
DEC 79 F DIBARTOLOMEO
UNCLASSIFIED AFIT/GE/EE/79D-11 NL

1 OF 2
AD
A080 367

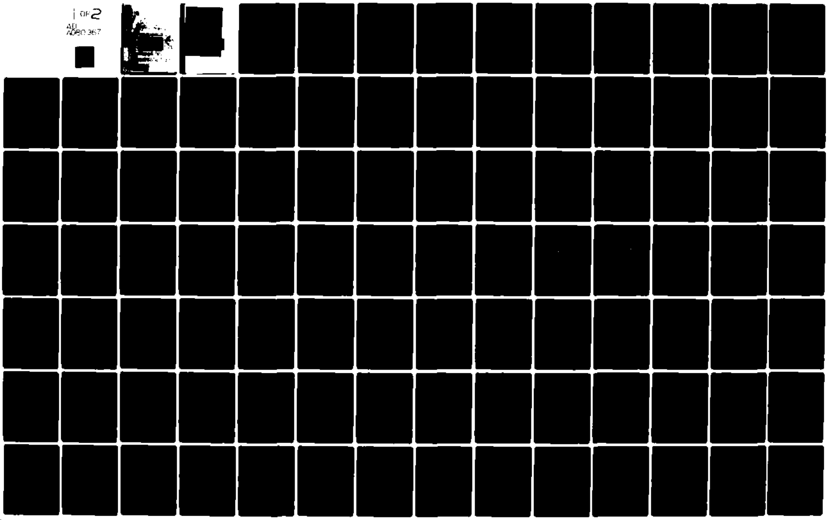

DISCLAIMER NOTICE

THIS DOCUMENT IS BEST QUALITY PRACTICABLE. THE COPY FURNISHED TO DDC CONTAINED A SIGNIFICANT NUMBER OF PAGES WHICH DO NOT REPRODUCE LEGIBLY.

AFIT/GE/EE/79D-11

6

PREDICTED MICROWAVE ELECTRO-MAGNETIC BACKSCATTERING RETURNS FOR SIMPLE REFLECTIVE TARGETS.

9 Master's THESIS,

14 AFIT/GE/EE/79D-11

Frank DiBartolomeo, Jr
2nd Lt. USAF

10

11 Dec 79

12 122

Approved for public release; distribution unlimited

012225

AFIT/GE/EE/79D-11

PREDICTIVE MICROWAVE ELECTROMAGNETIC BACKSCATTERING RETURNS FOR SIMPLE REFLECTIVE TARGETS

THESIS

Presented to the Faculty of the School of Engineering
of the Air Force Institute of Technology
Air University
in Partial Fulfillment of the
Requirements for the Degree of
Master of Science

by

Frank DiBartolomeo, Jr., B.S.E.E.
2nd Lt USAF
Graduate Electrical Engineering

December 1979

A 23 el

Approved for public release; distribution unlimited.

Preface

This thesis was stimulated by research in Tactical Target Identification performed by the United States Air Force Systems Command's Rome Air Development Center (RADC/OCTM), Griffiss AFB, New York. Engineers there are investigating the possibility of identifying aircraft from two dimensional cross range versus slant range image plots of the discrete electromagnetic scatterers on the aircraft. To identify the aircraft, it i. thought of as a collection of simple geometrical objects whose image plots are known at different aspect angles. For a known aircraft, the image plots of the individual geometrical objects are "pieced" together at their individual aspect angles with their spatial position observed, with respect to some reference point on the aircraft. Thus, what is produced is a composite image plot of the discrete point scatterers on the aircraft. The assumption made above is that secondary multiple scattering is negligible compared to primary scattering.

The goals of this thesis are to obtain a practical method of obtaining the backscattered signal for any known incident signal for the perfectly-conducting sphere and perfectly-conducting, infinitely-thin circular disk and also to investigate the sensitivity of the backscattered signal to changing aspect angle.

I ackowledge with thanks the advice and encouragement received from my thesis advisor, August Golden, Jr., Capt., USAF and to my thesis readers, Joseph W. Carl, Maj., USAF, and Professor Raymond Potter at the Air Force Institute of Technology. Also, my thanks and appreciation go to my sponsor, Mr. Richard Wood of the Surveillance Division, Rome Air Development Center and to Drs. D. L. Moffat and D. B. Hodge of the Ohio State University. Dr. Hodge's computer simulation for the scattering from the circular disk was extremely helpful. Also, Capt. Golden's many helpful suggestions were invaluable to the completion of this research.

Finally, I would like to thank my wife, Kathy, whose patience and understanding were of immeasurable value throughout my AFIT program.

FRANK DIBARTOLOMEO, JR.

Contents

List of Figures

Abstract

The problem of identifying the perfectly conducting sphere and perfectly-conducting, infinitely-thin circular disk via the backscattered far field from the object with a known incident signal is examined. A method utilizing Synthetic Aperture Radar principles to obtain slant range versus cross range image plots of the discrete point scatterers on an object is discussed. A computer program to calculate the far field backscattering from the sphere is developed. Another computer program, found in the literature, which calculates the far field backscattering from the infinitely-thin, circular disk, is extended for ka >15. In the above programs, the backscattering is obtained as a function of frequency and treated as the frequency response of a linear system. The input to this system is five cycles of 10GHz R-F. The return signal is the output of the system and is obtained by using conventional linear system theory. Since a sphere is symmetric, the same return is obtained at all aspect angles. This return from the sphere is examined. However, returns from the circular disk are different at different aspect angles. These returns from the disk are examined.

PREDICTED MICROWAVE ELECTRO-MAGNETIC BACKSCATTERING RETURNS FOR SIMPLE REFLECTIVE TARGETS

I. Introduction

Background

With the use of Synthetic Aperture Radar processing, it is theoretically possible to obtain two-dimensional slant range versus cross range image plots of the locations of the discrete point scatterers on simple geometrical shapes. These plots, it is hoped, will show a rough outline of the object and will aid in its identification. As was stated in the Preface, an aircraft will be thought of as a collection of these simple geometrical objects whose image plots are known at different aspect angles.

The two simple geometrical shapes considered here are the sphere and the circular disk. The sphere is unique in the fact that at any aspect angle the return signal will always be the same. This is due to spherical symmetry. Thus, at any specific aspect angle, the image plot obtained from the sphere will be the same as the image plot obtained at any other aspect angle. As will be shown in Chapter II, to obtain cross range information, the return signal must change with changing aspect angle. Thus, for the sphere, only slant range information can be obtained. The circular disk, however, has the advantage of returning an aspect-dependent signal. Therefore, cross range information can be obtained for the disk. The circular disk also possesses a known backscattered frequency response which is treated as the frequency response of a linear system. The backscattered signal is the output of the system and the incident signal is the input to the system. Although the backscattered signal from the sphere provides no cross range information, its backscattered signal can be obtained in the same way as the backscattered signal from the disk.

The method used for identification of the unknown shape is to compare the image obtained from the unknown shape to previously recorded images of different known shapes at known aspect angles. Hopefully, one of the known image plots will match up with the unknown plot. Taken that this is the case, the unknown object will be identified as the object which corresponds to the known matching image plot.

Problem and Scope

The specific problem studied in this thesis is how many distinct backscatter signature returns are obtained over a specified angle variation around the circular disk. The sphere is spherically symmetric and thus will backscatter the same return signal for all incident aspect angles. For this reason, the section on the sphere was used to show how the return signal was obtained by knowledge of the frequency response of the scattering. The return signal from the disk is obtained in the same manner. In this case, however, the frequency response of the scattering is aspect dependent.

Only the sphere and the circular disk are considered in depth since they are the only simple geometrical shapes for which the frequency response of the far field scattering can be numerically calculated.

General Approach and Presentation

The general approach used in the research was to firstly understand how two-dimensional images of the discrete point scatterers on simple geometrical objects can be obtained. Synthetic Aperture Radar processing was seen to aid in the development of a slant range versus cross range image of the discrete point scatterers of the object.

Secondly, there had to be discovered if there were any geometrical shapes for which the backscattered field as a function of frequency was numerically calculable. Once the sphere and the circular disk were found to possess this quality, they were the only shapes concentrated on. As was alluded to in the background section, this backscattered field, as a function of frequency, was treated as the frequency response of a linear system. The incident signal is the input to the system and the backscattered signal is the output. For the sphere, only the backscattered signal at one aspect angle is examined since the sphere is symmetric. For the disk, however, the returns from different aspect angles were examined.

The point of obtaining the backscattered signals from the sphere and the disk is that, theoretically, they can now become the inputs to the processor to produce the two-dimensional plots. Unfortunately, because of time constraints, this could not be attempted.

The sequence of presentation of the main chapters in thesis is:

I. Introduction

II. Signal Processing-Two Dimensional Images

III. Scattering from the Perfectly Conducting Sphere in the Far Field

IV. Scattering from the Perfectly Conducting, Infinitely-Thin Circular Disk in the Far Field

V. Conclusions, Findings and Recommendations.

II. Signal Processing Two-Dimensional Images

The processing used to obtain two-dimensional images of the scattering centers of objects in the far field is essentially Synthetic Aperture Radar processing (Ref 3, Ref 8). The following is an explanation of the processing used to obtain a two-dimensional image of two discrete point scatterers in the far field (Ref 7).

Figure 1 is representative of the situation of two discrete point scatterers in the far field. Scatterer 1 is at point one and scatterer 2 is at point two. Imagine, however, that instead of the scatterers moving around the radar, that the radar moves around the scatterers. The radar is at point three. With no loss in generality, let scatterer 1 be located at zero cross range and let scatterer 2 be located at cross range R_{c2}. Also let the distance from the radar to scatterer 1 be constant and be denoted R_0. Let the distance from the radar to scatterer 2 be varying and be denoted R. Also let $\Delta\theta/2$ and θ denote the angles shown in Figure 1. The angle $\Delta\theta/2 \cong 0°$ and $\theta \cong 90°$. Therefore, the cross range axis is perpendicular to the line from point one to point three.

The two dimensional image that will be obtained will be a plot of slant range versus cross range. Slant range can be obtained easily by noting the time delay of the signal from the radar to each point scatterer and back to the radar. Therefore, if the time delay to the i^{th} scatterer and back is denoted τ_i, the slant range R_{si}, is

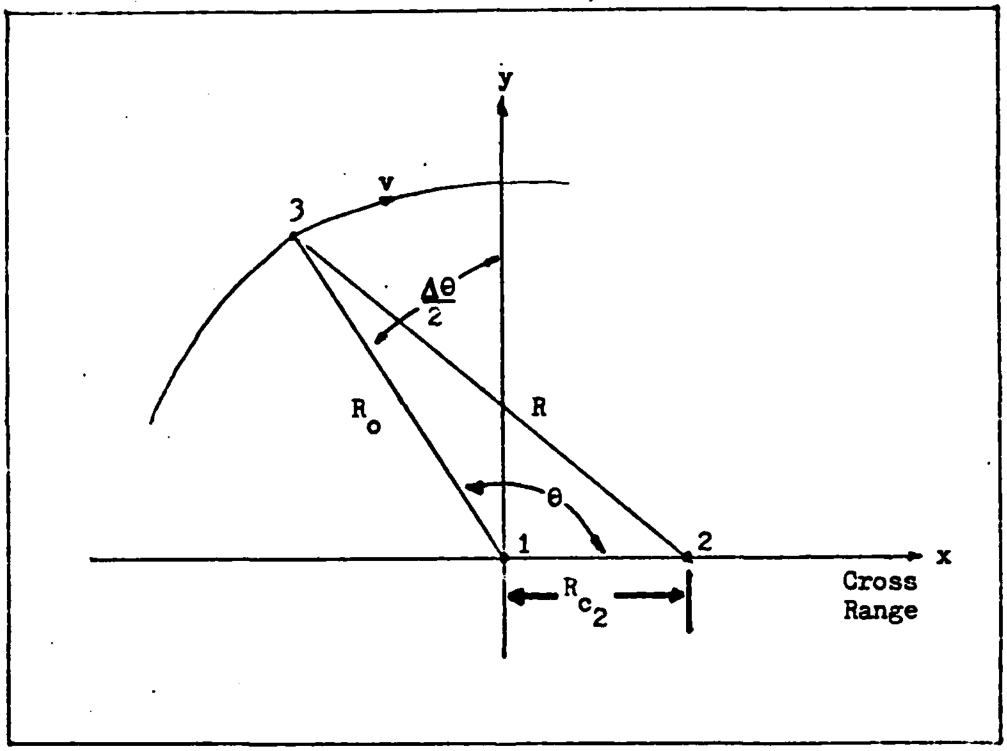

Figure 1. Two Discrete Point Scatterers in the Far Field

$$R_{si} = \frac{c\tau_i}{2} \tag{1}$$

where

$c \triangleq$ speed of light in free space

As can be seen, the processing required to obtain slant range is quite simple in principle. On the other hand, the processing required to obtain cross range is more complicated. The cross range of scatterer 2 will be examined since the processing involved to obtain its cross range is representative of the processing involved to obtain the cross range of any discrete point scatterer on the target.

Assuming the transmitted signal from the radar is

$$s_T(t) = e^{j\omega_c t} \tag{2}$$

the signal received back from scatterer 2 will be

$$s_{R2}(t) = e^{j(\omega_c t - 2kR_{s2})} \tag{3}$$

where

$$k = \frac{2\pi}{\lambda} \tag{4}$$

Also, assuming that cross range values will be much smaller than slant range values, R_{s2} can be approximated by

$$R_{s2} \cong R_0 - R_{c2} \cos\theta \tag{5}$$

therefore,

$$s_{R2}(t) = e^{j\omega_c t} \cdot e^{-j2kR_0} \cdot e^{j2R_{c2} \cos \theta} \tag{6}$$

note that

$$\theta = \theta_{(t)} = -\frac{v}{R_0}t + \frac{\pi}{2} + \frac{\Delta\theta}{2} \tag{7}$$

therefore

$$\begin{aligned} \cos \theta &= \cos \left(\frac{\pi}{2} + \frac{\Delta\theta}{2} - \frac{v}{R_0}t\right) \\ &= -\sin \left(\frac{\Delta\theta}{2} - \frac{v}{R_0}t\right) \end{aligned} \tag{8}$$

However, if $(\frac{\Delta\theta}{2} - \frac{v}{R_0}t)$ is small, then

$$\cos \theta \cong \frac{v}{R_0}t - \frac{\Delta\theta}{2} \tag{9}$$

Therefore,

$$s_{Rs}(t) = e^{j\omega_c t} \cdot e^{-j2kR_0} \cdot e^{-jk\Delta\theta R_{c2}} \cdot e^{j\frac{2kR_{c2}v}{R_0}t} \tag{10}$$

At the receiver, there will be a bank of matched filters. Each of them will be matched to a specific cross range on either side of zero cross range. There will also be a filter matched to zero cross range.

The bank of matched filters is represented in Figure 2 where Δx is the cross range resolution and T is the dwell time. If there is a discrete scatterer at a cross range which is an integer multiple of Δx, the outputs of the filters matched to those

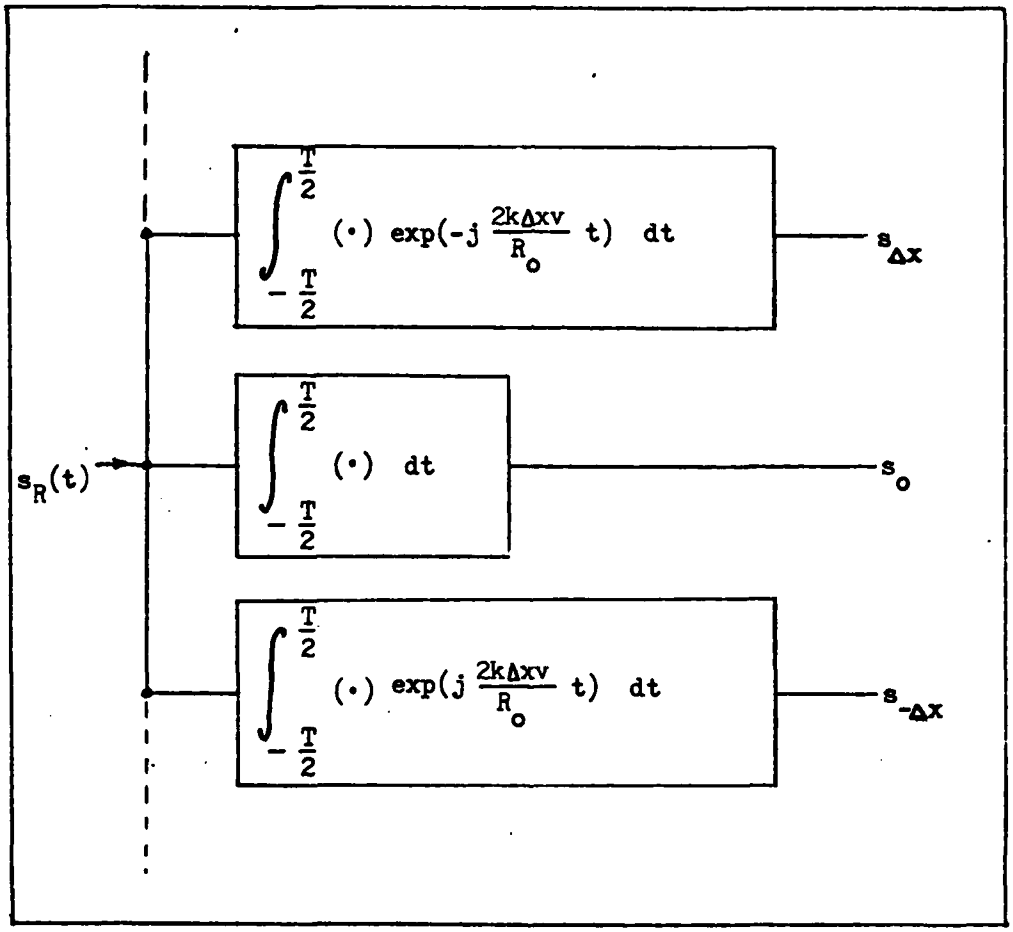

Figure 2. Bank of Matched Filters at Receiver

integer multiples will roll off with a sin x/x distribution. For example, suppose there is a scatterer at cross range R_c. Therefore

$$s_{R2}(t) = e^{j\omega_c t} \cdot e^{-j2kR_0} \cdot e^{-jk\Delta\theta R_c} \cdot e^{j\frac{2kR_c v}{R_0}t} \tag{11}$$

The $e^{j\omega_c t}$ term can be suppressed without loss in generality. Therefore,

$$s_{R2}(t) = e^{-j2kR_0} \cdot e^{-jk\Delta\theta R_c} \cdot e^{j\frac{2kR_c v}{R_0}t} \tag{12}$$

The output of the filter matched to R_{c2} would be

$$\int_{-T/2}^{T/2} e^{-jk(2R_0+\Delta\theta R_c)} \cdot e^{j\frac{2kR_c v}{R_0}t} \cdot e^{-j\frac{2kR_{c2}v}{R_0}t}\, dt$$

$$= e^{-jk(2R_0+\Delta\theta R_c)} \int_{-T/2}^{T/2} e^{j\frac{2kv}{R_0}(R_c-R_{c2})t}\, dt \tag{13}$$

$$= e^{-jk(2R_0+\Delta\theta R_c)} \quad \frac{T \sin[\frac{2\pi v}{\lambda R_0}(R_c-R_{c2})T]}{[\frac{2\pi v}{\lambda R_0}(R_c-R_{c2})T]}$$

A plot of the magnitude of the above equation as a function of R_c is shown in Figure 3. If $R_c = R_{c2}$, a maximum of T will be the output of the filter matched to R_{c2}. If $R_c \neq R_{c2}$, the output of that same filter will fall off as a sinc(x) distribution as a function of R_c.

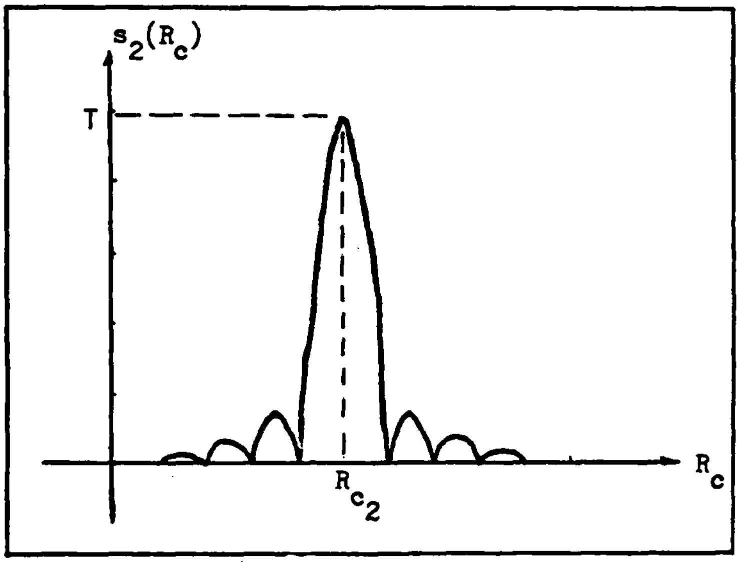

Figure 3. Plot of Magnitude of Equation (13)

To determine cross range resolution the criteria that will be used is that if the output of the filter matched to R_{c2} is above 0.707T in magnitude, then there is a scatterer at cross range R_{c2}: sinc(x)=0.707 at approximately 1.4 Rad. Therefore, $\Delta R_c = R_c - R_{c2}$ must be found in Eq. (14) and multiplied by two to obtain Δx.

$$\frac{\sin[\frac{2\pi v}{\lambda R_0}\Delta R_c T]}{[\frac{2\pi v}{\lambda R_0}\Delta R_c T]} = 0.707 \tag{14}$$

Therefore

$$\frac{2\pi v}{\lambda R_0}\Delta R_c T \cong 1.4 \tag{15}$$

$$\Delta R_c = \frac{1.4\lambda R_0}{2\pi v T} = \frac{0.22\lambda R_0}{vT} \tag{16}$$

$$\Delta x = 2\Delta R_c = \frac{0.44\lambda R_0}{vT} \tag{17}$$

After slant range and cross range of each scatterer are obtained, a two dimensional plot is made for a single target at a single aspect angle by locating these scatterers on a display.

III. Scattering from the Perfectly Conducting Sphere in the Far Field

The electromagnetic backscattering from an object can be thought of as a linear system characterized by a frequency response which is the normalized backscattered E-field as a function of frequency (Ref 2:6). Therefore, in theory, the frequency spectrum of the backscattered signal can be obtained by multiplying the Fourier Transform of the incident signal by the frequency response of the system. The backscattered signal is the inverse Fourier Transform of its frequency spectrum. Thus, by conventional linear system theory, the scattered signal from an object can be obtained.

The reason for obtaining the backscattered signal from the object is that it can now be inputed to the processor described in Chapter II in order to obtain a two-dimensional, slant range vs. cross range image of the discrete point scatterers on the object. The process is represented in a block diagram in Figure 4.

Frequency Response of the Sphere.

The Mie series solution of the scattering from the sphere at a point p as a function of ω is (Ref 14:142):

$$\bar{E}^s(p,\omega) = E_0 \sum_{n=1}^{\infty} (A_n \bar{M}ol_n + B_n \bar{N}el_n) \tag{18}$$

where,

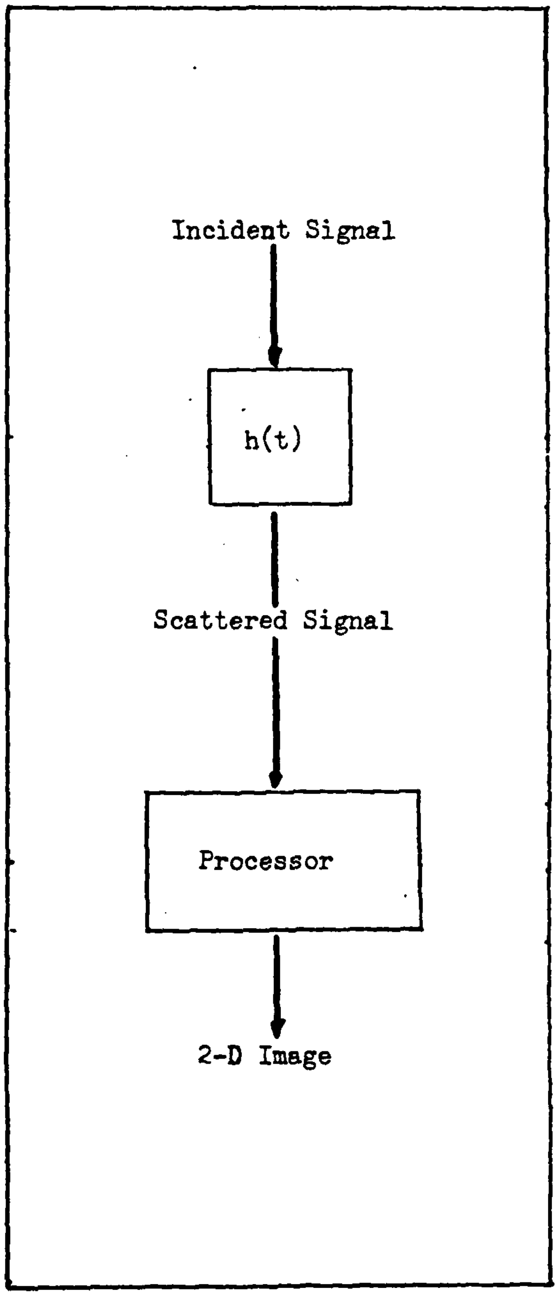

Figure 4. Identification Process

$$\mathrm{Mol}_n = \frac{1}{\sin\theta}\, h_n^1(kr)P_n^1(\cos\theta)(\cos\phi)\hat{\theta}$$

$$-h_n^1(kr)\frac{d}{d\theta}P_n^1(\cos\theta)(\sin\phi)\hat{\phi} \tag{19}$$

$$\mathrm{Nei}_n = \frac{n(n+1)}{kr}\, h_n^1(kr)P_n^1(\cos\theta)(\cos\phi)\hat{r}$$

$$+\frac{1}{kr}\frac{d}{d(kr)}[krh_n^1(kr)]\frac{d}{d\theta}P_n^1(\cos\theta)(\cos\phi)\hat{\theta} \tag{20}$$

$$-\frac{1}{kr\sin\theta}\frac{d}{d(kr)}[krh_n^1(kr)]P_n^1(\cos\theta)(\cos\phi)\hat{\phi}$$

$P_n^1(x) \triangleq$ Associated Legendre Polynomial of degree n and order 1.

$$= \frac{1}{2^n \cdot n!}\frac{d^n}{dx^n}(x^2-1)^n \tag{21}$$

$h_n^1(x) \triangleq$ Spherical Hankel Function of degree n and order 1.

$$= J_n(x) + jY_n(x) \tag{22}$$

$$Y_n(x) = \frac{J_n(x)\cos(n\pi) - J_{-n}(x)}{\sin(n\pi)} \tag{23}$$

n not an integer

$$A_n = -(-j)^n \frac{2n+1}{n(n+1)} \frac{j_n(ka)}{h_n^1(ka)} \tag{24}$$

$$B_n = (-j)^{n+1} \frac{2n+1}{n(n+1)} \frac{\frac{d}{d(ka)}[ka j_n(ka)]}{\frac{d}{d(ka)}[ka h_n^1(ka)]} \tag{25}$$

However, assuming r>>a, $e^{-j\omega t}$ time dependence and using far field approximations, with "a" the radius of the sphere (Ref 14:143):

$$\bar{E}^s(p,\omega) = \frac{E_0 e^{jkr}}{kr}[\cos\phi S_1(\theta)\hat{\theta} - \sin\theta S_2(\theta)\hat{\phi}] \tag{26}$$

where

$$S_1(\theta) = \sum_{n=1}^{\infty}(-j)^{n+1}\left[A_n \frac{P_n^1(\cos\theta)}{\sin\theta} + jB_n \frac{d}{d\theta} P_n^1(\cos\theta)\right] \tag{27}$$

$$S_2(\theta) = \sum_{n=1}^{\infty}(-j)^{n+1}\left[A_n \frac{d}{d\theta}P_n^1(\cos\theta) + jB_n \frac{P_n^1(\cos\theta)}{\sin\theta}\right] \tag{28}$$

let,

$$F(\theta,\phi)\,\hat{\tau} = \cos\phi S_1(\theta)\hat{\theta} - \sin\phi S_2(\theta)\hat{\theta} \tag{29}$$

In the backscattering direction, approximations are made for F(0) for four regions: the low-frequency region, the lower resonance region, the upper resonance region and the high frequency region (Ref 14:146-150):

In the low frequency region ($ka<0.4$) the approximation for $F(0)$ is (Ref 14:150):

$$F(0) = \frac{3}{2}(ka)^2 \tag{30}$$

therefore

$$rE^S(\omega) = \frac{E_0 e^{jkr}}{k} \cdot \frac{3}{2}(ka)^3 \tag{31}$$

In the lower resonance region ($0.4<ka<0.8$) the approximation for $F(0)$ is

$$F(0) = \frac{3}{2}(ka)^3\left[1-\frac{5}{54}(ka)^2+\frac{17}{900}(ka)^4 - \frac{6,651,923}{11,907,000}(ka)^6\right]$$

$$+ j\frac{1}{2}(ka)^6\left[1 + \frac{6}{5}(ka)^2\right] \tag{32}$$

$$= \sqrt{x^2+y^2}\, e^{j \tan^{-1} \frac{y}{x}}$$

where

$$x = \frac{3}{2}(ka)^3\left[1-\frac{5}{54}(ka)^2+\frac{17}{900}(ka)^4 - \frac{6,651,923}{11,907,000}(ka)^6\right] \tag{33}$$

$$y = \frac{1}{2}(ka)^6[1 + \frac{6}{5}(ka)^2] \tag{34}$$

therefore

$$rE^s(\omega) = \frac{E_0\sqrt{x^2+y^2}}{k} \cdot e^{j(kr + \tan^{-1}\frac{y}{K})} \tag{35}$$

In the upper resonance region (0.8<ka<20) the approximation for F(0) consists of a specular component, $F^o(0)$, added to a creeping wave term, $F^c(0)$. Therefore,

$$F(0) = F^o(0) + F^c(0) \tag{36}$$

The approximations of $F^o(0)$ and $F^c(0)$ are:

$$F^o(0) = -\frac{ka}{2} e^{-j2ka}[1 - \frac{i}{2ka}] \tag{37}$$

$$F^c(0) = (ka)^{\frac{4}{3}} e^{j\pi(ka - \frac{7}{6})} [1.357588 +$$

$$+ (0.741196 + j1.283788)(ka)^{-\frac{2}{3}}] .$$

$$\cdot \exp\left[-(ka)^{\frac{1}{3}}(2.200002 - j1.270172)\right.$$

$$\left. + (ka)^{-\frac{1}{3}}(0.445396 + j0.257150)\right]$$

$$+\left[0.695864 + (0.964654 + j1.670829)(ka)^{-\frac{2}{3}}\right] \cdot$$

$$\cdot \exp\left[-(ka)^{\frac{1}{3}}(7.014224 - j4.049663)\right.$$

$$\left. - (ka)^{-\frac{1}{3}}(0.444477 + j0.256619)\right]$$

$$- \left[0.807104 + (0.798821 + j1.383598)(ka)^{-\frac{2}{3}}\right] \cdot$$

$$\cdot \exp\left[-(ka)^{\frac{1}{3}}(5.048956 - j2.915016)\right.$$

$$\left. - (ka)^{-\frac{1}{3}}(0.312321 + j0.180319)\right] \tag{38}$$

let

$$F^{o}(0) + F^{c}(0) = \sqrt{x^2+y^2}\, e^{\tan^{-1}\frac{y}{x}} \tag{39}$$

where

$$x = \mathrm{Re}\{F^{o}(0) + F^{c}(0)\} \tag{40}$$

$$y = \operatorname{Im}\{F^{o}(0) + F^{c}(0)\} \tag{41}$$

therefore

$$rE^{s}(\omega) = E_0 \frac{\sqrt{x^2+y^2}}{k} \; e^{j(kr+\tan^{-1}\frac{y}{x})} \tag{42}$$

In the high frequency region (ka>20) the approximation for F(0) is

$$F(0) = -\frac{1}{2}kae^{-j2ka} \tag{43}$$

therefore

$$\begin{aligned} rE^{s}(\omega) &= -\frac{E_0 ka}{2k} e^{-j[kr-2ka]} \\ &= -\frac{E_0 a}{2} e^{j[kr-2ka]} \end{aligned} \tag{44}$$

A computer program is listed in Appendix A which calculates the frequency response of the far field E-field backscattering from a perfectly conducting sphere. To give an idea of the shape of the backscattered E-field frequency response, a sample of the response is shown in Figure 5 as a function of ka up to ka=30. Since the scattering from the sphere is aspect independent, the response shown in Figure 5 is valid at any aspect angle.

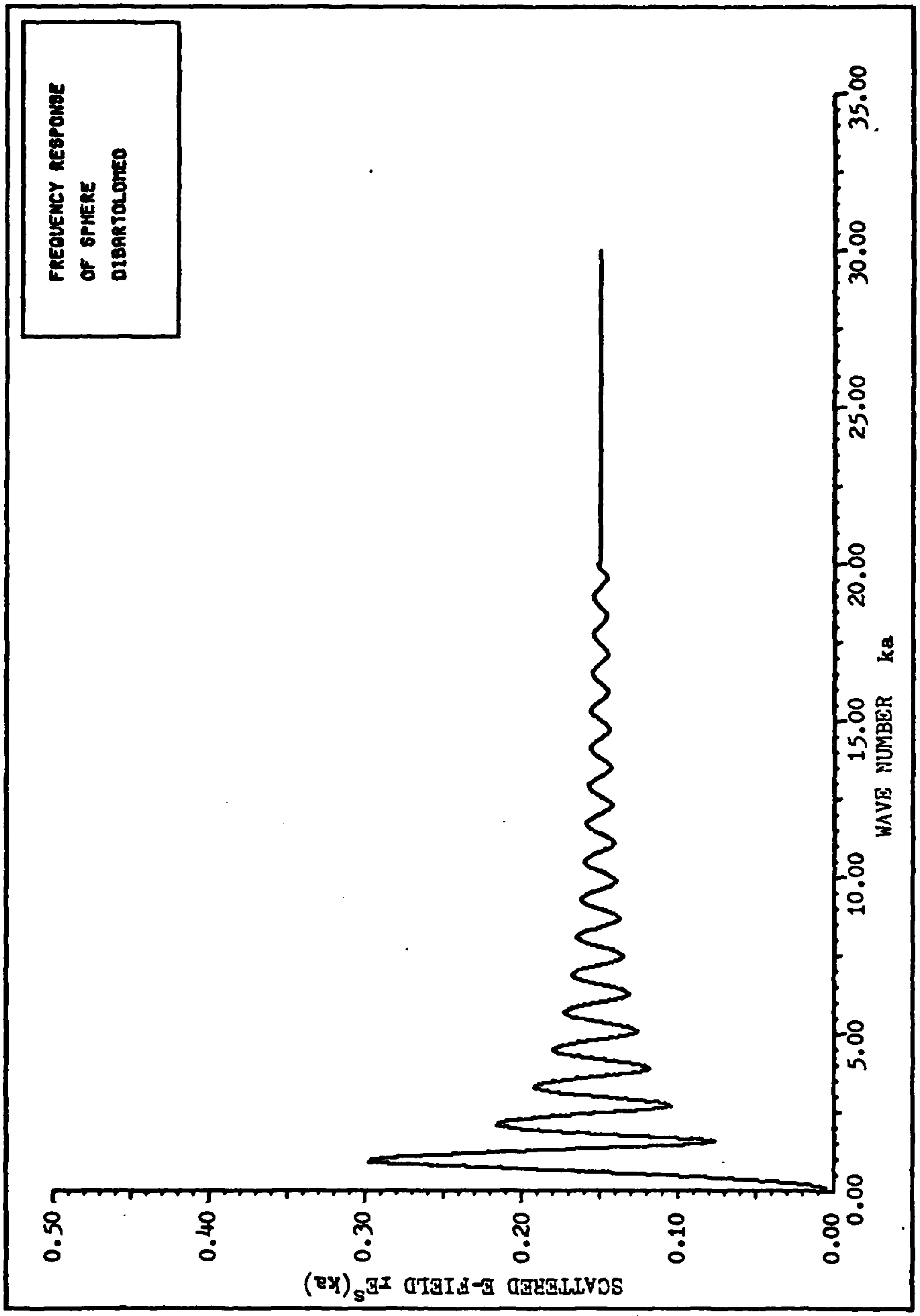

Figure 5. Frequency Response of the Scattering from the Sphere as a function of ka

The facility for obtaining Fourier Transforms and Inverse Fourier Transforms in this thesis is the Fast Fourier Transform (FFT). An explanation as well as a listing of the computer program for the FFT is provided in Appendix C. A review of the proper selection of FFT parameters is provided in Appendix D.

Process to Obtain Backscattered Signal

The incident signal used is a pulse of five cycles of 10GHz R-F. The selection of the proper way to sample the incident pulse is explained in Appendix D. From Appendix D, the pulse is shown to be sampled ten times each cycle, or fifty times each pulse. The pulse is shown in Figure 6 centered at t=0. The pulse is shown split in two parts. One part is at t=0 while the other part is at t=10.24 nsec. This is done because the FFT cannot see negative time. The FFT assumes periodicity of the time signal and its frequency spectrum. Therefore, the pulse would repeat around t=10.24 nsec (NOTE: 1024 samples, samples are 0.01 nsec apart). An expanded view of the left half of the pulse is shown in Figure 7. The spectrum of the pulse is shown in Figure 8. Note that the spectrum is simply a sinc(x) function shifted in frequency and centered on 10GHz. As outlined in Appendix D, the frequency response of any object must go out to the 250th sample, with Δf between samples being 97,656,000Hz, to fully enclose the appreciable frequency components of the incident 10GHz pulse. The frequency response for the sphere is shown in Figure 9, with the left half frequency reversed, conjugated and shifted up in frequency. The conjugation occurs, because when this frequency response is inverse transformed, the result should be a real impulse response.

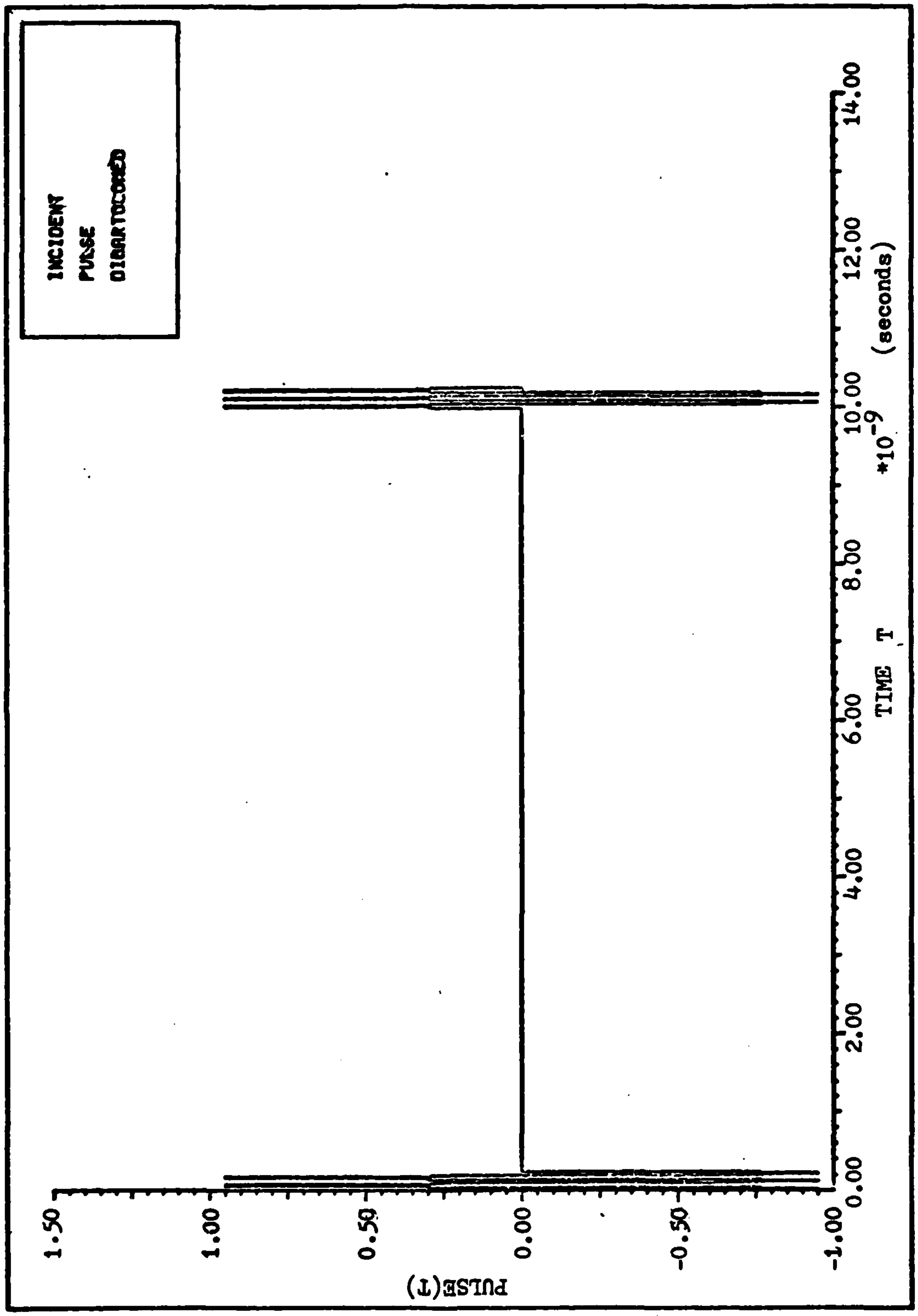

Figure 6. Incident Pulse of R-F at 10 GHz

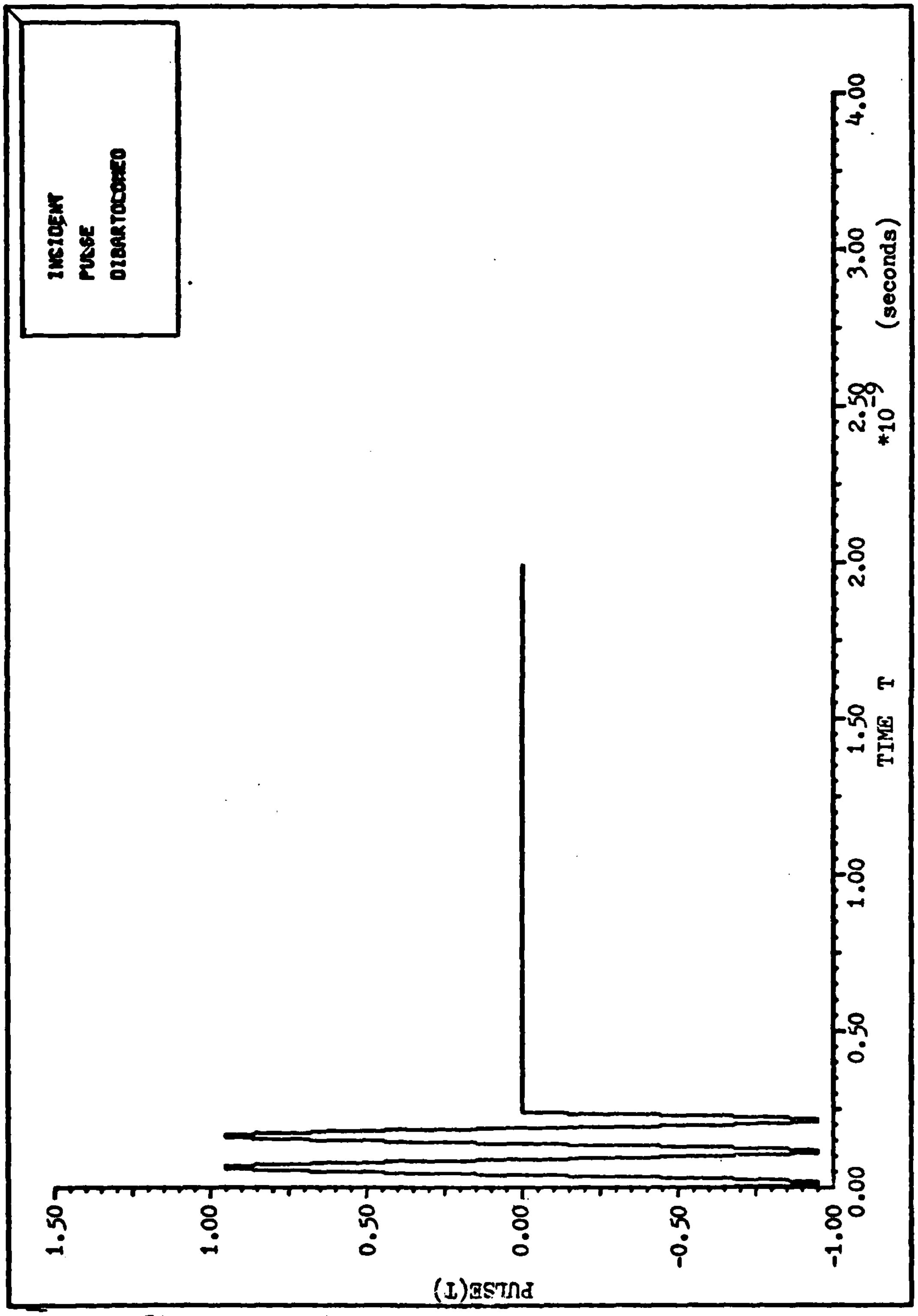

Figure 7. Expanded View of Incident R-F Pulse

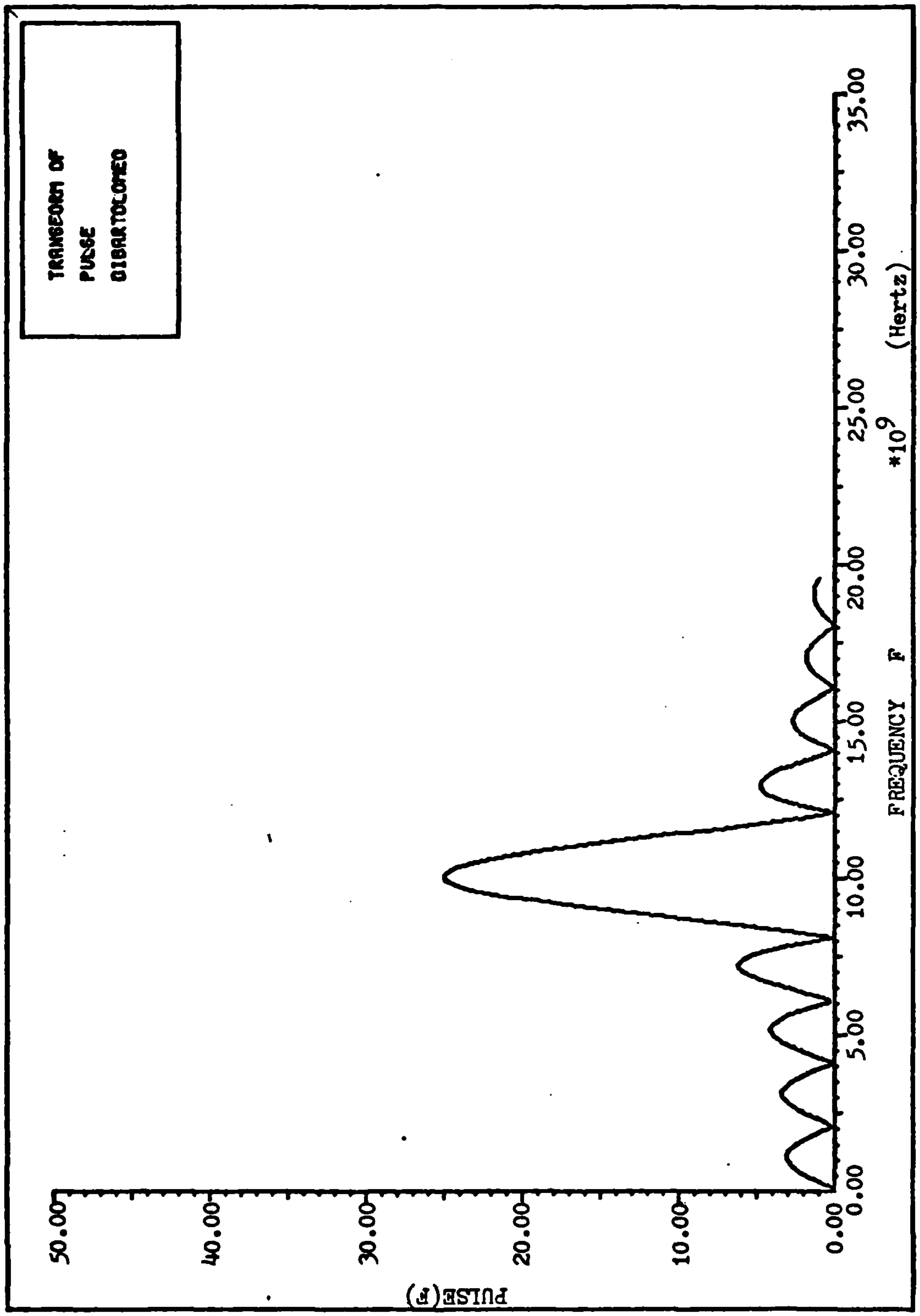

Figure 8. Spectrum of Incident R-F Pulse

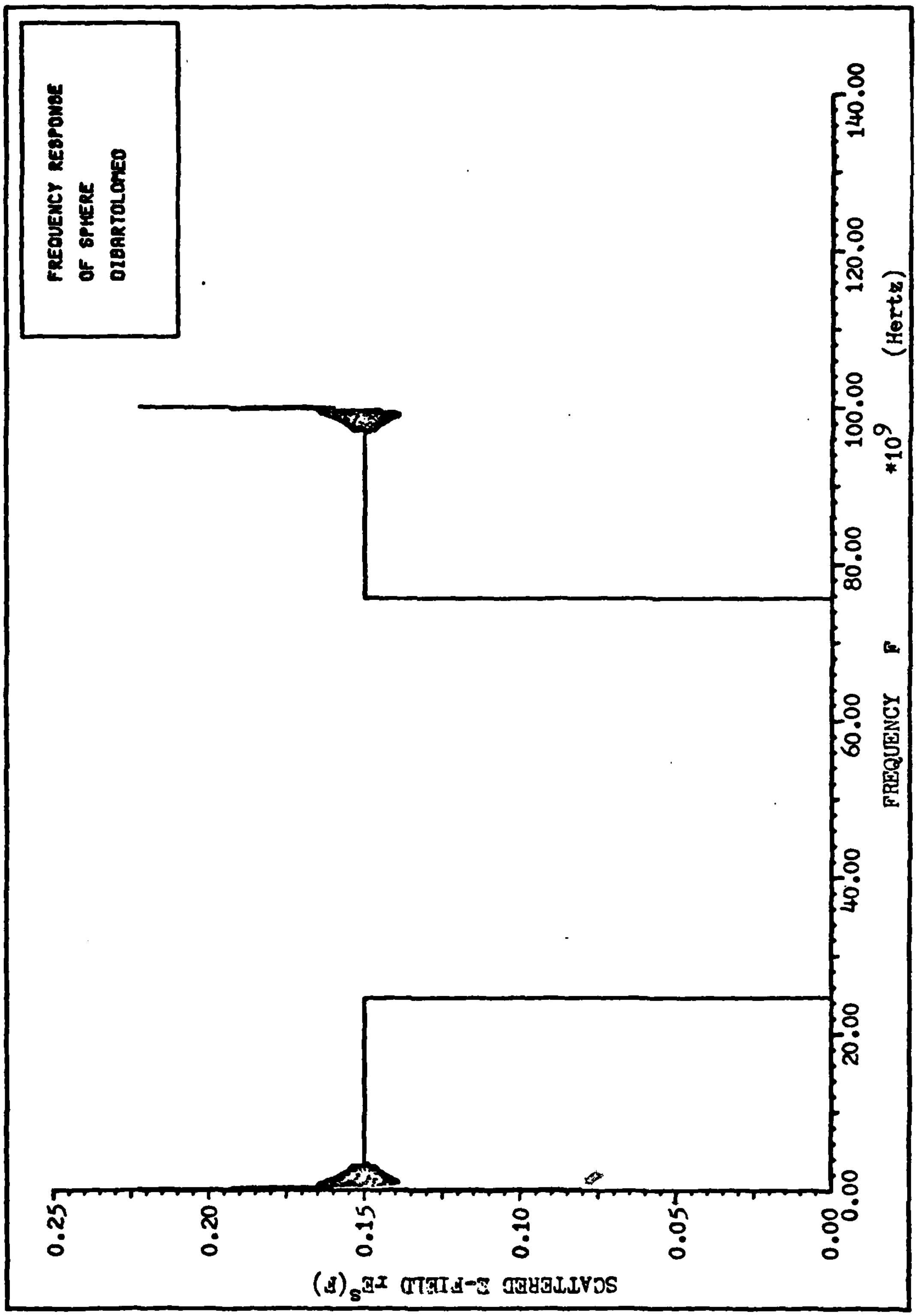

Figure 9. Frequency Response of the Scattering of the Sphere

It will be real if the frequency response has even magnitude and odd phase. The real part of the inverse Fourier Transform of the frequency response in Figure 9, is shown in Figure 10.

In Figure 11 is shown the real part of the result that is obtained when the frequency response of the sphere is multiplied by the Fourier Transform of the 10GHz incident pulse and inverse Fourier Transformed. Figures 12-14 show the same process done on a video pulse of the same width as the 10GHz pulse. Figure 12 is the video pulse with Figure 13 its spectrum, and Figure 14 the real part of the backscattered signal. Figures 11 and 14 will be compared. Because the video pulse has frequency components down very low in frequency where the frequency response of the sphere is oscillatory, the response obtained by linearly convolving this pulse with the impulse response of the sphere is not exactly the video pulse returned as is shown in Figure 14. However, the appreciable frequency components of the frequency spectrum of the 10GHz pulse are out in frequency where the frequency response of the sphere is essentially flat. Therefore, as shown in Figure 11, the 10GHz pulse is returned almost intact with only a time delay. The slight negative response at the end of the graph in Figure 11 also holds much significance. This is the return from the incident signal creeping around the sphere. The significant point is that as the incident pulse gets shorter and shorter in duration, more and more physical features of the object that the pulse is illuminating will become noticeable. In the case of the sphere, there are only two returns; the specular return and the creeping wave return. An unfortunate result is

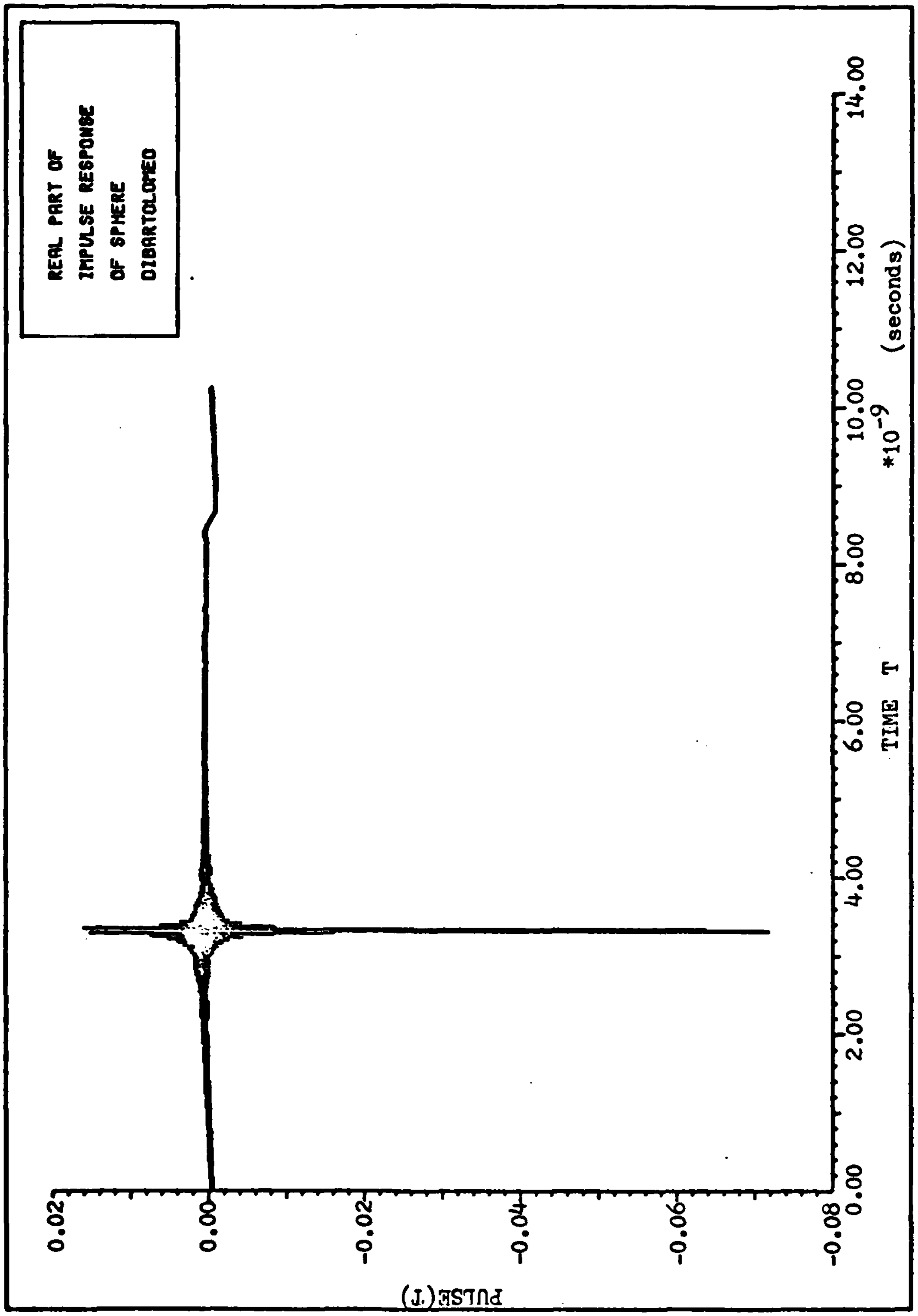

Figure 10. Real Part of Inverse Fourier Transform of the Frequency Response of the Scattering from the Sphere

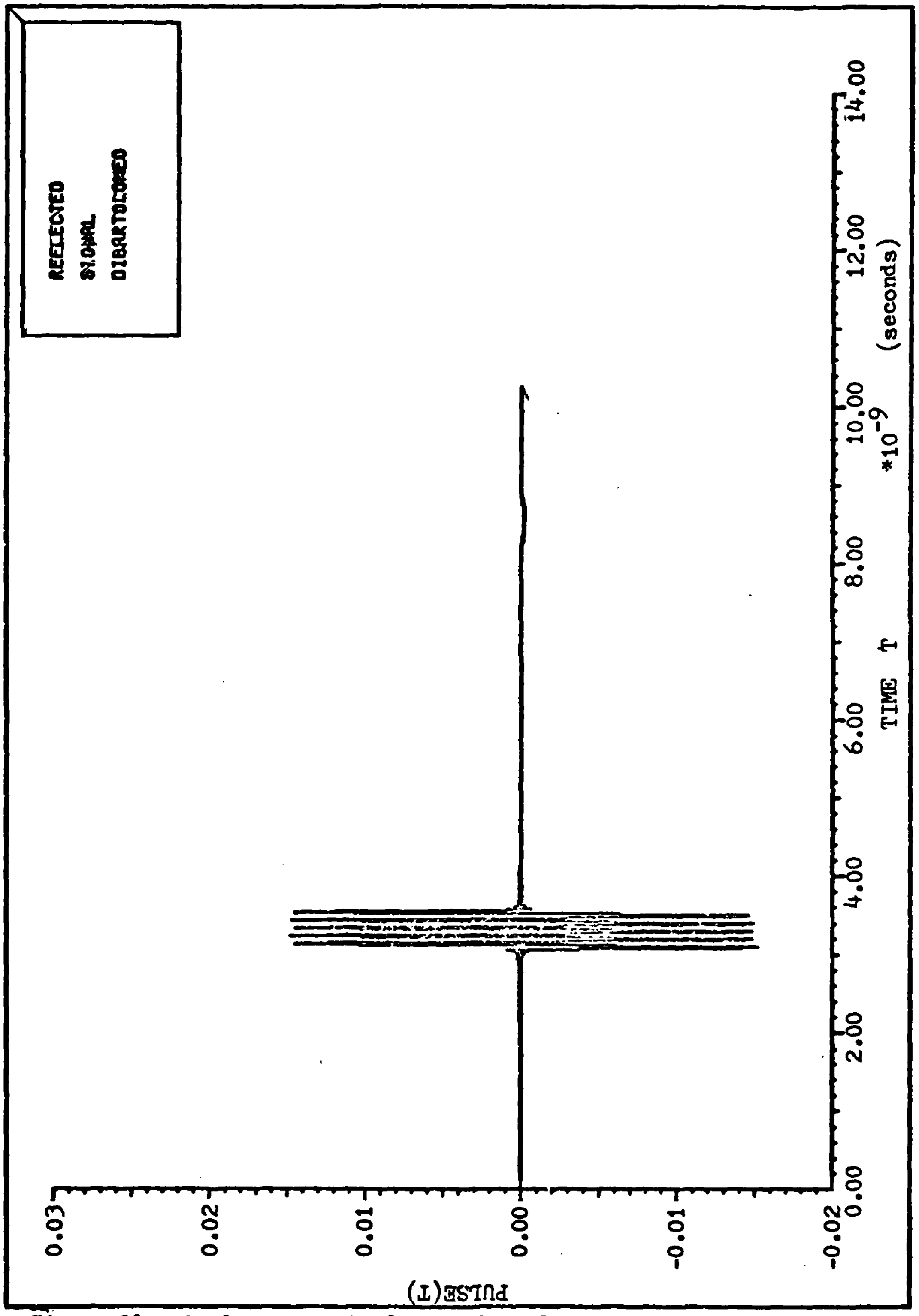

Figure 11. Real Part of Reflected Signal with R-F Pulse Incident

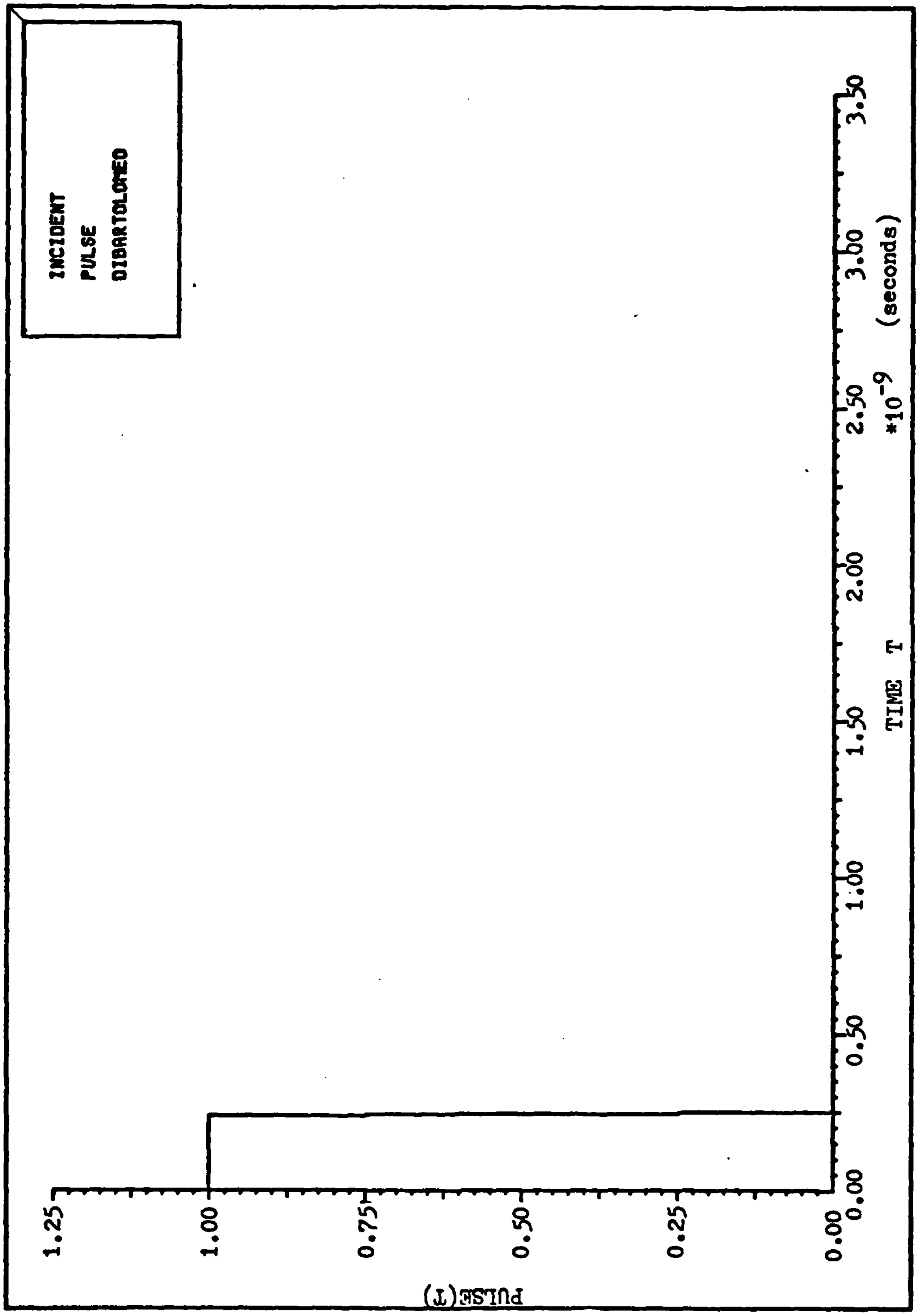

Figure 12. Video Pulse

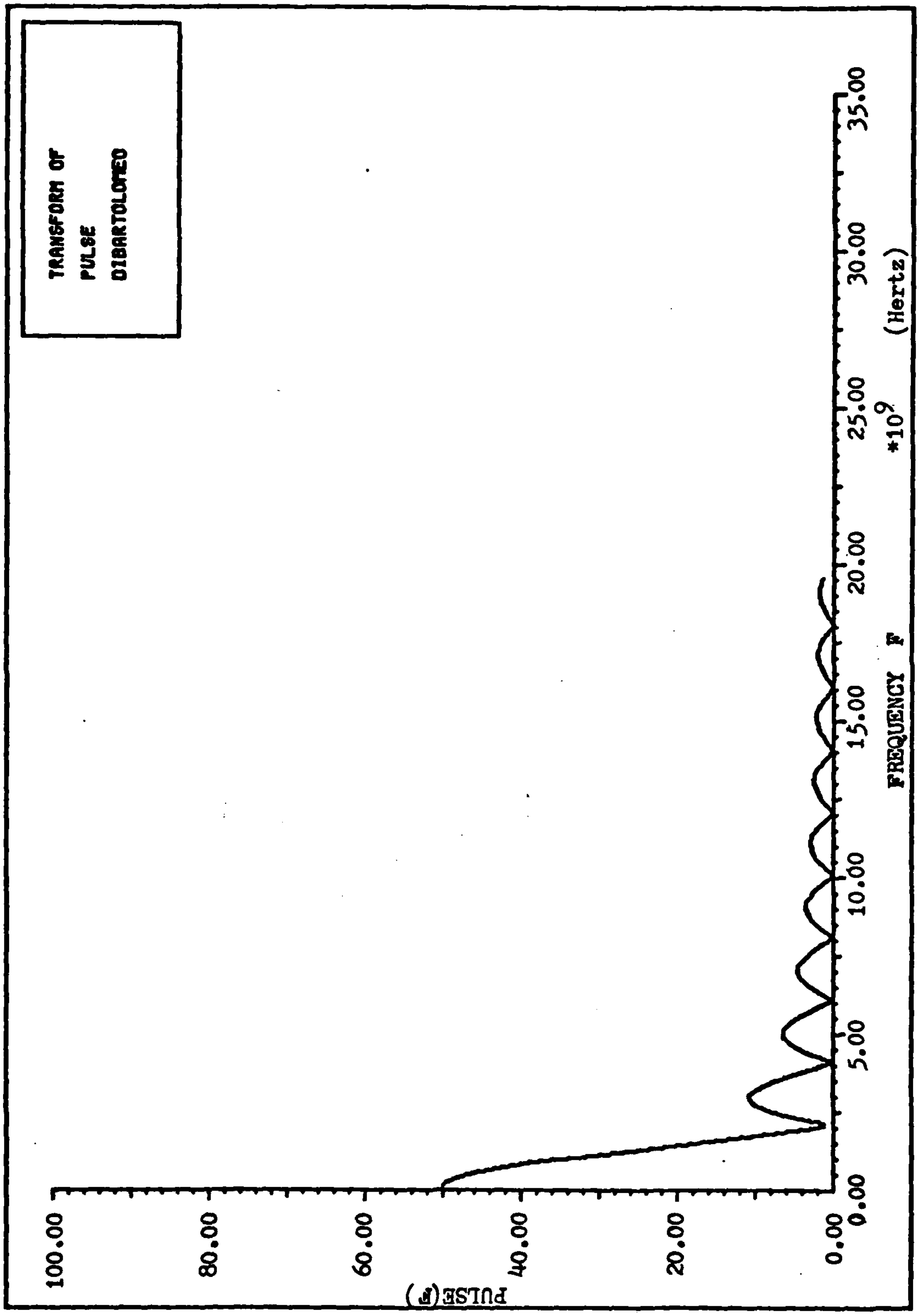

Figure 13. Spectrum of Video Pulse

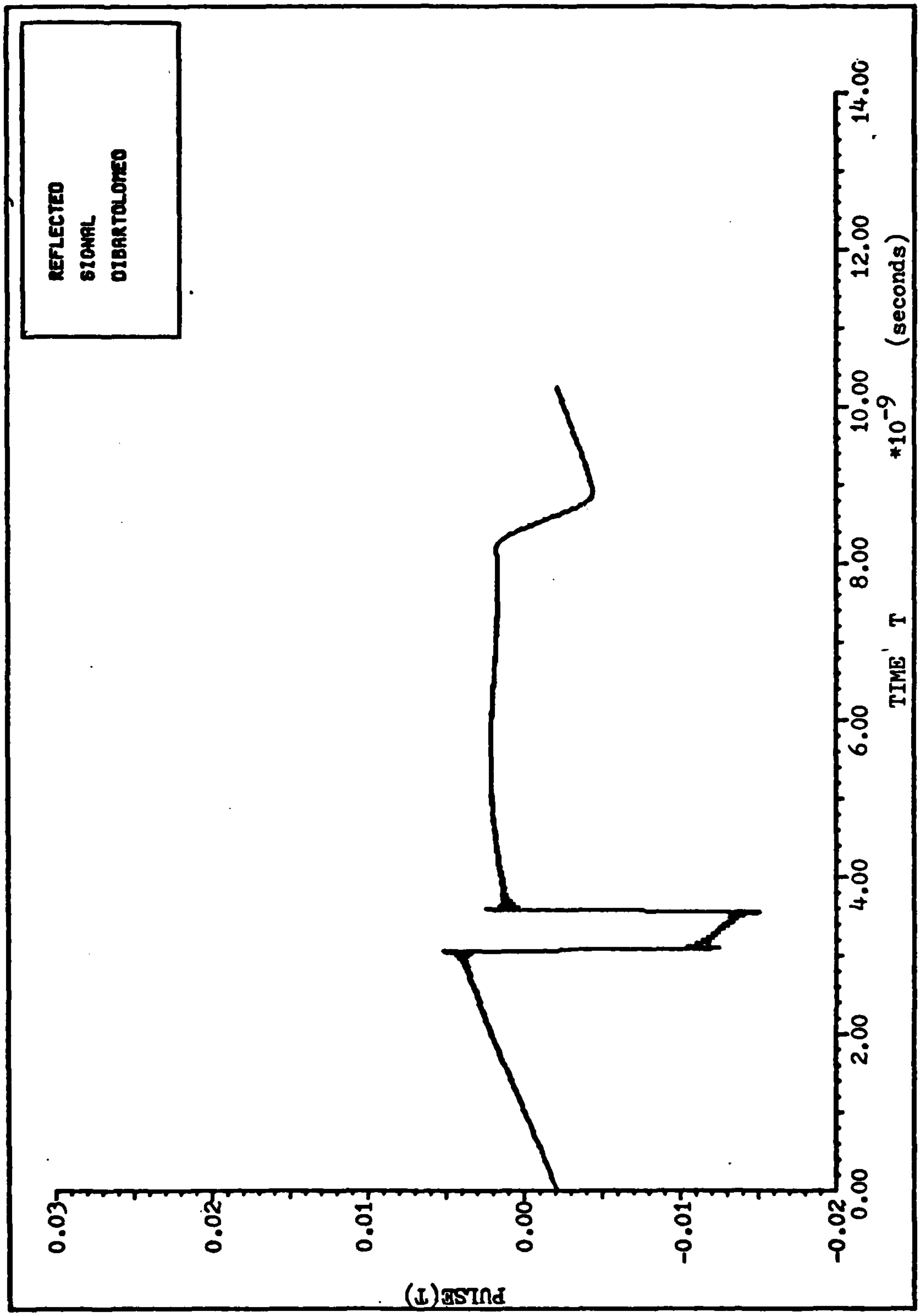

Figure 14. Real Part of Reflected Signal with Video Pulse Incident

that as the frequency of the pulse is increased, the creeping wave term will become less apparent. So only the specular return will be noticeable. At lower frequencies, the creeping wave return will become more apparent. Refer back to Eq. (17) in Chapter II, written here for convenience.

$$\Delta x = 2\Delta R_c = \frac{0.44\lambda R_0}{vT} \tag{17}$$

As the frequency is decreased in order to notice the creeping wave return, the wave length, λ, will be increased and thus increase Δx and thus decrease the cross range resolution. As the frequency is increased in order to decrease λ and Δx and therefore increase the cross range resolution of the discrete point scatterers, the creeping wave return will disappear. Thus, for all practical purposes, only the specular return will be detected.

IV. Scattering from the Perfectly Conducting, Infinitely-Thin Circular Disk in the Far Field

As was stated in the Introduction, the sphere, until recently was the only geometrical object for which numerical scattering results could be obtained. Although the rigorous eigenfunction solution of the scattering from the thin circular disk has been available in the literature for some time (Ref 1), only limited numerical results have been available due to the complexity of the numerical computations involved. However, in February 1979, a report out of the Electrosciences Laboratory at the Ohio State University was published for the Department of the Navy, Office of Naval Research, which made available the rigorous eigenfunction solution of the plane wave scattering problem from the infinitely-thin circular disk (Ref 9). The author, Dr. D. B. Hodge, develops a computer program to obtain the far field scattering from the thin metallic disk. The program allows an incident plane wave of arbitrary incidence angle and polarization and calculates the far field radar cross section as well as the scattered E-field. The geometry of the disk is shown in Figure 15. The direction of the incident wave is specified by k^i and θ_0. The incident direction is restricted to the x-z plane. Because of circular symmetry, this is no restriction. The angle "α" is the polarization angle. When α=0°, the incident field is parallel to the x-z plane. When α=90°, the incident field is perpendicular to the x-z plane. The radius of the disk is "a." While the incident

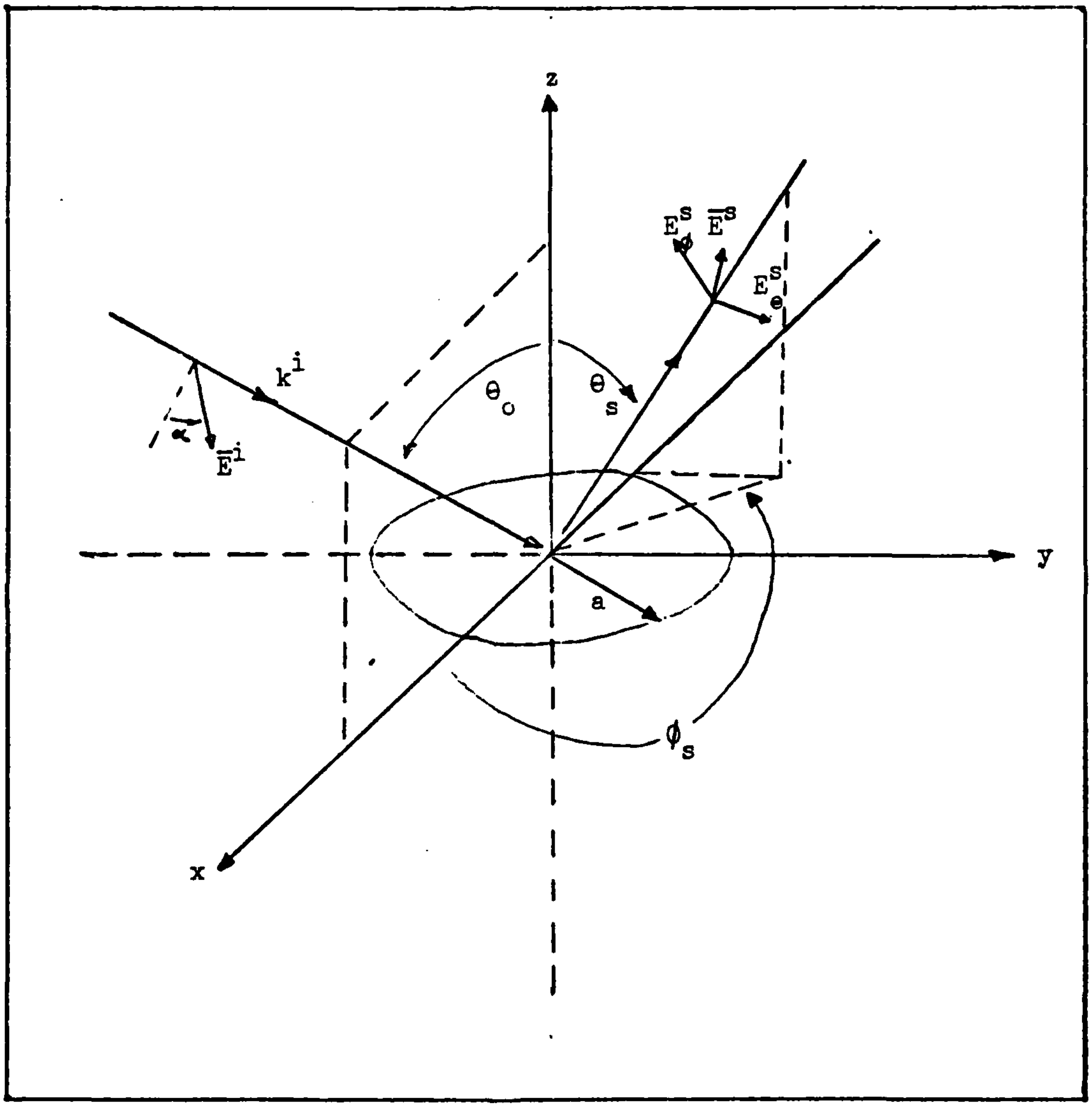

Figure 15. Geometry of Disk

field is restricted to the x-z plane, the scattered field can be in any direction specified by θ_s and ϕ_s. However, since backscattering is only considered, $\theta_s=\theta_0$ and $\phi_s=0$. A listing of Dr. Hodge's program is contained in Appendix B along with a sample I/O and an explanation of how to input values to the program.

The program is valid up to ka=15. A high-frequency approximation was used to extend the program past ka=15. This approximation is a modification of the Sommerfield-MacDonald technique by Ufimitsev (Refs 16 and 17). For $0°<\theta_0<90°$ and $\theta_s=\theta_0$, the theta component of the E-field normalized by the radius of the disk and divided by two is (Ref14:514-515).

$$rE\theta_N^s \cong -j\left[\left\{A_1{}^2(\theta)\left(\frac{1-\sin\theta_0}{2\sin\theta_0}\right) + A_2{}^2(\theta)\left(\frac{1+\sin\theta_0}{2\sin\theta_0}\right)\right\}\cdot\right.$$

$$\cdot\, J_1(2ka\sin\theta_0) - j\left\{A_1{}^2(\theta)\left(\frac{1-\sin\theta_0}{2\sin\theta_0}\right)\right. \tag{45}$$

$$\left.\left.-A_2{}^2(\theta)\left(\frac{1+\sin\theta_0}{2\sin\theta_0}\right)\right\}J_2(2ka\sin\theta_0)\right]$$

where

$$A_{\frac{1}{2}}(\theta) = \sqrt{2}\exp[-j\tfrac{\pi}{4}]\left[C[2\sqrt{\tfrac{2ka}{\pi}}|\cos(\tfrac{\pi}{4} \mp \tfrac{\theta_0}{2})|]\right.$$

$$\left. + jS[2\sqrt{\tfrac{2ka}{\pi}}|\cos(\tfrac{\pi}{4} \mp \tfrac{\theta_0}{4})|]\right] \quad (46)$$

$$C(\eta) = \int_0^{\eta} \cos \tfrac{\pi}{2}t^2 \, dt \quad (47)$$

$$S(\eta) = \int_0^{\eta} \sin \tfrac{\pi}{2}t^2 \, dt \quad (48)$$

$$\sigma_{||} = 4\pi r^2 |E_\theta|^2 \quad (49)$$

To limit the extent of the programs listed in Appendix B, α=0, in Figure 15. Since, such is the case, only E_θ^S need be considered since E_ϕ^S will be zero. The program used to implement the above equations for E_θ^S and $\sigma_{||}$ is in Appendix B with an output following the first program. The computer program that incorporates the extension to the first program is the third program listed in Appendix B.

Sensitivity of Returns from the Circular Disk at Five Different Aspect Angles

The following discussion is divided into three sections. The first section concerns backscattering from the circular disk at

1° off normal incidence. The second section is a sensitivity study of the backscattering from the disk at 71°, 72°, 73°, 74°, and 75° off normal incidence. The last section examines backscattering from the disk at 89° off normal incidence.

Backscattering from the Circular Disk at 1° Off Normal. Figure 16 shows the frequency response of the backscattered E-field from the circular disk at 1° off normal. The large oscillatory portion of the response is the backscattering in accordance with the physical optics model. If the frequency of the incident E-field is constant and is directed at a specific aspect angle off the normal of the disk, a lobing pattern, quite similar to an antenna lobing pattern, will be created with the maximum of the major lobe pointed at the same angle off normal as the incident E-field and 180° around the disk from the incidence direction. This pattern is the magnitude of the scattered E-field as a function of aspect angle. As the frequency is increased and the incidence angle is kept constant, the beam widths of the lobes of the lobing pattern become smaller and consequently maxima and minima of the lobing pattern pass by the fixed incident angle resulting in the oscillatory nature of the frequency response of the backscattered E-field. The oscillatory response riding on the physical optics response is due to diffraction off the edges of the disk. If this response were to be plotted out by itself, it would be seen to be oscillatory in nature although of much smaller magnitude than the physical optics response. Figure 17 is a plot of the phase of the frequency response whereas Figure 16 is a plot of the magnitude of the frequency response. Figure 18

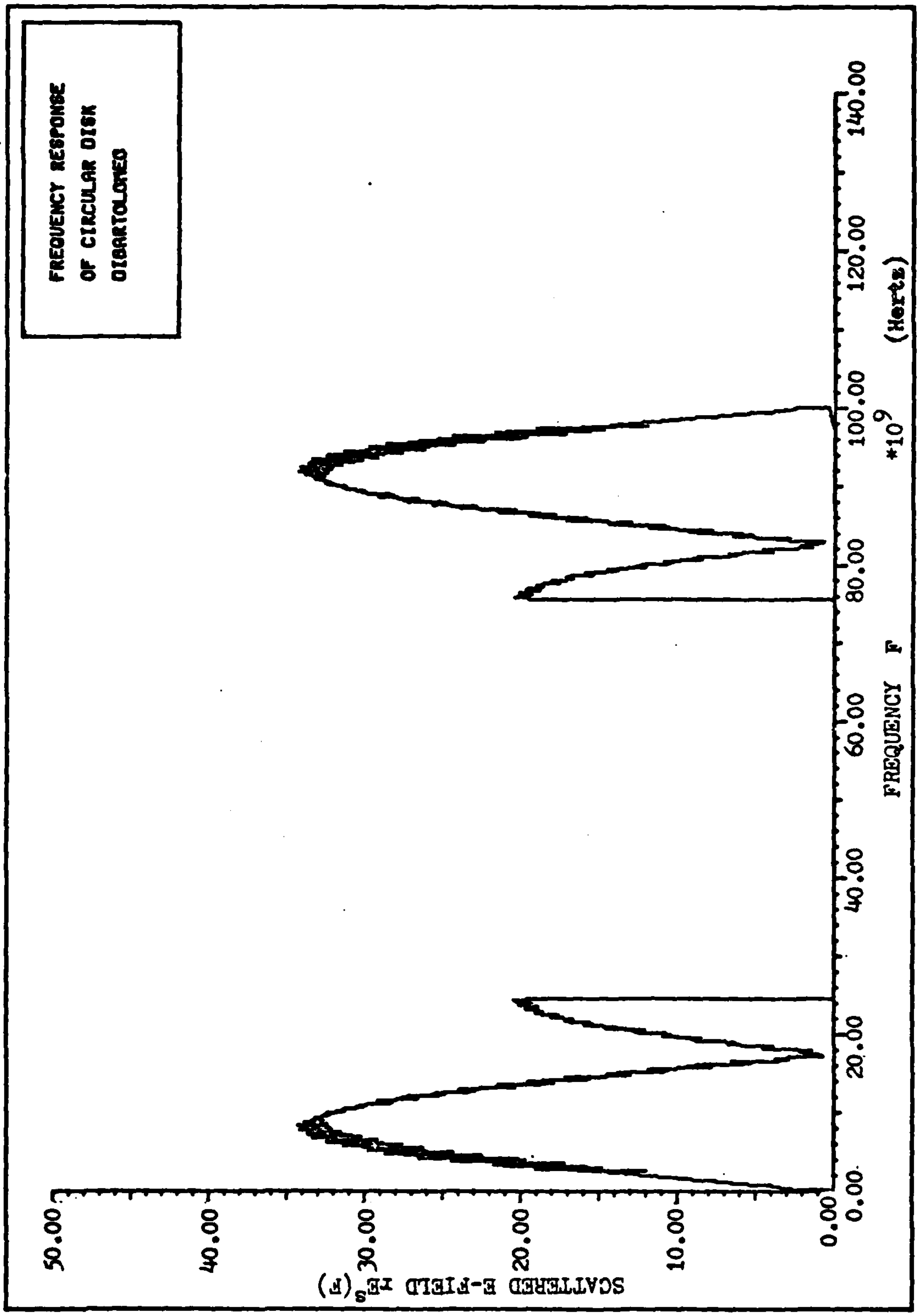

Figure 16. Frequency Response of the Scattering from the Circular Disk with θ_0=1°

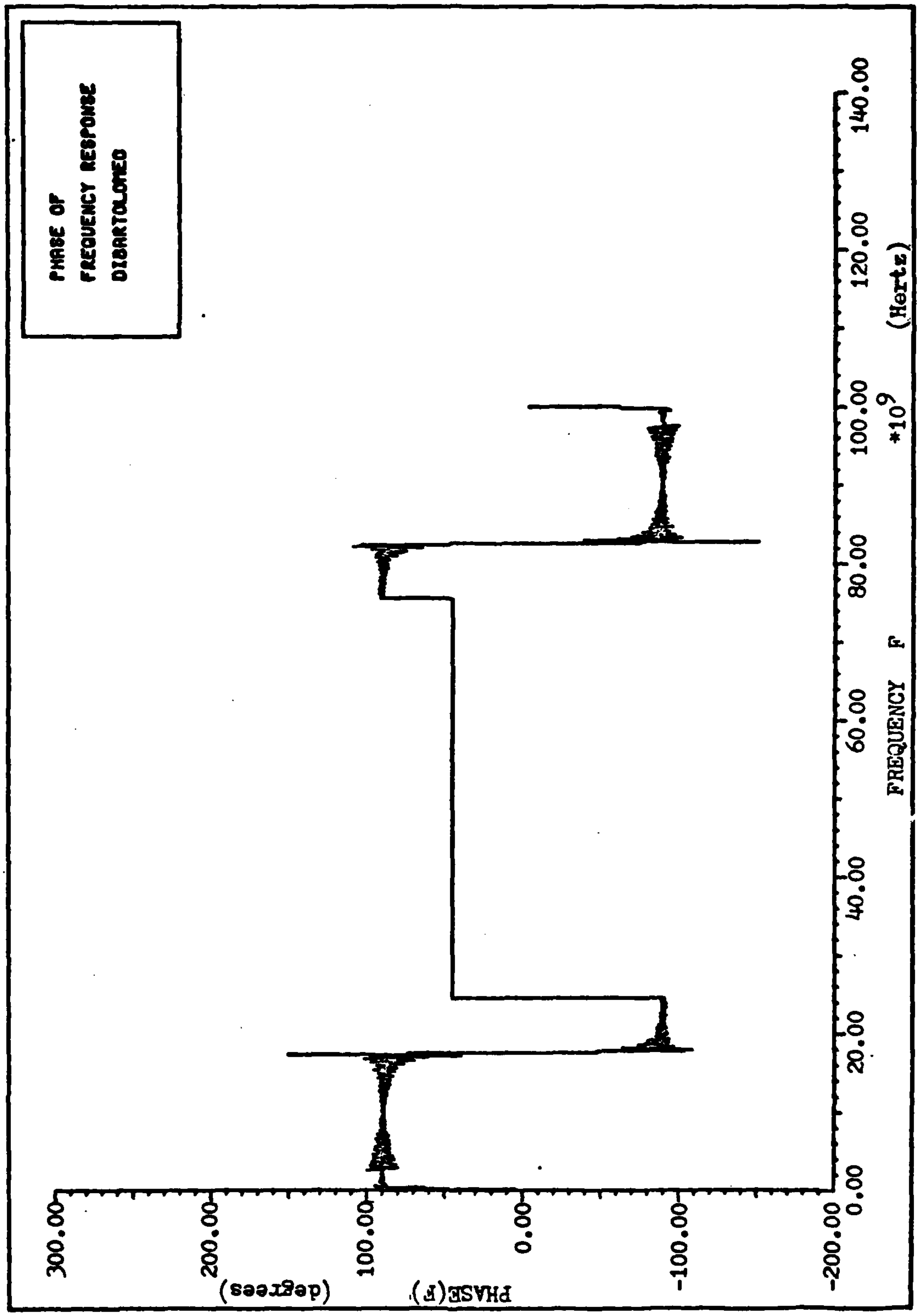

Figure 17. Phase of the Frequency Response of the Scattering from the Circular Disk with θ_0=1°

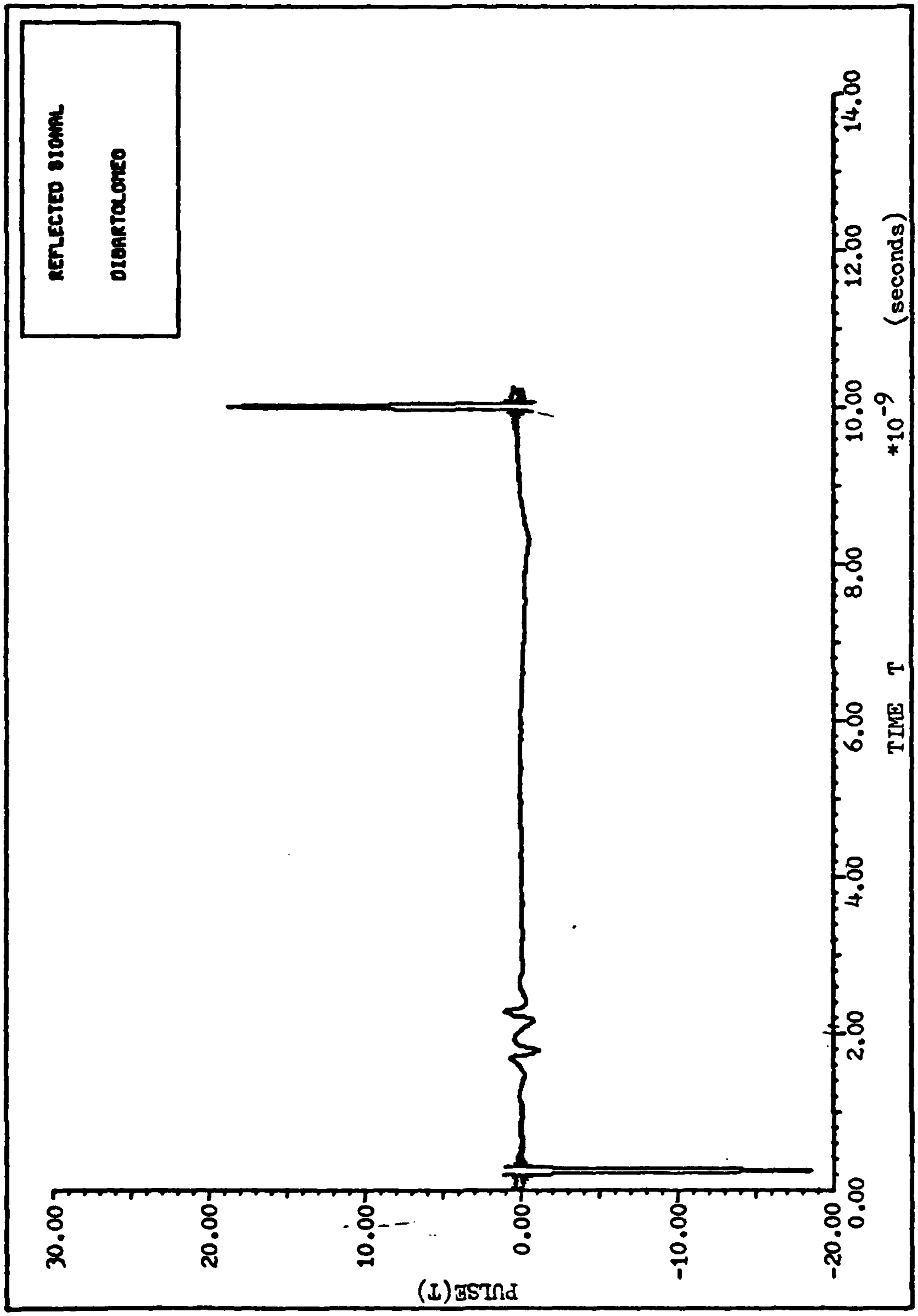

Figure 18. Reflected Signal from Circular Disk with Video Pulse Incident at 1°

is a plot of the backscattered signal at 1° off normal incidence when a video pulse 0.5 nsec wide with a pulse repetition frequency of 100MHz is incident. This "impulse response" is seen to have a doublet at the leading edge of the response. This contribution is due to a term proportional to ka in the scattered electric field and is predicted by both physical optics and the geometrical theory of diffraction (Ref 10:559). Although the response in Figure 18 is not truly the impulse response since the incident pulse is not an impulse but a video pulse of width 0.5 nsec, the response obtained closely resembles results obtained in the literature (Ref 10:p.559). The backscattered signals obtained when a pulse of five cycles of 10GHz R-F is incident at 1° is shown in Figure 19. The effect of the doublet is still seen as the phase of the signal immediately to the right of t=0 has a phase of 180° relative to the incident signal shown in Figure 6.

Backscattering from the Circular Disk from 71°, 72°, 73°, 74°, and 75° off Normal. As was stated in the Introduction, the specific problem studied in this thesis is how many distinct backscatter signature returns are obtained over a specified angle variation around the circular disk. The vehicle for accomplishing this was to find the angle for which the backscatter frequency response had the lowest minimum at 10GHz (remember the incident pulse is five cycles of 10GHz R-F). The angle is 73° and was obtained with the use of the combination program or 3rd program in Appendix B. The angle variation, mentioned above, was centered on 73°. This variation in angle was from 71° to 75° in one degree increments. The frequency responses

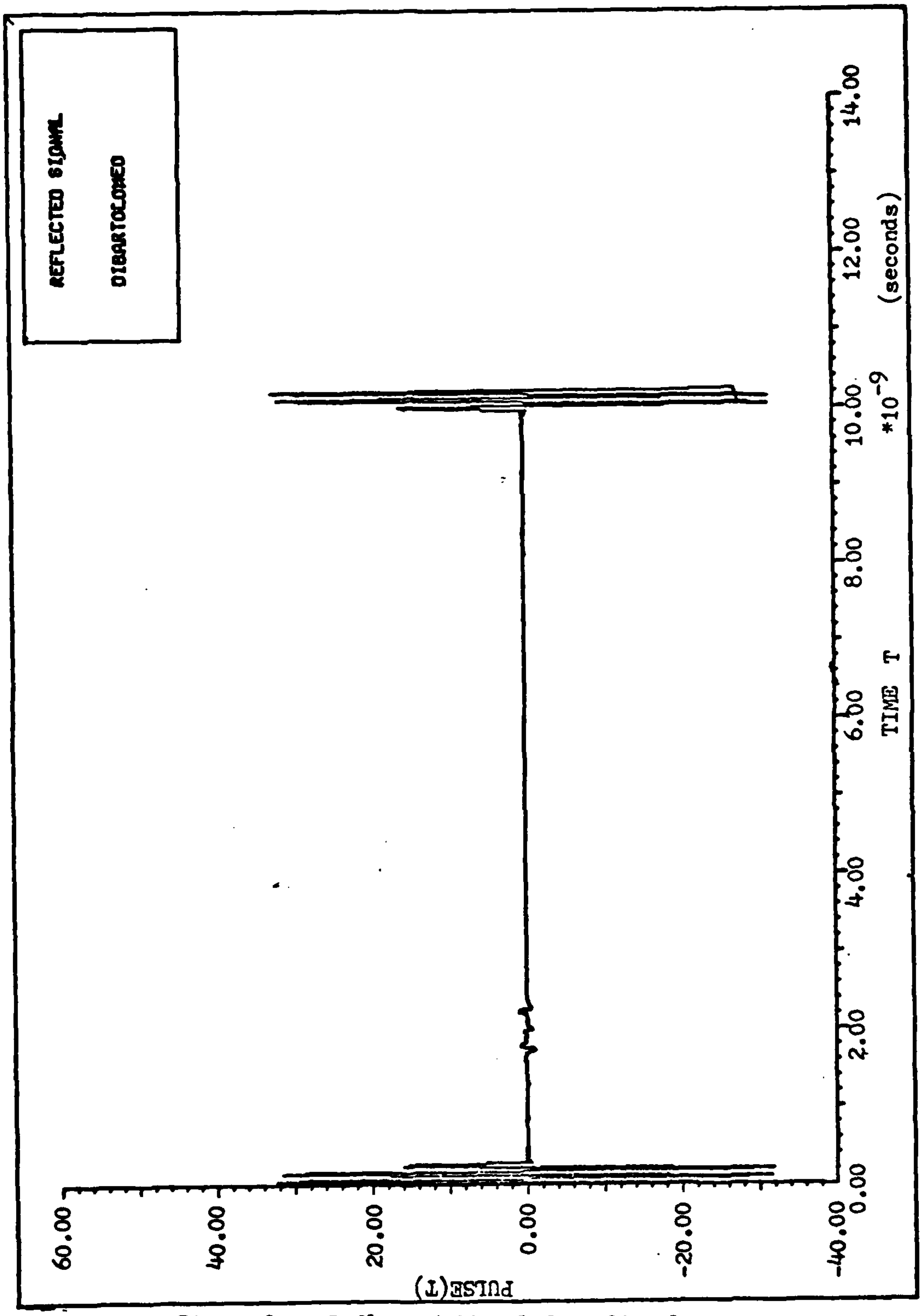

Figure 19. Reflected Signal from Circular Disk with R-F Pulse Incident at 1°

which correspond to the five angles are shown in Figures 20-24. The backscattered signals at these angles are shown in Figures 25-29. If more time were available, the backscattered signals would have been inputed to the signal processor outlined in Chapter II, but because of time constraints only the backscattered frequency responses and backscattered signals will be compared. Their similarities and dissimilarities will be pointed out as well as conclusions that can be dervied from the figures.

In Figure 20 is shown the frequency response of the backscattering when the incidence direction is 71° off normal. Note the minimum is at approximately 8GHz. As the angle is increased from 71° through 75°, this minimum will move to the right and would pass through 10GHz when the incident angle equals 73° to approximately 13GHz when the angle equals 75°.

If images were able to be made from the backscattered signals corresponding to angle variations around the five angles discussed, one of two things would be true. If the images were virtually the same, then only one of the images would be recorded. Thus, this would reduce the number of image plots to characterize the object. If the image plots were quite dissimilar, then all the image plots obtained would definitely be needed and the angle variations would further have to be subdivided to see if the image plots corresponding to the smaller angle variations were similar or not. This process is repeated until image plots which were virtually the same were obtained. At this point, only the previous image plots are retained for comparison to the image plot obtained from the unknown object.

In Figures 25 to 29 are shown the backscattered signals when the angle of incidence is 71°, 72°, 73°, 74° and 75° off normal, respectively. Notice that the backscattered signal when θ_0=73° is the smallest return out of the 5 returns. This makes sense since at 73° the frequency response of the backscattering has a minimum at 10GHz which is the frequency of the incident signal. As θ_0 is increased and decreased around 73° the backscattered signals are shown to increase in amplitude. This indicates that a valley in the frequency response has been passed through. At the right side of the curves shown in Figures 25-29 there is another response. This is conjectured to be the diffracted return with the dominant curve on the left being the specular return.

<u>Backscattering from the Circular Disk at 89° off normal</u>. In Figure 30 is shown the frequency response when θ_0=89°. This case is considered to illustrate what the return signal looks like at almost edge-on incidence.

In Figures 31 and 32 are shown the backscattered signals at θ_0=89° for the 10GHz R-F Pulse and video pulse. Note that the amplitudes of the returns are reduced from the amplitudes of the returns centered around θ_0=73° by 2 orders of magnitude. It can thus be concluded that the diffracted returns are always smaller than the physical optics returns. It is interesting to note the curve on the right side of Figure 32. This return quite possibly could be the pulse traversing the disk and being diffracted back. From

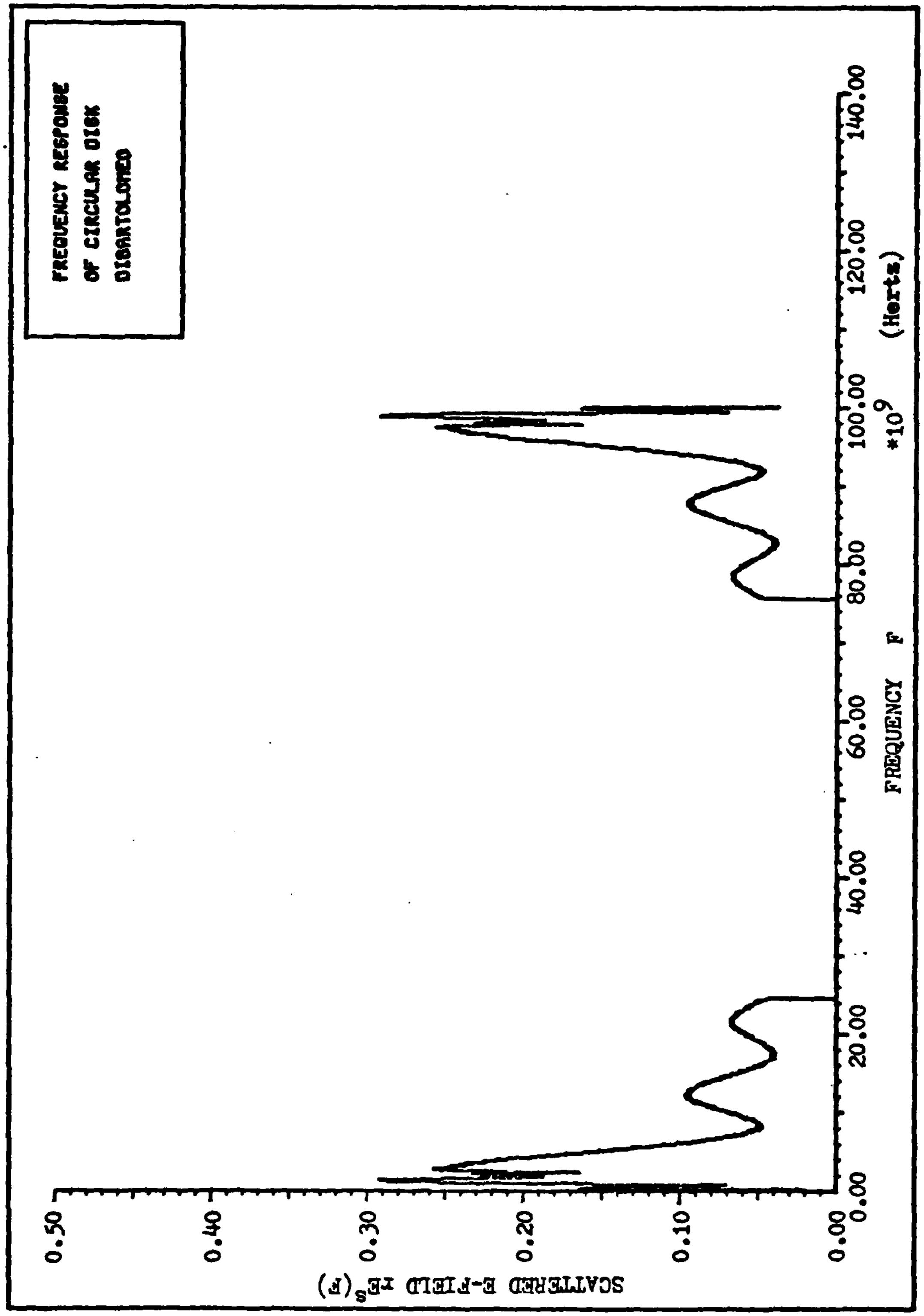

Figure 20. Frequency Response of the Scattering from the Circular Disk with θ_0=71°

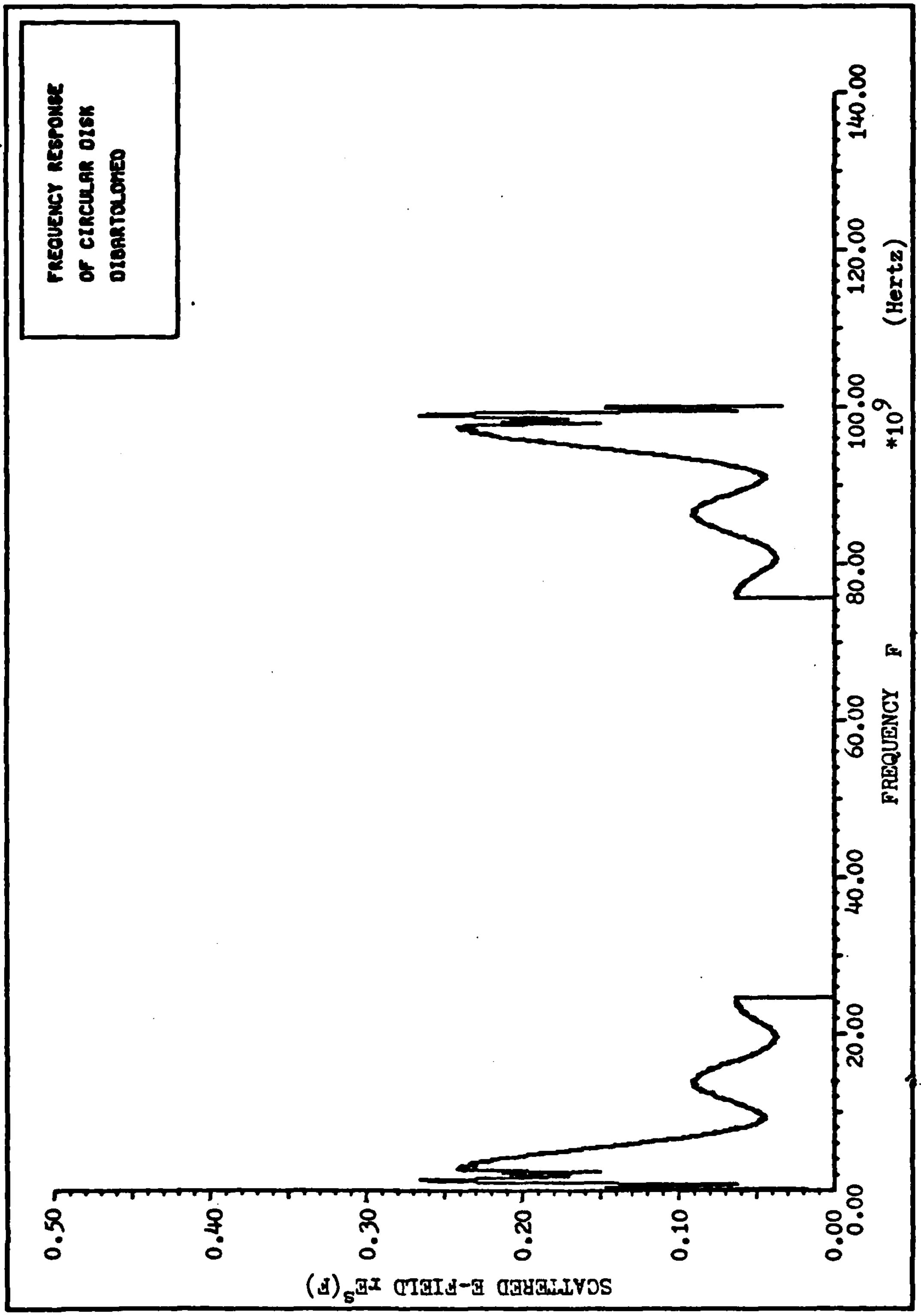

Figure 21. Frequency Response of the Scattering from the Circular Disk with θ_0=72°

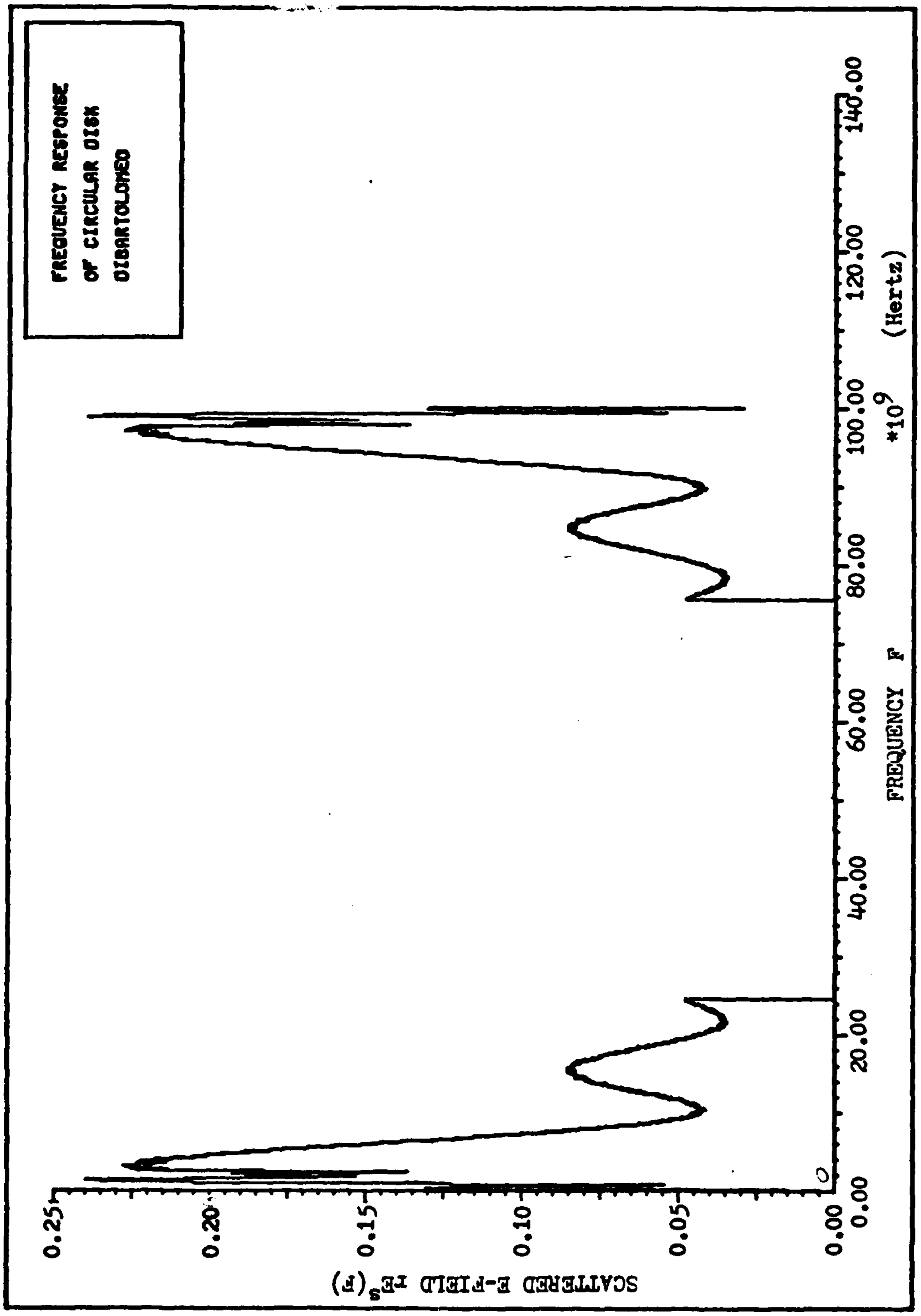

Figure 22. Frequency Response of the Scattering from the Circular Disk with θ_0=73°

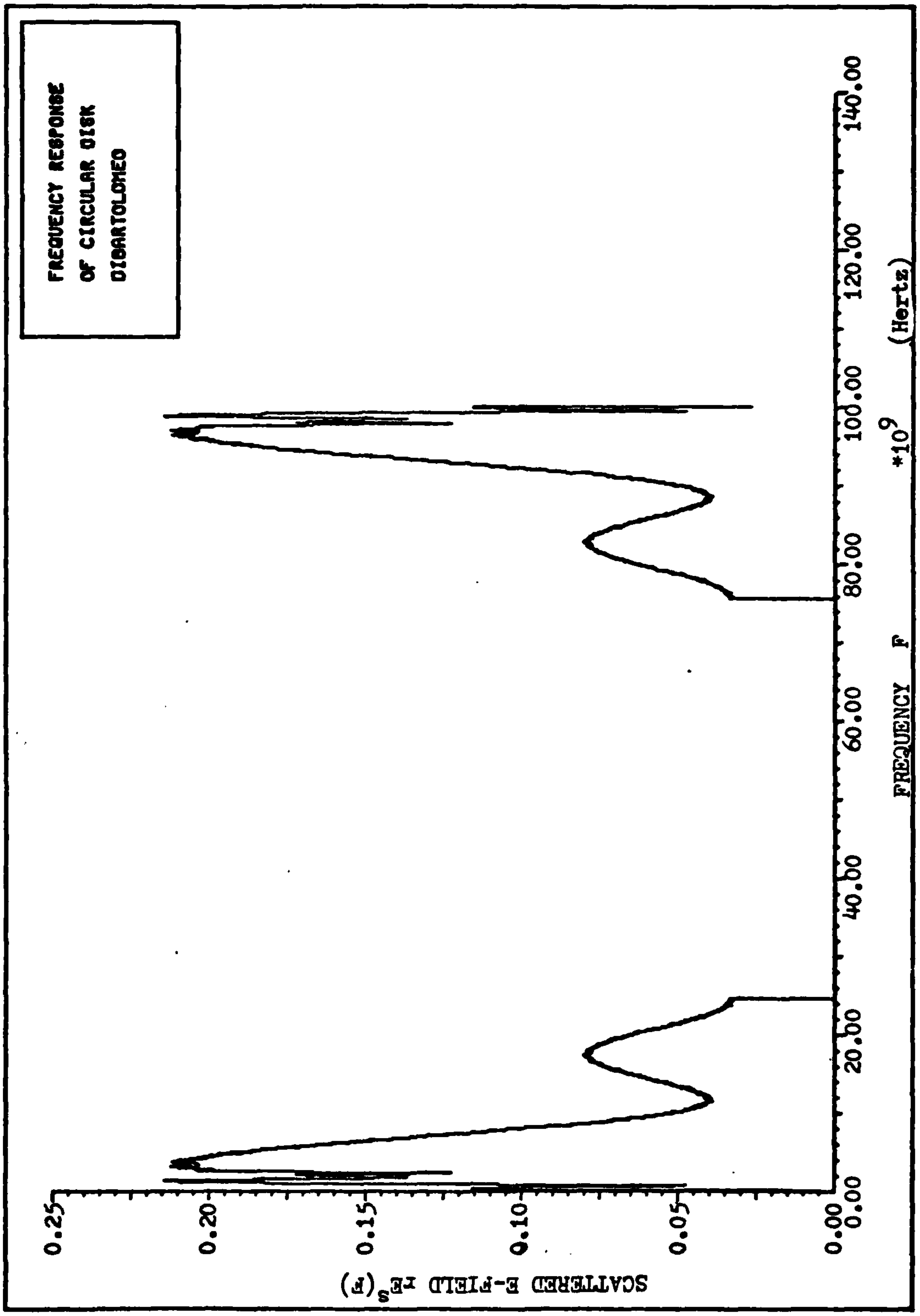

Figure 23. Frequency Response of the Scattering from the Circular Disk with θ_0=74°

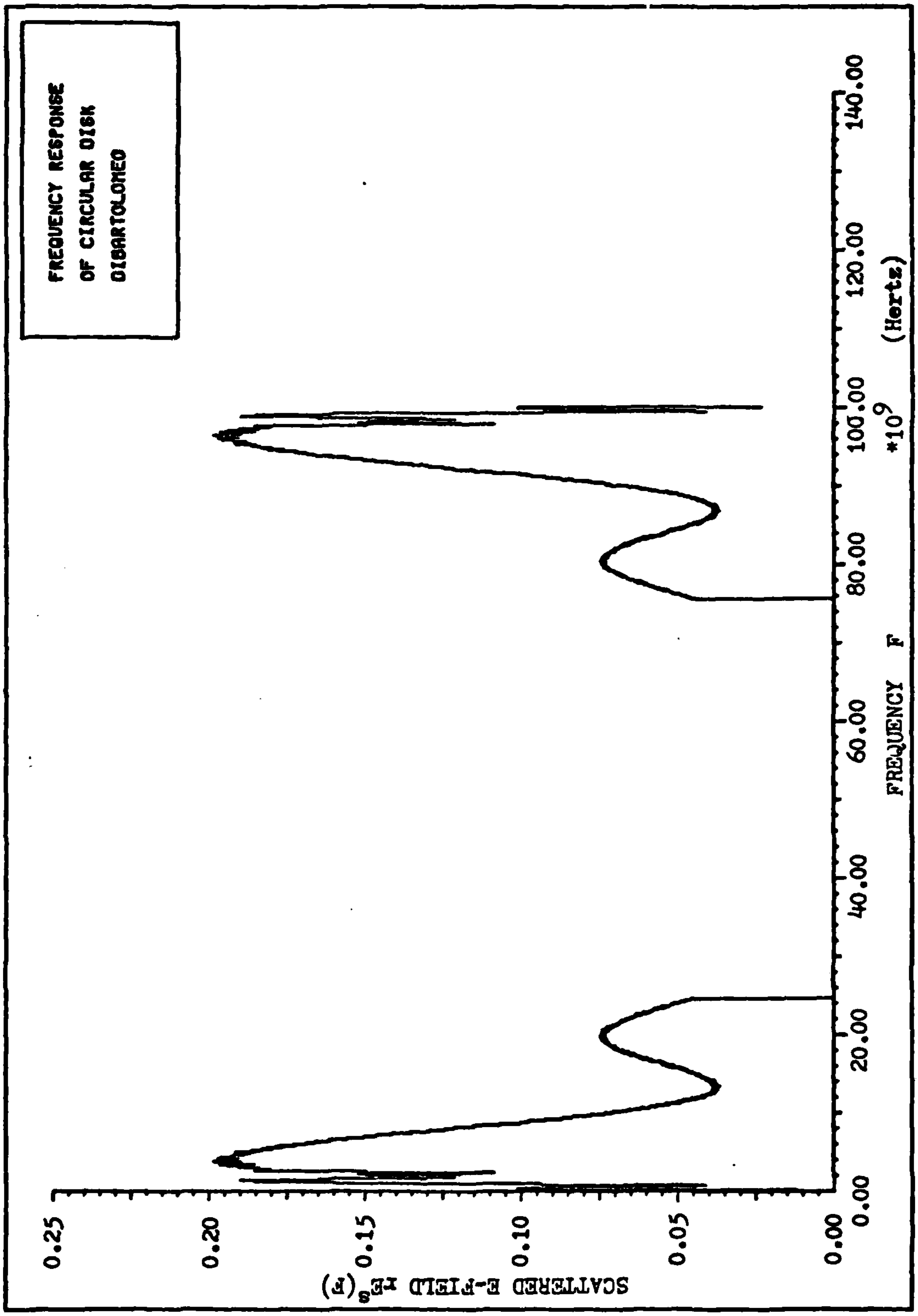

Figure 24. Frequency Response of the Scattering from the Circular Disk with θ_0=75°

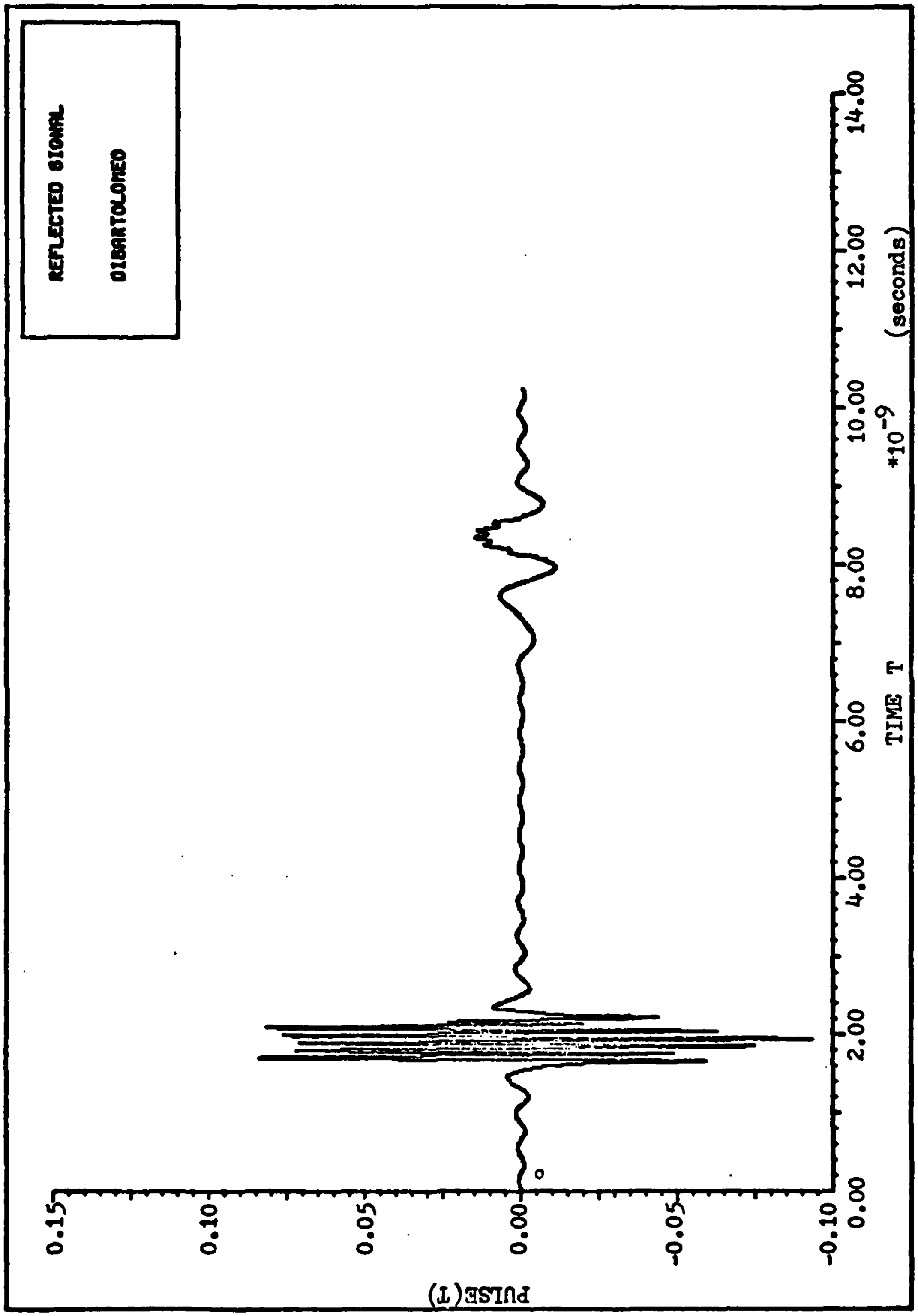

Figure 25. Reflected Signal from the Circular Disk with R-F Pulse Incident at 71°

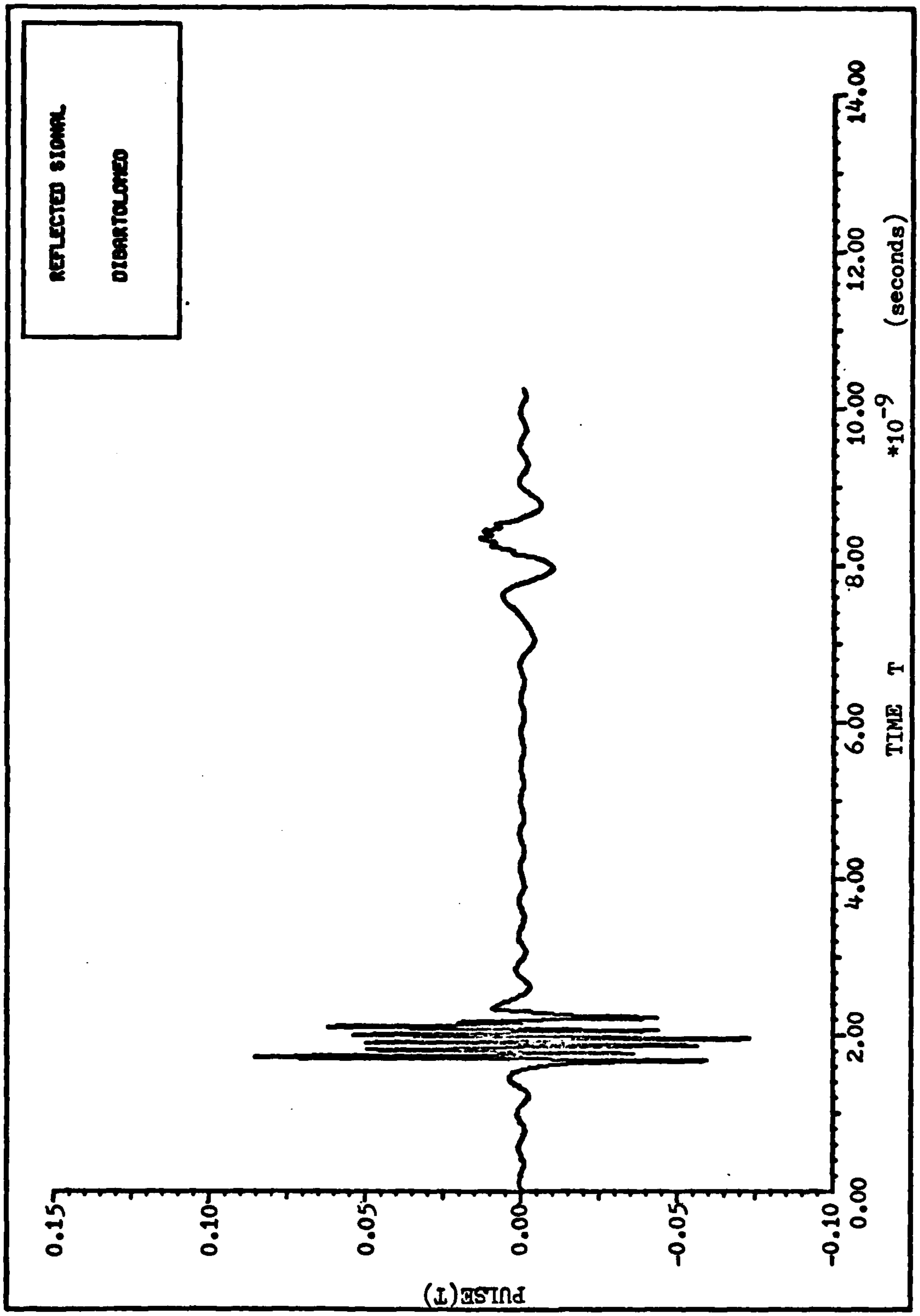

Figure 26. Reflected Signal from the Circular Disk with R-F Pulse Incident at 72°

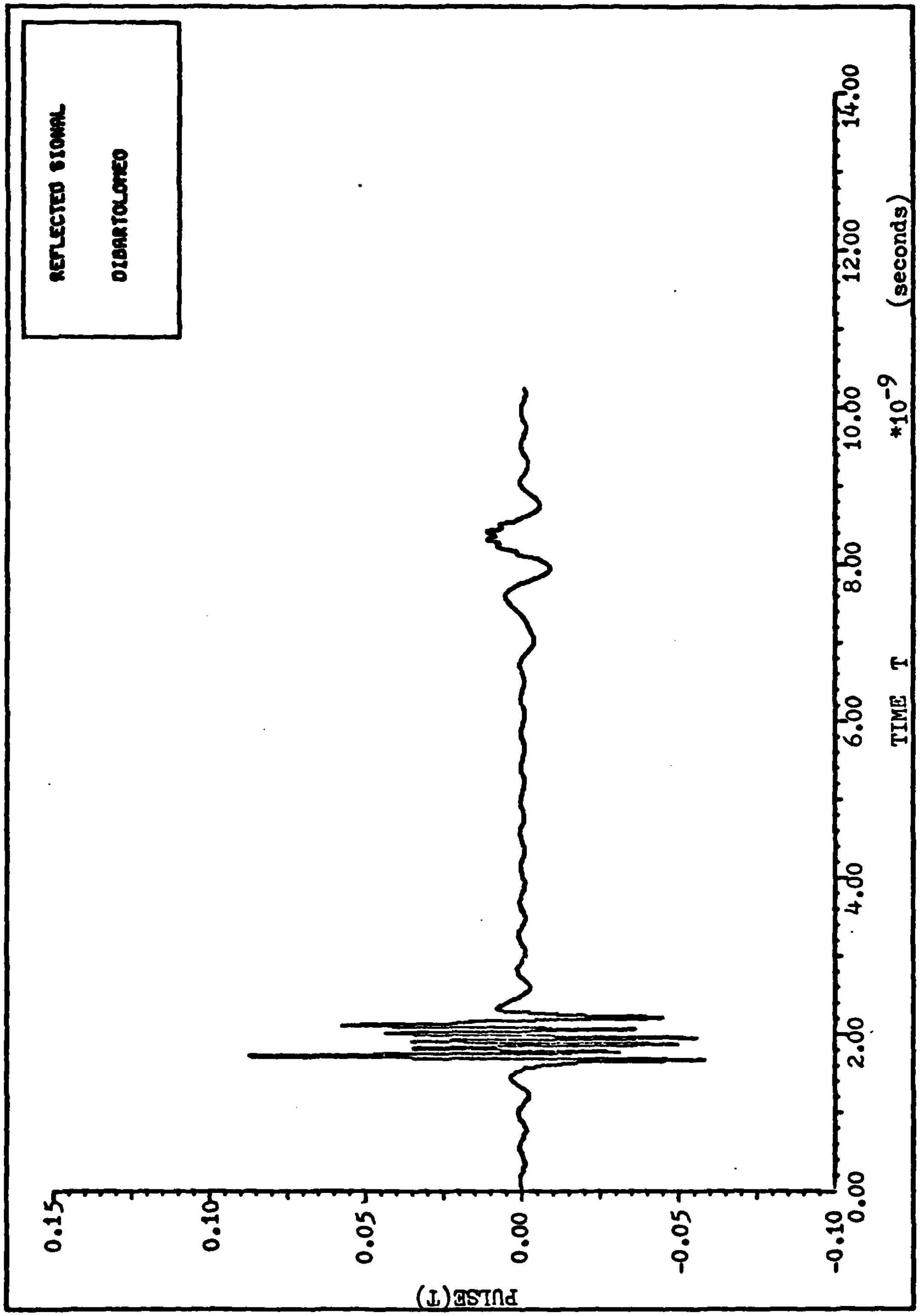

Figure 27. Reflected Signal from the Circular Disk with R-F Pulse Incident at 73°

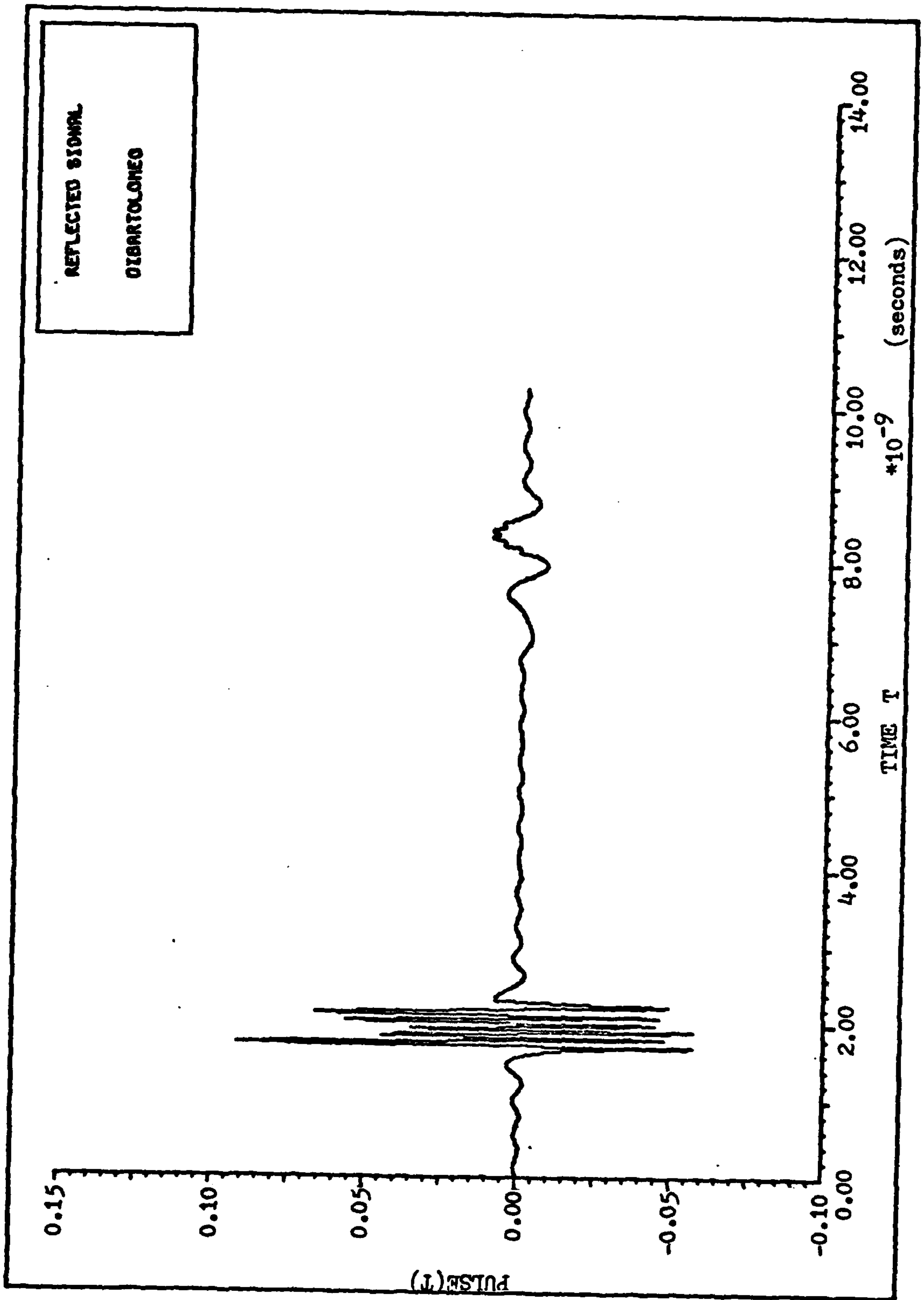

Figure 28. Reflected Signal from the Circular Disk with R-F Pulse Incident at 74°

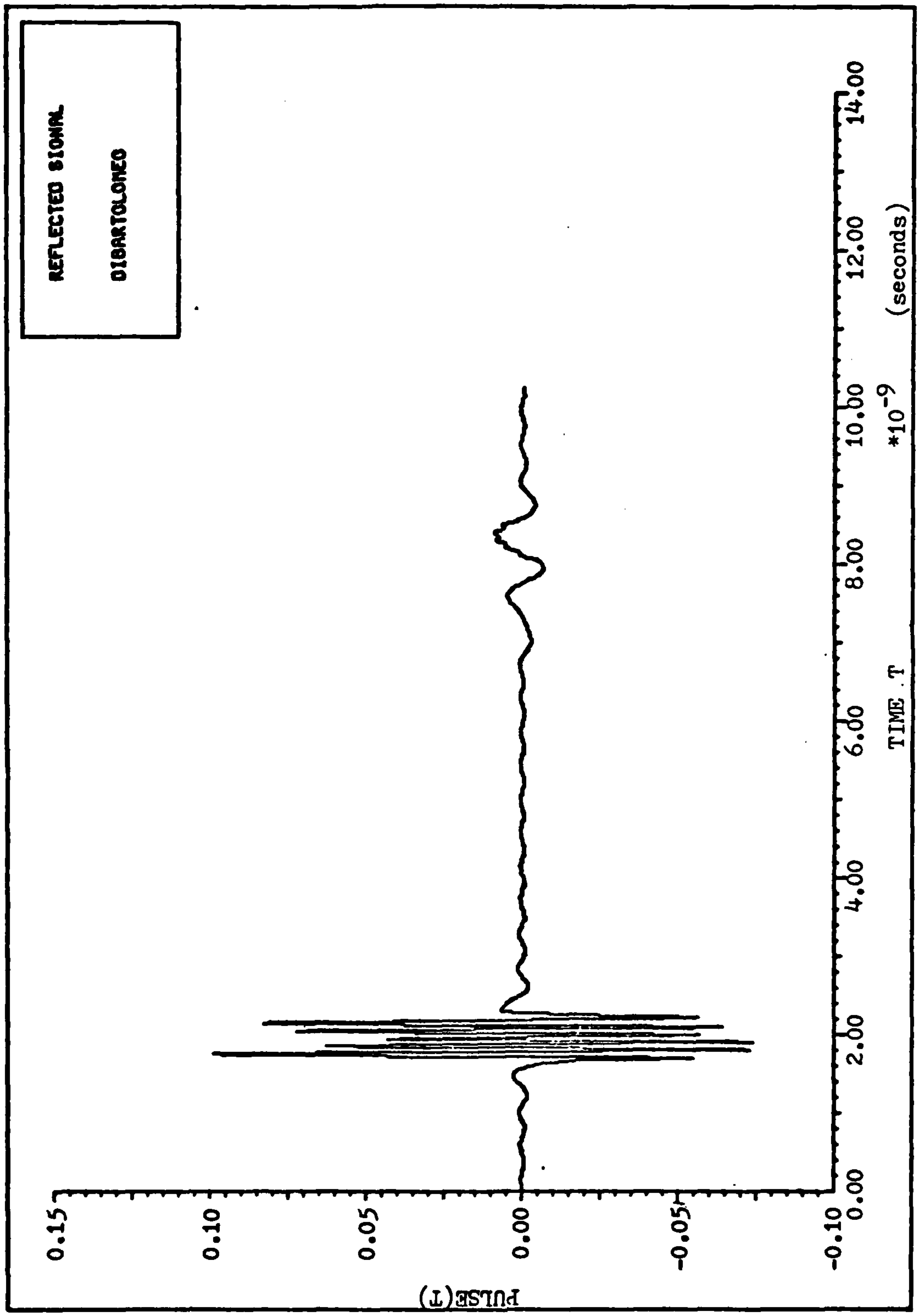

Figure 29. Reflected Signal from the Circular Disk with R-F Pulse Incident at 75°

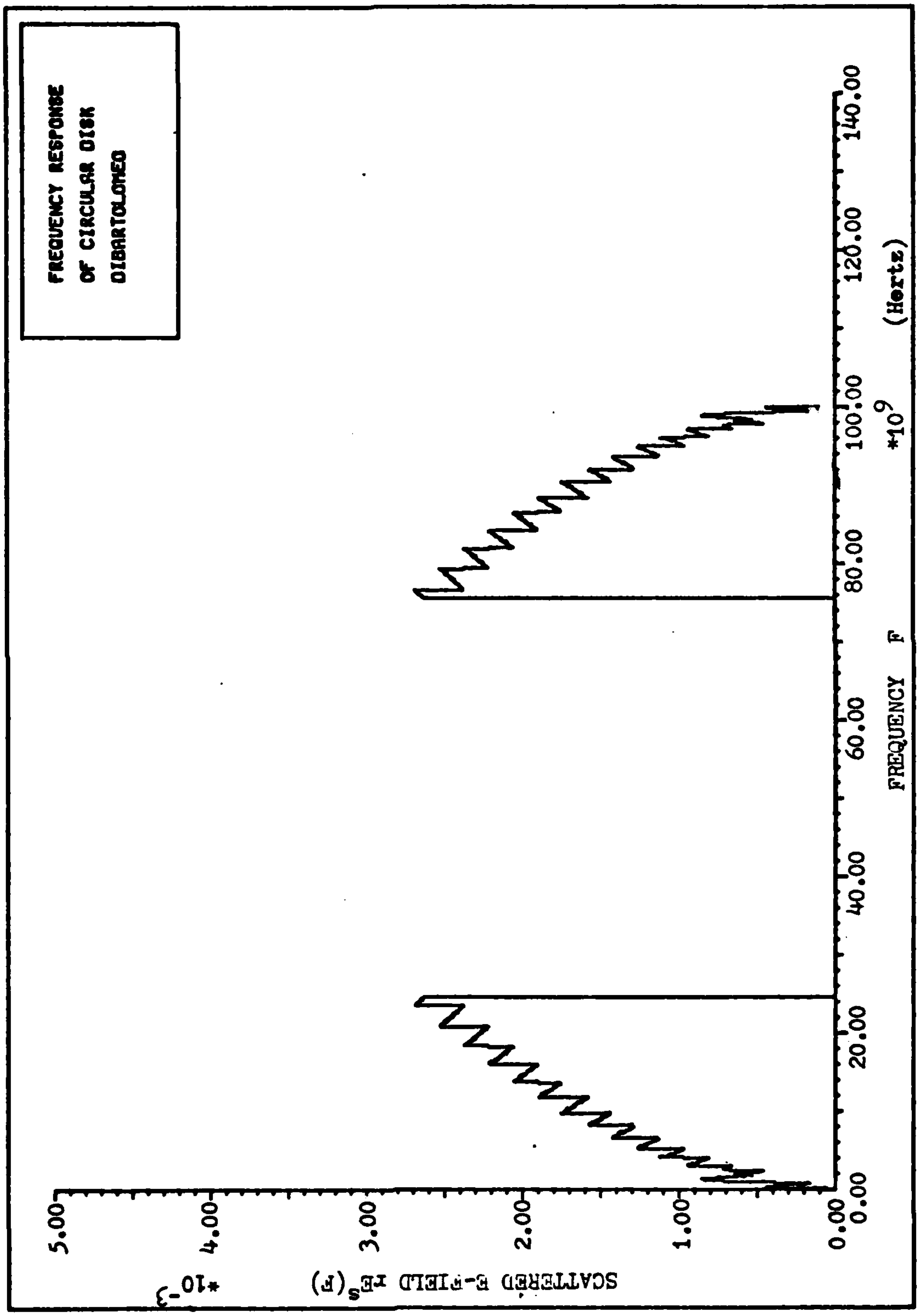

Figure 30. Frequency Response of the Scattering from the Circular Disk with θ_0=89°

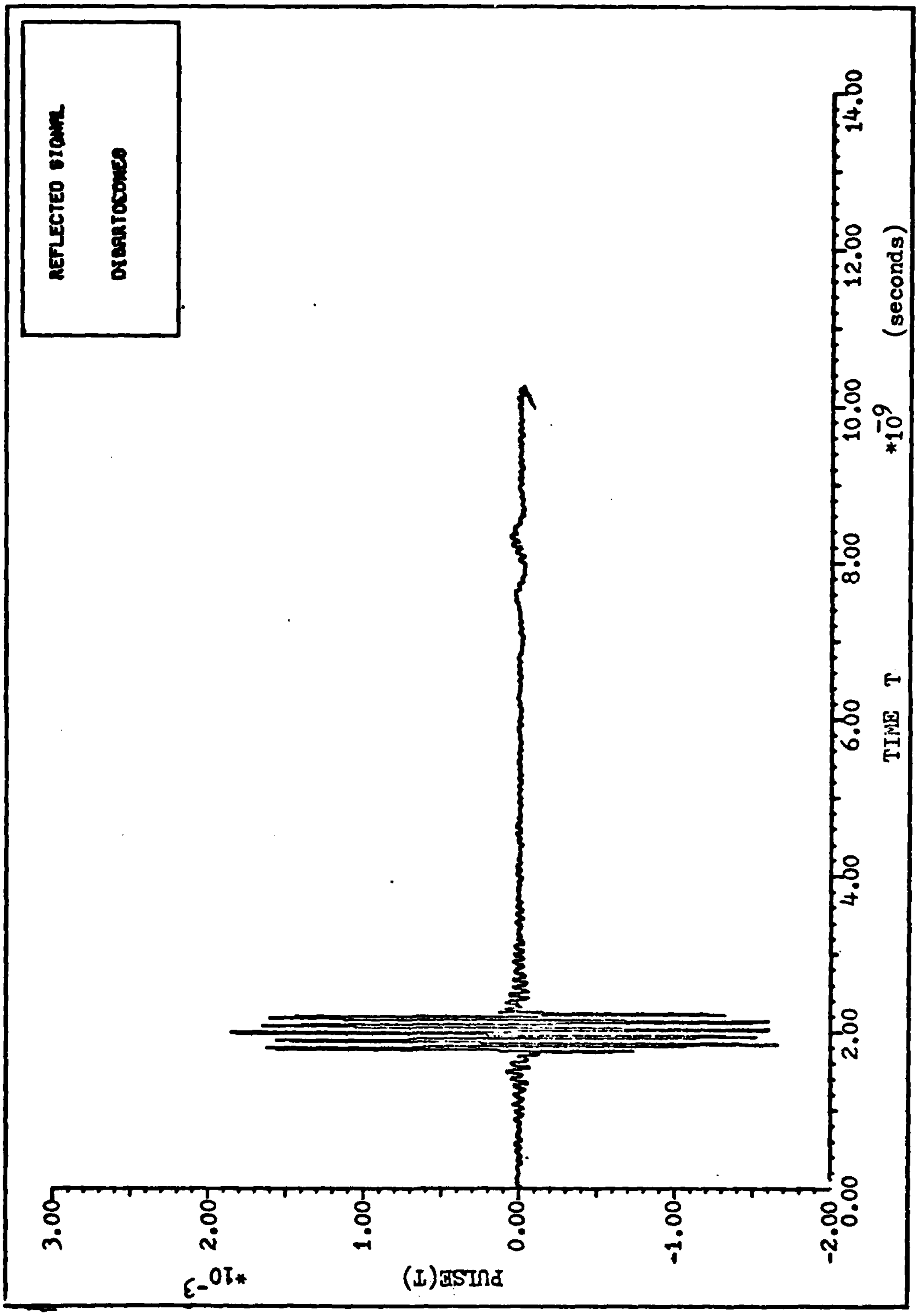

Figure 31. Reflected Signal from the Circular Disk with R-F Pulse Incident at 89°

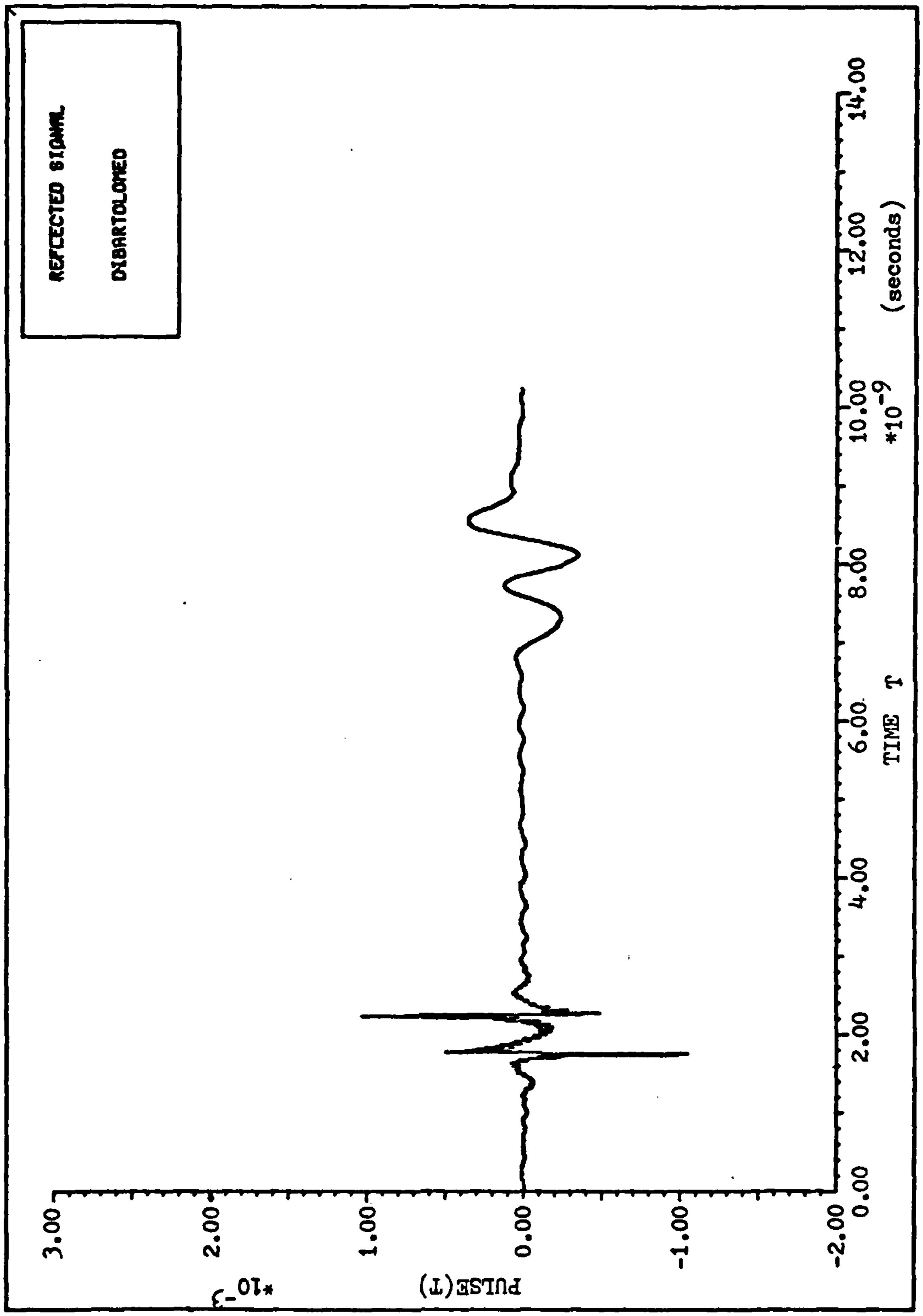

Figure 32. Reflected Signal from the Circular
Disk with Video Pulse Incident at 89°

Figure 32 it can be observed that the time delay between the beginning of the first return and the beginning of the second return is approximately 5.20 nsec. It can be calculated that the distance in space that corresponds to a time delay of 5.2 nsec is equal to approximately 1.56 m. This means that the incident pulse has to travel an additional 1.56 m to produce the second return than it had to travel to produce the first return. The first return in Figure 32 is considered the physical optics return from the edge of the disk. The second return in Figure 32 is conjectured to be the return caused by the incident pulse traversing the disk and then traveling half way around the disk to the point of incidence. With the radius of the disk equal to 0.30 m, the additional distance that the second return travels is approximately 1.54 m which provides a time delay of approximately 5.20 nsec which corresponds to the time delay between returns in Figure 32.

VI. Conclusions, Findings, and Recommendations

Conclusions

There are two major conclusions that can be derived from this thesis.

The first conclusion is that no cross-range information can be obtained from the perfectly-conducting sphere due to the aspect independent nature of the backscattered return. The second conclusion is that, with the 10GHz pluse incident, due to cross-range resolution constraints, only the specular scatterer and not both the specular and creeping wave scatterers will be detected on an image plot. Thus, the image plots obtained from the processing discussed in Chapter II would only show one scatterer and would not aid in the identification of the sphere.

Findings

The backscattered signals centered around $\theta_0 = 73°$ for the circular disk are quite similar. The above indicates that maybe the image plots that would be obtained from angle variations around 71°, 72°, 73°, 74° and 75° off normal, quite possibly could be quite similar. If this were the case, the five image plots could be replaced by one image plot. If such were not the case, then these five image plots would definitely be needed in the series of image plots used to characterize the circular disk.

Recommendations

It is recommended that the processor described in Chapter II be implemented and that the number of distinct image plots that are obtained for the circular disk be investigated. The effect of increasing or decreasing the frequency or, equally, decreasing or increasing the wavelength of the incident E-field, on the cross range resolution in reference to the disk should be investigated. In other words, are the diffraction returns off the edges of the circular disk attenuated as the frequency is increased and is Δx, as defined in Chapter II, too large to resolve the diffraction scatterers as the frequency is decreased.

Bibliography

1. Andrejewski, W. "Die Beugung Elektromagnetischer Wellen an der Leitenden Kreisscheibe und an der Kreisformigen Offnung in Leitenden Ebenen Schieum," Dissertation for Rheinich-Westfalichen Technischen Hochschule, Aachen, Germany, 1952.

2. Bennett, C. L., et al. "Space-Time Integral Equation Approach to the Large Body Scattering Problem," Sperry-Rand Research Center Technical Report SRRC-CR-73-1 (RADC-TR-73-70), Sudbury, Mass., May, 1973.

3. Brown, William M. and Leonard J. Porcello. "An Introduction to Synthetic Aperture Radar," IEEE Spectrun, 52-62, September, 1969.

4. Carl, Joseph W., Professor, Air Force Institute of Technology, Wright-Patterson Air Force Base, Ohio: Personal Communication, 1979.

5. Carswell, A. I. "Microwave Scattering Measurements in the Rayleigh Region Using a Focused Beam System," Canadian Journal of Physics 43: 1962 (1965).

6. Crispin, J. W. Jr. and K. M. Siegel. Methods of Radar Cross--Section Analysis. New York, N.Y.: Academic Press, 1968.

7. Golden, August Jr., Professor, Air Force Institute of Technology, Wright-Patterson Air Force Base, Ohio: Personal Communication, 1979.

8. Harger, Robert O. Synthetic Aperture Radar Systems-Theory and Design. New York, N.Y.: Academic Press, 1970.

9. Hodge, D. B. "The Calculation of Far Field Scattering by a Circular Metallic Disk," The Ohio State University-Electrosciences Laboratory, Technical Report 710816-2 on contract no. N00014-78-0049, February 1979.

10. Hodge, D.B. "Spectral and Transient Response of a Circular Disk to Plane Electromagnetic Waves," IEEE Transactions on Antennas and Propagation, 558-561, July 1971.

11. Jahnke, E. and F. Emde. Tables of Functions, Fourth Edition, New York, N.Y.: Dover Publications, 1945.

12. Keller, Joseph B. "Geometrical Theory of Diffraction," Journal of the Optical Society of America, 54: 116-130 (February 1962).

13. Oppenheim, Alan V. and Ronald W. Schafer. Digital Signal Processing, Englewood Cliff, N.J.: Prentice Hall Inc., 1975.

14. Ruck, George J., et al. Radar Cross-Section Hand-book, Vol. I and Vol. II, New York, N.Y.: Plenum Press, 1970.

15. Stanley, William D. Digital Signal Processing, Reston, Va.: Reston Publishing Co., Inc., 1975.

16. Ufimtsev, P. Ya. "Approximate Calculation of the Diffraction of Plane Waves by Certain Metal Objects," II, Zh. Tekh. 28: 2604, USSR (1958).

17. Ufimtsev, P. Ya. "Secondary Diffraction of Electromagnetic Waves by the Disk," Zh. Tekh. 28: 583, USSR (1958).

18. Wood, Richard J. Rome Air Development Center, Griffiss AFB, New York, Project Engineer and Thesis Sponsor. Personal communication, 1979.

Appendix A

Explanation and Program Listing for the Frequency Response of the Sphere

The following listing is the computer program that was used to generate Figures' 6, 7, 8, 9, 10, and 11. The program is a straightforward application of the equations for the different frequency regions as outlined in Chapter III. However, a few words will be stated to explain the plotting.

First of all, the plotting was done using a library which is unique to the computer system at the Air Force Institute of Technology. The library of subroutines used is called SAPL. The subroutine within SAPL used to do the plotting is called HGRAPH. As an example, generation of one of the graphs will be explained.

Figure 10 is a graph of the real part of the impulse response of the sphere. The computer program statements which generate this graph are statements 1140 to 1220 inclusive. The array IE which has 17 locations is used for labeling. IE(1) to IE(8) are used to label the upper righthand corner box. IE(9) and IE(10) are used to label the abscissa and IE(11) and IE(12) are used to label the ordinate. IE(13) to IE(17) are used to title the graph (NOTE: 10 hollerith characters fit in one array location). This title goes on the outside of the graph box along the ordinate coordinate. The CALL PLOT statements merely position the pen on the plotter. The CALL HGRAPH statement calls the correct subroutine for plotting. The argument list contains seven arguments. In the example, V is the array of x-axis values of dimension 1026. ROESR is the array of y-axis values of dimension 1026. Both arrays are two more locations than 1024 for internal scaling purposes. The "1024" is the number of points to be plotted. The IE is the labeling array. The "1" specifies internal scaling by the program. The first "0" means connect successive points by a straight line. And, finally, the second "0" means to draw dots at points as opposed to other symbols (i.e., triangles, circles, etc.).

The preceding is all that is needed to plot graphs using the HGRAPH subroutine in the SAPL library.

```
      PROGRAM IMAG512(INPUT,OUTPUT,PLOT)
      REAL C1,C2,E1,E2,F1,F2,G1,G2,H1,H2,I1,I2,J1,J2,K1,K2,
     $L1,L2,M1,M2,N1,N2,P1,P2,KA
      INTEGER Z
      COMPLEX C,E,F,G,H,I,J,K,L,M,N,P
     $,PULSE(1024),PULSER(1024),ROES(1024)
      DIMENSION X(1026),Y(1026),W(1026),V(1026),ID(17)
     $,IA(17),IB(17),IC(17),IE(17),ROESR(1026),ROESI(1026)
     $,IF(17)
C
C       FIX DIAMETER OF SPHERE,A, AND DISTANCE TO TARGET,RO.
C
      A=0.3
      RO=0.0
      B=0.45
C
C       COMPUTE WHAT THE SCATTERED FIELD, ROES, AS A FUNCTION
C       OF WAVE NUMBER, IS FOR THE LOW FREQUENCY REGION, THE
C       LOWER RESONANCE REGION, THE UPPER RESONANCE REGION,
C       AND THE HIGH FREQUENCY REGION.
C
      FREQ=97656000
      DO 10 Z=1,251
      KA=((0.3)*(2)*(3.14159)*FREQ*(Z-1))/(300000000)
      IF(KA.EQ.0)GO TO 55
      C1=0.0
      C2=(KA*RO)/(A)
      C=CMPLX(C1,C2)
      E1=(3./2.)*(KA**3.)*(1. - (5./54.)*(KA**2.)
     $ + (17./900.)*(KA**4.) - (6651923./11907000.)*(KA**6.))
      E2=(1./2.)*(KA**6.)*(1. + (6./5.)*(KA**2.))
      E=CMPLX(E1,E2)
      F1=1.0
      F2=1./(2.*KA)
      F=CMPLX(F1,F2)
      G1=0.0
      G2=-(2.*KA)
      G=CMPLX(G1,G2)
      H1=0.0
      H2=(3.141593)*(KA-(1./6.)-1.)
      H=CMPLX(H1,H2)
      I1=1.357588 + (0.741196)*(KA**(-2./3.))
      I2=(1.283788)*(KA**(-2./3.))
      I=CMPLX(I1,I2)
      J1=-(KA**(1./3.))*(2.200002) +
     $ (KA**(-1./3.))*(0.445396)
      J2=(KA**(1./3.))*(1.270172) +
     $ (KA**(-1./3.))*(0.257150)
      J=CMPLX(J1,J2)
      K1=0.695864 + (0.964654)*(KA**(-2./3.))
      K2=-(1.670829)*(KA**(-2./3.))
      K=CMPLX(K1,K2)
      L1=-(KA**(1./3.))*(7.014224) -
     $ (KA**(-1./3.))*(0.444477)
      L2=(KA**(1./3.))*(4.049663) -
     $ (KA**(-1./3.))*(0.256619)
```

```
      L=CMPLX(L1,L2)
      M1=0.807104 + (0.798821)*(KA**(-2./3.))
      M2=(1.383598)*(KA**(-2./3.))
      M=CMPLX(M1,M2)
      N1=-(KA**(1./3.))*(5.048956) -
     $ (KA**(-1./3.))*(0.312321)
      N2=(KA**(1./3.))*(2.915016) -
     $ (KA**(-1./3.))*(0.180319)
      N=CMPLX(N1,N2)
      P1=0.0
      P2=((KA*RO)/(A)) - (2.)*(KA)
      P=CMPLX(P1,P2)
      IF(KA.LE.0.4)GO TO 20
      IF(KA.GT.20.0)GO TO 50
      IF(KA.LE.0.8)GO TO 30
      IF(KA.GE.0.9)GO TO 40
20     ROES(Z)=(B/KA)*(KA**3.)*(CEXP(C))
      GO TO 10
30     ROES(Z)=(((2./3.)*B)/(KA))*(CEXP(C))*(E)
      GO TO 10
40     ROES(Z)=((((2./3.)*B)/(KA))*(CEXP(C)))*
     $ (-(KA/2.)*(CEXP(G))*F + (KA**(4./3.))*
     $ (CEXP(H))*(I)*(CEXP(J)) + (K)*(CEXP(L)) -
     $ (M)*(CEXP(N)))
      GO TO 10
50     ROES(Z)=(-B/3.)*(CEXP(P))
      GO TO 10
55    ROES(Z)=(0.,0.)
10     CONTINUE
      DO 60 Z=1,251
      A=REAL(ROES(Z))
      B=AIMAG(ROES(Z))
      ROES(Z)=CMPLX(A,-B)
      X(Z)=REAL(ROES(Z))
      Y(Z)=AIMAG(ROES(Z))
60    W(Z)=((((X(Z))**2.)+((Y(Z))**2.)))**(1./2.)
      DO 65 Z=252,774
      ROES(Z)=(0.,0.)
65    W(Z)=0.0
      DO 68 Z=1,250
      ROES(1025-Z)=CMPLX(X(Z+1),-(Y(Z+1)))
68    CONTINUE
      CALL FFT(ROES,10,-1.)
       DO 1 Z=1,1024
       ROESR(Z)=REAL(ROES(Z))
       ROESI(Z)=AIMAG(ROES(Z))
       V(Z)=(Z-1.)/(10**11.)
1      CONTINUE
       DATA IE(1)/20H REAL PART OF        /
      DATA IE(3)/20H IMPULSE RESPONSE    /
      DATA IE(5)/20H OF SPHERE           /
      DATA IE(7)/20H DIBARTOLOMEO        /
      DATA IE(9)/20H          T          /
      DATA IE(11)/20H  IMPULSE RESPONSE  /
      DATA IE(13)/50H
/
```

```
      CALL PLOT(0.,-4.,-3.) $ CALL PLOT(0.,.03,-3.)
      CALL HGRAPH(V,ROESR,1024,IE,1,0,0)
      DATA IF(1)/20H IMAGINARY PART OF   /
      DATA IF(3)/20H IMPULSE RESPONSE    /
      DATA IF(5)/20H OF SPHERE           /
      DATA IF(7)/20H DIBARTOLOMEO        /
      DATA IF(9)/20H               T     /
      DATA IF(11)/20H  IMPULSE RESPONSE  /
      DATA IF(13)/50H
     /
      CALL PLOT(0.,-4.,-3.) $ CALL PLOT(0.,.03,-3.)
      CALL HGRAPH(V,ROESI,1024,IF,1,0,0)
      CALL FFT(ROES,10,1.)
      DO 69 Z=775,1024
      X(Z)=REAL(ROES(Z))
      Y(Z)=AIMAG(ROES(Z))
      W(Z)=((((X(Z))**2.)+((Y(Z))**2.)))**(1./2.)
69    CONTINUE
      DO 70 Z=1,20
      PRINT*,X(Z),Y(Z),W(Z)
70    CONTINUE
      DO 80 Z=1,1024
      V(Z)=FREQ*Z
80    CONTINUE
      DATA ID(1)/20H FREQUENCY RESPONSE /
      DATA ID(3)/20H OF SPHERE          /
      DATA ID(5)/20H DIBARTOLOMEO       /
      DATA ID(7)/20H                    /
      DATA ID(9)/20H              F     /
      DATA ID(11)/20H       ROES(F)       /
      DATA ID(13)/50H            FREQUENCY RESPONSE OF SPHERE
     /
      CALL PLOT(0.,-4.,-3.) $ CALL PLOT(0.,.03,-3.)
      CALL HGRAPH(V,W,1024,ID,1,0,0)
      DO 90 Z=1,25
      X=(Z+25)/(10**11.)
      PULSE1=SIN(2*3.14159*(10**10.)*X)
      PULSE2=0.0
      PULSE(Z)=CMPLX(PULSE1,PULSE2)
90    CONTINUE
      DO 100 Z=26,999
      PULSE1=0.0
      PULSE2=0.0
      PULSE(Z)=CMPLX(PULSE1,PULSE2)
100   CONTINUE
      DO 105 Z=1000,1024
      X=(Z-999)/(10**11.)
      PULSE1=SIN(2*3.14159*(10**10.)*X)
      PULSE2=0.0
      PULSE(Z)=CMPLX(PULSE1,PULSE2)
105   CONTINUE
      DO 110 Z=1,1024
      X(Z)=REAL(PULSE(Z))
      V(Z)=(Z-1.)/(10**11.)
110   CONTINUE
      DATA IA(1)/20H INCIDENT           /
      DATA IA(3)/20H PULSE              /
```

```
      DATA IA(5)/20H DIBARTOLOMED       /
      DATA IA(7)/20H                    /
      DATA IA(9)/20H          T         /
      DATA IA(11)/20H      PULSE(T)      /
      DATA IA(13)/50H           INCIDENT PULSE OF RF AT 10 GHZ
     /
      CALL PLOT(0.,-4.,-3.) $ CALL PLOT(0.,.03,-3.)
      CALL HGRAPH(V,X,1024,IA,1,0,0)
      CALL PLOT(0.,-4.,-3.) $ CALL PLOT(0.,.03,-3.)
      CALL HGRAPH(V,X,200,IA,1,0,0)
      CALL FFT(PULSE,10,1.)
      DO 120 Z=1,1024
      X(Z)=REAL(PULSE(Z))
      Y(Z)=AIMAG(PULSE(Z))
      W(Z)=(((X(Z))**2.)+((Y(Z))**2.)))**(1./2.)
  120 V(Z)=FREQ*Z
      DATA IB(1)/20H TRANSFORM OF       /
      DATA IB(3)/20H PULSE              /
      DATA IB(5)/20H DIBARTOLOMED       /
      DATA IB(7)/20H                    /
      DATA IB(9)/20H          F         /
      DATA IB(11)/20H     PULSE(F)       /
      DATA IB(13)/50H                FOURIER TRANSFORM OF PULSE
     /
      CALL PLOT(0.,-4.,-3.) $ CALL PLOT(0.,.03,-3.)
      CALL HGRAPH(V,W,200,IB,1,0,0)
      DO 140 Z=1,1024
      PULSER(Z)=(ROES(Z))*(PULSE(Z))
  140 CONTINUE
      CALL FFT(PULSER,10,-1.)
      DO 150 Z=1,1024
      X(Z)=REAL(PULSER(Z))
      Y(Z)=AIMAG(PULSER(Z))
      W(Z)=(((X(Z))**2.)+((Y(Z))**2.)))**(1./2.)
      V(Z)=(Z-1.)/(10**11.)
  150 CONTINUE
      DATA IC(1)/20H REFLECTED          /
      DATA IC(3)/20H SIGNAL             /
      DATA IC(5)/20H DIBARTOLOMED       /
      DATA IC(7)/20H                    /
      DATA IC(9)/20H          T         /
      DATA IC(11)/20H      PULSER(T)     /
      DATA IC(13)/50H                    REFLECTED PULSE OF RF
     /
      CALL PLOT(0.,-4.,-3.) $ CALL PLOT(0.,.03,-3.)
      CALL HGRAPH(V,X,1024,IC,1,0,0)
      CALL PLOT(0.,-4.,-3.) $ CALL PLOT(0.,.03,-3.)
      CALL HGRAPH(V,Y,1024,IC,1,0,0)
      CALL FFT(PULSE,10,-1.)
      DO 160 Z=1,1024
      X(Z)=REAL(PULSE(Z))
  160 V(Z)=(Z-1)/(10**11.)
      CALL PLOT(0.,-4.,-3.) $ CALL PLOT(0.,.03,-3.)
      CALL HGRAPH(V,X,1024,IA,1,0,0)
      CALL PLOTE(M)
      STOP
      END
      SUBROUTINE FFT(X,M,XI)
```

```
      COMPLEX X(1),U,W,T
      N=2**M
      NV2=N/2
      NM1=N-1
      J=1
      DO 7 I=1,NM1
      IF(I.GE.J) GO TO 5
      T=X(J)
      X(J)=X(I)
      X(I)=T
5     K=NV2
6     IF(K.GE.J) GO TO 7
      J=J-K
      K=K/2
      GO TO 6
7     J=J+K
      PI=3.14159265358979
      DO 20 L=1,M
      LE=2**L
      LE1=LE/2
      U=(1.0,0.0)
      W=CEXP(CMPLX(0.,-XI*PI/LE1))
      DO 20 J=1,LE1
      DO 10 I=J,N,LE
      IP=I+LE1
      T=X(IP)*U
      X(IP)=X(I)-T
10    X(I)=X(I)+T
20    U=U*W
      IF(XI.GT.0.) RETURN
      DO 30 I=1,N
30    X(I)=X(I)/N
      RETURN
      END
```

Appendix B

Explanation and Program Listings for the Frequency Response of the Far Field Scattering of the Perfectly-Conducting Infinitely-Thin, Circular Disk

The first computer program shown on the following pages calculates the far field radar cross section and associated E-field for the infinitely thin circular disk (Ref 9). A sample of the program I/O is shown after the program listing. The user need only input eight variables for the initial case to be executed. They are:

1. KA = electrical radius of the disk = $(2\pi/\lambda)a$.
2. THETA INCIDENT = θ_0 (degrees)
3. POLARIZATION = α (degrees)
4. THETA SCATTERED = θ_s (degrees)
5. PHI SCATTERED = ϕ_s (degrees)

WHICH VARIABLE IS TO BE INCREMENTED? :

if 1 through 5: the variable associated with that index above will be incremented

if 1 through 5: then only the initial case will be calculated. In this event, the remaining parameters are not requested.

TYPE NUMBER OF CASES: enter the total number of computations to be performed.

WHAT IS THE INCREMENT?: enter the increment by which the variable selected should be increased after each execution.

All inputs may be made in free format. The program labels the first column with the name of the variable to be incremented. The second and third columns contain the cross sections associated with the θ and ϕ components of the scattered field. The last four columns list the magnitudes and phases (in degrees) of both the θ and ϕ components of the normalized scattered electric field.

On completion of the cases desired, the program will ask for a new KA and proceed as before. If a 0 is entered, the program will terminate. If a -1 is entered, a brief statement of the problem geometry will be given. Following this statement, the program will ask for a new value of KA.

The program works fine up to KA=15. For KA>15, a high frequency approximation is used as is outlined in Chapter IV. The program to implement the high frequency approximation is called SCATTER and follows the I/O of the first program. The output for $\theta_0=45°$ follows SCATTER's program listing. It is important to note that in relation to the input parameters of the first program, SCATTER is restrictive in the sense that it returns only the theta components of cross section and E-field and assumes the phi components of cross section and E-field are zero ($\alpha=0$). Also the incident angle is equal to the scattered angle (backscattering) and is restricted between 0° and 90°. It is also restrictive because it will only increment KA.

Although the first program's output and the output from SCATTER have values for the cross section and E-field from KA=1-25, the first program is invalid for KA>15 and SCATTER is invalid for the lower values of KA. What is needed is a program that combines the two. This combination program follows the output from SCATTER. The output from the combination program follows its listing. Note that for KA$\leq$15, it uses values from the first program and for KA>15, it uses values from SCATTER.

In the SCATTER program, the Fresnel Integrals were calculated using the trapezoidal rule for approximation. The values obtained from the FRESNEL subroutine agree with the literature out to three decimal places (Ref 11:34).

```
      PROGRAM DISK24(INPUT,OUTPUT,TAPE5=INPUT,TAPE6=OUTPUT)
C     FAR FIELD SCATTERING BY A CIRCULAR METALLIC DISK
      DIMENSION LABEL(5),VAR(5)
      COMPLEX F4,PSI,W,YO,YETAO,U,X,Z,ZA,ZB,ZC,ZD
     1,IX,EPAPT,EPARP,EPERT,EPERP,ESNT,ESNP
      COMMON EIG(50),D(50,50),DNEG(50),R1(50),F4(50)
     1,SO(50),P(50),SETA(50),SETAO(50),PSI(50),W(50),YO(50)
     1,YETAO(50),U(50),X(50),CMPHI(50),SMPHI(50)
      DATA LABEL(1)/10H    KA    /
      DATA LABEL(2)/10H THETA I  /
      DATA LABEL(3)/10H   POL    /
      DATA LABEL(4)/10H THETA S  /
      DATA LABEL(5)/10H  PHI S   /
      IX=(0.,1.)
      WRITE(6,11)
 11   FORMAT(1X,///,1X,"SCATTERING BY A METALLIC CIRCULAR DISK",
     1/,5X,"(HODGE -- VERSION 12/17/78)")
      WRITE(6,26)
 26   FORMAT(1X,///,1X,"(TYPE KA=0 TO STOP PROGRAM)",/,
     11X,"(TYPE KA=-1 FOR A DESRIPTION OF THE",
     1" PARAMETERS)",/,1X,"(NORMALIZATION:  ESCAT=A*EINC*ENORM"
     1"/(2*R)*EXP(-J*K*R))",/,1X,"(ALL ANGLES IN DEGREES)")
 4    NOC=1
      INDEX=1
      WRITE(6,27)
 27   FORMAT(1X,///,1X,"1.  KA",14X,"= ")
      READ(5,*) VAR(1)
      IF(VAR(1).EQ.-1)GO TO 41
      IF(VAR(1).LE.0.)GO TO 5
      WRITE(6,28)
 28   FORMAT(1X,"2.  THETA INCIDENT  = ")
      READ(5,*) VAR(2)
      WRITE(6,29)
 29   FORMAT(1X,"3.  POLARIZATION    = ")
      READ(5,*) VAR(3)
      WRITE(6,30)
 30   FORMAT(1X,"4.  THETA SCATTERED = ")
      READ(5,*) VAR(4)
      WRITE(6,31)
 31   FORMAT(1X,"5.  PHI SCATTERED   = ")
      READ(5,*) VAR(5)
      WRITE(6,3)
 3    FORMAT(1X,//,1X,"WHICH VARIABLE IS TO BE INCREMENTED?")
      READ(5,*) NVAR
      IF((NVAR.LE.0).OR.(NVAR.GT.5))GO TO 23
      WRITE(6,21)
 21   FORMAT(1X,"TYPE NUMBER OF CASES:")
      READ(5,*) NOC
      WRITE(6,32)
 32   FORMAT(1X,"WHAT IS THE INCREMENT?")
      READ(5,*) VINCRE
 23   CONTINUE
      WRITE(6,24) LABEL(NVAR)
 24   FORMAT(1X,//,A10,4X,"CROSS SECTION",22X,"E NORM",/,
     113X,"SIGMA/(PI*A**2)",11X,"THETA",15X,"PHI",/,13X,
     1"THETA",7X,"PHI",8X,"MAG",5X,"PHASE",6X,"MAG",5X,
```

```
     1"PHASE",/)
6     C=VAR(1)
      MMMAX=45
      NNMAX=45
      IRRMAX=45
      THED=VAR(2)*3.14159/180
      ETAD=COS(THED)
      THE=VAR(4)*3.14159/180
      ETA=COS(THE)
      PHI=VAR(5)*3.14159/180
      ALF=VAR(3)*3.14159/180
      CALF=COS(ALF)
      SALF=SIN(ALF)
34    DO 10 MM=1,MMMAX
      M=MM-1
      IQ=0
      CALL SMND(M,NNMAX)
      CALL DBEIGN(C,M,NNMAX)
      CALL DBCOFN(C,M,MMMAX,NNMAX,IRRMAX)
      CALL DNEGN(C,M,NNMAX)
      CALL DBRAD(C,M,IQ,MMMAX,NNMAX,IRRMAX)
      IF(IQ.EQ.1)GO TO 10
      CALL FPSI(M,NNMAX)
      CALL POLYN(ETAD,M,IRRMAX)
      CALL DBANG(NNMAX,IRRMAX)
      DO 7 I=1,NNMAX
7     SETAD(I)=SETA(I)
      CALL FW(M,NNMAX)
      CALL POLYN(ETA,M,IRRMAX)
      CALL DBANG(NNMAX,IRRMAX)
      CALL FY(M,NNMAX)
10    CONTINUE
      DO 13 MM=1,MMMAX
      CALL FXU(MM,MMMAX)
      IF(MMMAX.LT.MM)GO TO 13
      CALL CSPHI(MM,PHI)
13    CONTINUE
      CALL FZ(MMMAX,Z,ZA,ZB,ZC,ZD)
      EPART=ETA*(-2*Z*CMPHI(2)+ZA)
      EPARP=-2*Z*SMPHI(2)+ZB
      EPERT=ETA*(2*Z*SMPHI(2)-ZC)
      EPERP=-2*Z*CMPHI(2)+ZD
      IF(ETAD.EQ.0.)GO TO 2
      ESNT=2*IX*(CALF*EPART/ETAD+SALF*EPERT)/C
      ESNP=2*IX*(CALF*EPARP/ETAD+SALF*EPERP)/C
      GO TO 8
2     ESNT=2*IX*SALF*EPERT/C
      ESNP=2*IX*SALF*EPERP/C
8     EMAGT=CABS(ESNT)
      EMAGP=CABS(ESNP)
      SIGTHE=EMAGT*EMAGT
      SIGPHI=EMAGP*EMAGP
      E1=REAL(ESNT)
      E2=AIMAG(ESNT)
      IF(E1.EQ.0.)GO TO 16
```

```
      ARG=E2/E1
      EPHAT=180/3.14159*ATAN(ARG)
      IF((E1.LT.0.).AND.(E2.GT.0.))EPHAT=EPHAT+180
      IF((E1.LT.0.).AND.(E2.LT.0.))EPHAT=EPHAT-180
      GO TO 17
 16   EPHAT=90
      IF(E2.LT.0.)EPHAT=-90
 17   E1=REAL(ESNP)
      E2=AIMAG(ESNP)
      IF(E1.EQ.0.)GO TO 18
      ARG=E2/E1
      EPHAP=180/3.14159*ATAN(ARG)
      IF((E1.LT.0.).AND.(E2.GT.0.))EPHAP=EPHAP+180
      IF((E1.LT.0.).AND.(E2.LT.0.))EPHAP=EPHAP-180
      GO TO 19
 18   EPHAP=90
      IF(E2.LT.0.)EPHAP=-90
 19   IF(NVAR.EQ.0)NVAR=1
      WRITE(6,25) VAR(NVAR),SIGTHE,SIGPHI,EMAGT,EPHAT,
     1EMAGP,EPHAP
 25   FORMAT(1X,F7.2,2(1X,E10.3),2(1X,E10.3,1X,F7.2))
 37   IF(INDEX.EQ.NOC)GO TO 4
      INDEX=INDEX+1
      VAR(NVAR)=VAR(NVAR)+VINCRE
      GO TO 6
 5    CALL EXIT
 41   WRITE(6,40)
 40   FORMAT(1X,//,1X,"THE DISK OF RADIUS A LIES IN THE X-Y PLANE
",/,
     11X,"CENTERED AT THE ORIGIN.  THE CONVENTIONAL (R, THETA,",/
,1X,
     1"PHI) COORDINATE SYSTEM IS USED IN THE FAR FIELD.  ",/,1X,
     1"THE PLANE OF INCIDENCE OF THE PLANE WAVE IS THE",/,1X,
     1"X-Z (PHI=0) PLANE.  THE POLARIZATION ANGLE (POL)",/,1X,
     1"OF EINC IS MEASURED FROM THE PLANE OF INCIDENCE ",/,1X,
     1"IN THE PHI-DIRECTION. I.E., POL=0 IS THE PARALLEL",/,1X,
     1"(THETA) CASE AND POL=90 IS THE PERPENDICULAR (PHI)",/,1X,
     1"CASE.",2X,"THE RESULT IS A SOLUTION OF THE RIGOROUS",/,
     11X,"EIGENFUNCTION SCATTERING PROBLEM.")
      GO TO 4
 42   CONTINUE
      GO TO 4
      END
C
C     OBLATE SPHEROIDAL ANGULAR FUNCTION,S,OF ARGUMENT 0;
C     ORDERM,N; WITH N-M EVEN;UP TO ORDER N=M+2*NNMAX-2.
C     (EQUAL TO PMN(0))
C
      SUBROUTINE SMNO(M,NNMAX)
      COMPLEX F4
      COMMON EIG(50),D(50,50),DNEG(50),R1(50),F4(50)
     1,SO(50)
      SO(1)=1
      IF(M.EQ.0.)GO TO 1
      DO 2 MM=1,M
 2    SO(1)=(2*MM-1)*SO(1)
 1    DO 3 NN=1,NNMAX
```

```
      N=2*(NN-1)+M
    3 SO(NN+1)=-(N+M+1)*SO(NN)/(N-M+2)
      RETURN
      END
C
C     SIN AND COSINE FUNCTIONS OF PHI
C
      SUBROUTINE CSPHI(MM,PHI)
      COMPLEX F4,PSI,W,YO,YETAO,U,X
      COMMON EIG(50),D(50,50),DNEG(50),R1(50),F4(50)
     1,SO(50),P(50),SETA(50),SETAO(50),PSI(50),W(50),YO(50)
     1,YETAO(50),U(50),X(50),CMPHI(50),SMPHI(50)
      M=MM-1
      CMPHI(MM)=COS(M*PHI)
      SMPHI(MM)=SIN(M*PHI)
      RETURN
      END
C
C     OBLATE SPHEROIDAL EIGENVALUES OF ARGUMENT C, ORDER M,N
C     WITH N-M EVEN UP TO ORDER N=M+2*NNMAX-2
C
      SUBROUTINE OBEIGN(C,M,NNMAX)
      COMMON EIG(50)
      DIMENSION IP(50),ALPHA(50),BETA(50),P(50)
    4 CONTINUE
      M2=2*M
      C2=C*C
      ACC=1.0E-05
      NN2=NNMAX+2
      NI=NN2+1
      P(1)=1
      IP(1)=1
      DO 2 IQQ=1,NN2
      IV=2*IQQ-1
      IW=M2+2*IQQ
      IX=M2+4*IQQ-1
      ALPHA(IQQ)=(C2*(M2*(2*IV-1)+2*IV*(IV-1)-1))/(IX*(IX-4))
     1-(M+IV-1)*(IV+M)
    2 BETA(IQQ+1)=C2/IX*SQRT(IV*(IV+1)*IW*(IW-1)/(IX*IX-4.0))
      BETA(NN2+1)=0.
      BO=ABS(ALPHA(1))+ABS(BETA(2))
      DO 3 IQQ=2,NN2
      AO=ABS(BETA(IQQ))+ABS(ALPHA(IQQ))+ABS(BETA(IQQ+1))
      BETA(IQQ)=BETA(IQQ)*BETA(IQQ)
      IF(AO.GT.BO) BO=AO
    3 CONTINUE
      AO=-BO
      BOI=BO
   13 CONTINUE
      BO=BOI
      DO 20 IQQ=1,NNMAX
      N=2*IQQ-2+M
      A=AO
      B=BO
      IERR=-1
```

```
21    IIS=0
      CO=(A+B)/2
      IF(CO)50,22,50
50    ERR=(B-A)/ABS(CO)
      IERR=IERR+1
      IF(IERR-60)40,41,41
41    WRITE(6,42) N
42    FORMAT(2X,"ITERATIONS EXCEEDED FOR EIGENVALUE ",I3)
      GO TO 700
40    IF(ERR-ACC)24,24,22
22    P(2)=ALPHA(1)-CO
      DO 5 I=3,NI
      P(I)=(ALPHA(I-1)-CO-BETA(I-1)*(P(I-2)/P(I-1)))*P(I-1)
      PMAG=ABS(P(I))
      IF(PMAG.GT.1.0E+33) GO TO 7
5     CONTINUE
12    CONTINUE
      DO 6 I=2,NI
      IF(P(I))14,8,9
8     IF(P(I-1))9,9,14
14    IP(I)=-1
      GO TO 10
9     IP(I)=1
10    IF(IP(I)-IP(I-1))6,11,6
11    IIS=IIS+1
6     CONTINUE
      IF(IIS-IQQ)16,15,15
15    A=CO
      GO TO 21
16    B=CO
      GO TO 21
24    BO=CO
700   EIG(IQQ)=-CO
20    CONTINUE
      RETURN
7     NNMAX=I-4
      NI=NNMAX+3
      GO TO 4
      END
C
C     OBLATE SPHEROIDAL EIGENFUNCTION EXPANSION COEFFICIENTS
C     OF ARGUMENT C; ORDER M,N,R; WITH N-M EVEN, UP TO ORDER
C     N=M+2*NNMAX-2,R=2*IRRMAX+2
C
      SUBROUTINE OBCOFN(C,M,MMMAX,NNMAX,IRRMAX)
      COMMON EIG(50),D(50,50)
      DIMENSION DP(50)
      C2=C*C
      MM=M+1
      DO 1 NN=1,NNMAX
      N=M+2*NN-2
4     DP(IRRMAX+3)=0
      DP(IRRMAX+2)=1.0E-30
      D(NN,1)=0
      D(NN,2)=1
```

```
      JJ=(N-M)/2+1
      DO 107 LL=1,IRRMAX
      L=LL-1
      IF(LL.GE.JJ)  L=IRRMAX+JJ-LL
      IR=2*L
      IRM=M+IR
      AR=(M+IRM+2)*(M+IRM+1)*C2/((2*IRM+3)*(2*IRM+5))
      BR=(2*IRM*(IRM+1)-2*M*M-1)*C2/((2*IRM-1)*
     1  (2*IRM+3))-IRM*(IRM+1)
      CR=IR*(IR-1)*C2/((2*IRM-3)*(2*IRM-1))
      IF(LL-JJ)105,106,106
105   D(NN,L+3)=-(CR*D(NN,L+1)+(BR+EIG(NN))*D(NN,L+2))/AR
      DMAG=ABS(D(NN,L+3))
      IF(DMAG.GT.1.0E+30)  GO TO 3
      GO TO 107
106   DP(L+1)=-(AR*DP(L+3)+(BR+EIG(NN))*DP(L+2))/CR
      DMAG=ABS(DP(L+1))
      IF(DMAG.GT.1.0E+30)  GO TO 3
107   CONTINUE
      DL=ABS(D(NN,JJ+1))
      DL=ALOG10(DL)
      DLP=ABS(DP(JJ+1))
      DLP=ALOG10(DLP)
      DL=ABS(DL)
      DLP=ABS(DLP)
      DL=DL+DLP
      IF(DL.GT.30.)  GO TO 5
      CON=D(NN,JJ+1)/DP(JJ+1)
      ACON=ABS(CON)
      IF(ACON.GE.1.0E+32)  GO TO 2
      DO 118 J=JJ,IRRMAX
118   D(NN,J+2)=CON*DP(J+2)
      F=1
      IF(M)198,198,199
199   DO 110 I=1,M
110   F=F*(M+I)
198   SUM=0
      MMX=IRRMAX+1
      DO 113 I=1,MMX
      IR=2*I
      SUM=SUM+F*D(NN,I+1)
      IF(I-JJ)  113,197,113
197   FNM=F
113   F=(-F*(IR+2*M-1))/IR
      ALF=FNM/SUM
      DO 114 I=1,MMX
      D(NN,I)=ALF*D(NN,I+1)
114   CONTINUE
1     CONTINUE
      RETURN
3     IRRMAX=LL-1
      GO TO 4
2     IRRMAX=IRRMAX-1
      GO TO4
5     NNMAX=NN-1
```

```
      RETURN
      END
C
C     NEGATIVE D COEFFICIENT SUBROUTINE
C
      SUBROUTINE DNEGN(C,M,NNMAX)
      COMMON EIG(50),D(50,50),DNEG(50)
      DO 4 NN=1,NNMAX
      C2=C*C
      IF(M.GE.1) GO TO 2
      DO 5 II=1,NNMAX
    5 DNEG(II)=D(II,1)
      GO TO 3
    2 B1=1.0
      B2=0.0
      EI=EIG(NN)
      DO 1 IRR=1,M
      IR=2*IRR-2*M-2
      AR=(2*M+IR+2)*(2*M+IR+1)*C2/((2*M+2*IR+3)
     1*(2*M+2*IR+5))
      BR=(M+IR)*(M+IR+1)-EI-(2*(M+IR)*(M+IR+1)-2*M*M-1)
     1*C2/((2*M+2*IR-1)*(2*M+2*IR+3))
      CR=(IR)*(IR-1)*C2/((2*M+2*IR-3)*(2*M+2*IR-1))
      B3=B2
      B2=B1
    1 B1=(BR*B2-CR*B3)/AR
      A=D(NN,1)/B1
      DNEG(NN)=A
      DDM=ABS(DNEG(NN))
      IF(DDM.LT.1.0E-35) GO TO 6
    4 CONTINUE
    3 RETURN
    6 NNMAX=NN-1
      RETURN
      END
C
C     OBLATE SPHEROIDAL RADIAL FUNCTION R(4) OF ARGUMENT C;
C     ORDER M,N; WITH N-M EVEN; UP TO ORDER N=M+2*NNMAX-2.
C     ALSO NORMALIZATION FUNCTION, N.
C
      SUBROUTINE OBRAD(C,M,IQ,MMMAX,NNMAX,IRRMAX)
      COMMON EIG(50),D(50,50),DNEG(50),R1(50),F4(50)
      COMPLEX IX,R4,F4
      IX=(0.0,1.0)
      EEAC=1
      EAC=1
      EAC2=1
      GRO=1
      IF(M.EQ.0) GO TO 20
      MAXM=M+1
      DO 19 MM=2,MAXM
      IM=MM-1
      GRO=(2*IM-1)*(2*IM)*GRO
      EEAC=(2*IM-1)*EEAC
      EAC2=(2*IM-1)*(2*IM)*EAC2
```

```
19    EAC=IM*EAC
      IF(EEAC.GE.1.0E+17) GO TO 4
      IF(EAC2.GE.1.0E+30) GO TO 4
20    DO 17 NN=1,NNMAX
      N=2*(NN-1)+M
      SUM=0
      GR=GRO
      ENORM=0.
      DO 18 NR=1,IRRMAX
      IR=2*(NR-1)
      SUMP=GR*D(NN,NR)
      SUM=SUM+SUMP
      DMAG=ABS(D(NN,NR))
      IF(DMAG.LT.1.0E-30) GO TO 1
      ENORMP=2*GR*(D(NN,NR))**2/(2*IR+2*M+1)
2     ENORM=ENORM+ENORMP
      GRMAG=ABS(GR)
      IF(GRMAG.GT.1.0E+30) GO TO 5
      GR=(IR+2*M+1.)/(IR+1.)*(IR+2*M+2.)/(IR+2.)*GR
18    CONTINUE
      R1(NN)=(-1)**(NN-1)*2**M*EAC*C**M*D(NN,1)/((2*M+1)*SUM)
      R2=(-1)**(NN-1)*(2*M-1)*EAC*C**(M-1)/(2*EAC2)*3.14159
     1*(EEAC**2/SUM)*2**M/DNEG(NN)
      RR2=ABS(R2)
      IF(RR2.GE.1.0E+30) GO TO 4
      EEAC=(N+M+1)*EEAC/(N-M+2)
      IF(EEAC.GE.1.0E+17) NNMAX=NN
      R4=R1(NN)-IX*R2
      A5=ABS(ENORM)
      A1=ALOG10(A5)
      A4=ABS(R2)
      A2=ALOG10(A4)
      A3=A1+A2
      IF(A3.GT.30.) GO TO 3
      A5=ABS(R1(NN))
      A1=ALOG10(A5)
      A3=ABS(A1)+ABS(A2)
      IF(A3.GT.30.) GO TO 3
      F4(NN)=1/(ENORM*R4)
17    CONTINUE
      RETURN
1     ENORMP=0
      GO TO 2
3     F4(NN)=(0.,0.)
      GO TO 17
5     GR=0
      GO TO 18
4     MMMAX=M
      IQ=1
      RETURN
      END
C
C     PSI FUNCTION
C
      SUBROUTINE FPSI(M,NNMAX)
```

```
      COMPLEX IX,F4,PSI
      COMMON EIG(50),D(50,50),DNEG(50),R1(50),F4(50)
     1,SO(50),P(50),SETA(50),SETAO(50),PSI(50)
      IX=(0.,1.)
      MM=M+1
      PSI(MM)=(0.,0.)
      DO 1 NN=1,NNMAX
      N=M+2*NN-2
      PSI(MM)=PSI(MM)+IX**(N)*SO(NN)**2*F4(NN)
    1 CONTINUE
      RETURN
      END
C
C     ASSOCIATED LEGENDRE POLYOMIALS,OP,OF ARGUMENT ETAO;
C     ORDERPM,N; WITH N-M EVEN; OF TO ORDER N=M+2*NNMAX-2.
C
      SUBROUTINE POLYN(ETAO,M,NNMAX)
      DIMENSION PP(3)
      COMPLEX F4
      COMMON EIG(50),D(50,50),DNEG(50),R1(50),F4(50)
     1,SO(50),P(50)
      SQ=SQRT(1-ETAO*ETAO)
      PP(1)=0
      PP(2)=1
      IF(M.EQ.0) GO TO 1
      DO 2 L=1,M
    2 PP(2)=(2*L-1)*SQ*PP(2)
    1 P(1)=PP(2)
      DO 3 NN=2,NNMAX
      N=M+2*NN-3
      DO 4 L=1,2
      PP(3)=((2*N-1)*ETAO*PP(2)-(N+M-1)*PP(1))/(N-M)
      N=N+1
      PP(1)=PP(2)
    4 PP(2)=PP(3)
    3 P(NN)=PP(3)
      RETURN
      END
C
C     OBLATE SPHEROIDAL ANGULAR FUNCTIONS, S, OF ARGUMENTS
C     C AND ETAO; ORDER M,N; WITH N-M EVEN; UP TO ORDER
C     N=M+2*NNMAX-2.
C
      SUBROUTINE OBANG(NNMAX,IRRMAX)
      COMPLEX F4
      COMMON EIG(50),D(50,50),DNEG(50),R1(50),F4(50)
     1,SO(50),P(50),SETA(50),SETAO(50)
      DO 1 NN=1,NNMAX
      SETA(NN)=0
      DO 2 IRR=1,IRRMAX
    2 SETA(NN)=SETA(NN)+D(NN,IRR)*P(IRR)
    1 CONTINUE
      RETURN
      END
C
```

```
C       W FUNCTION
C
        SUBROUTINE FW(M,NNMAX)
        COMPLEX IX,F4,W,PSI
        COMMON EIG(50),D(50,50),DNEG(50),R1(50),F4(50)
       1,SD(50),P(50),SETA(50),SETAD(50),PSI(50),W(50)
        IX=(0.,1.)
        MM=M+1
        W(MM)=(0.,0.)
        DO 1 NN=1,NNMAX
        N=M+2*NN-2
 1      W(MM)=W(MM)+IX**N*SETAD(NN)*SD(NN)*F4(NN)
        RETURN
        END
C
C       Y FUNCTION
C
        SUBROUTINE FY(M,NNMAX)
        COMPLEX F4,YD,YETAD,PSI,W
        COMMON EIG(50),D(50,50),DNEG(50),R1(50),F4(50)
       1,SD(50),P(50),SETA(50),SETAD(50),PSI(50),W(50),YD(50)
       1,YETAD(50)
        MM=M+1
        YD(MM)=(0.,0.)
        YETAD(MM)=(0.,0.)
        DO 1 NN=1,NNMAX
        N=M+2*NN-2
        YD(MM)=YD(MM)+(-1)**N*R1(NN)*SD(NN)*SETA(NN)*F4(NN)
 1      YETAD(MM)=YETAD(MM)+(-1)**N*R1(NN)*SETAD(NN)*SETA(NN)*F4(NN
)
        RETURN
        END
C
C       S AND U FUNCTIONS
C
        SUBROUTINE FXU(MM,MMMAX)
        COMPLEX IX,F4,PSI,W,YD,YETAD,U,X,PT
        COMMON EIG(50),D(50,50),DNEG(50),R1(50),F4(50)
       1,SD(50),P(50),SETA(50),SETAD(50),PSI(50),W(50),YD(50)
       1,YETAD(50),U(50),X(50)
        IX=(0.,1.)
        IF(MM.EQ.1) GO TO 1
        IF(MM.EQ.MMMAX) GO TO 2
        PT=PSI(MM-1)*PSI(MM+1)
        PTT=CABS(PT)
        IF(PTT.EQ.0.) GO TO 3
        U(MM)=2*IX**(MM-2)*(W(MM-1)+W(MM+1))/(PSI(MM-1)+PSI(MM+1))
        X(MM)=2*IX**(MM-2)*(W(MM-1)-W(MM+1))/(PSI(MM-1)+PSI(MM+1))
        RETURN
 1      U(1)=-IX*W(2)/PSI(2)
        X(1)=(0.,0.)
        RETURN
 2      U(MM)=IX**(MM-2)*2*W(MM-1)/PSI(MM-1)
        X(MM)=U(MM)
        RETURN
 3      MMMAX=MM-1
```

```
      RETURN
      END
C
C     Z FUNCTIONS
C
      SUBROUTINE FZ(MMMAX,Z,ZA,ZB,ZC,ZD)
      COMPLEX IX,IQ,Z,ZA,ZB,ZC,ZD,F4,PSI,W,YD,YETAD,U,X
      COMMON EIG(50),D(50,50),DNEG(50),R1(50),F4(50)
     1,SD(50),P(50),SETA(50),SETAD(50),PSI(50),W(50),YD(50)
     1,YETAD(50),U(50),X(50),CMPHI(50),SMPHI(50)
      IX=(0.,1.)
      Z=(0.,0.)
      ZA=Z
      ZB=Z
      ZC=Z
      ZD=Z
      MAXMM=MMMAX-1
      DO 3 MM=1,MAXMM
      M=MM-1
      A=2
      B=1
      C=1
      IF(MM.EQ.1) A=1
      IF(MM.EQ.2) B=2
      IF(MM.EQ.2) C=0
      IQ=IX**(-M)
      Z=Z+A*YETAD(MM)*CMPHI(MM)
      IF(MM.EQ.1) GO TO 2
      ZA=ZA+IQ*(U(MM+1)*CMPHI(MM+1)-B*U(MM-1)*CMPHI(MM-1))
     1*YD(MM)
      ZB=ZB+IQ*(U(MM+1)*SMPHI(MM+1)+U(MM-1)*SMPHI(MM-1))
     1*YD(MM)
      ZC=ZC+IQ*(X(MM+1)*SMPHI(MM+1)-X(MM-1)*SMPHI(MM-1))
     1*YD(MM)
      ZD=ZD+IQ*(X(MM+1)*CMPHI(MM+1)+C*X(MM-1)*CMPHI(MM-1))
     1*YD(MM)
      GO TO 1
 2    ZA=ZA+U(2)*CMPHI(2)*YD(1)
      ZB=ZB+U(2)*SMPHI(2)*YD(1)
      ZC=ZC+X(2)*SMPHI(2)*YD(1)
      ZD=ZD+X(2)*CMPHI(2)*YD(1)
 1    CONTINUE
 3    CONTINUE
      RETURN
      END
```

```
SCATTERING BY A METALLIC CIRCULAR DISK
     (HODGE -- VERSION 12/17/78)


(TYPE KA=0 TO STOP PROGRAM)
(TYPE KA=-1 FOR A DESRIPTION OF THE PARAMETERS)
(NORMALIZATION:  ESCAT=A*EINC*ENORM/(2*R)*EXP(-J*K*R))
(ALL ANGLES IN DEGREES)


1.  KA                 =1
2.  THETA INCIDENT     =45
3.  POLARIZATION       =0
4.  THETA SCATTERED    =45
5.  PHI SCATTERED      =0


WHICH VARIABLE IS TO BE INCREMENTED?1
TYPE NUMBER OF CASES: 25
WHAT IS THE INCREMENT?1
```

KA	CROSS SECTION SIGMA/(PI*A**2) THETA	PHI	E NORM THETA MAG	PHASE	PHI MAG
1.00	.351E+00	0.	.593E+00	-22.65	0.
2.00	.903E+00	0.	.950E+00	-110.86	0.
3.00	.263E+00	0.	.513E+00	148.85	0.
4.00	.353E+00	0.	.594E+00	85.18	0.
5.00	.334E+00	0.	.578E+00	-3.41	0.
6.00	.447E+00	0.	.669E+00	-105.68	0.
7.00	.149E+00	0.	.387E+00	148.80	0.
8.00	.738E-01	0.	.272E+00	58.53	0.
9.00	.659E-02	0.	.812E-01	43.29	0.
10.00	.194E-01	0.	.139E+00	-45.88	0.
11.00	.534E-01	0.	.231E+00	-95.93	0.
12.00	.456E-01	0.	.213E+00	167.71	0.
13.00	.102E+00	0.	.319E+00	87.48	0.
14.00	.627E-01	0.	.250E+00	-11.15	0.
15.00	.982E-01	0.	.313E+00	-103.23	0.
16.00	.637E-01	0.	.252E+00	159.30	0.
17.00	.570E-01	0.	.239E+00	86.09	0.
18.00	.119E-01	0.	.109E+00	21.45	0.
19.00	.800E-02	0.	.894E-01	-127.06	0.
20.00	.244E-01	0.	.156E+00	124.65	0.
21.00	.122E+00	0.	.349E+00	88.27	0.
22.00	.172E+00	0.	.414E+00	71.90	0.
23.00	.631E-01	0.	.251E+00	10.06	0.
24.00	.116E+00	0.	.340E+00	-120.81	0.
25.00	.164E+00	0.	.405E+00	72.44	0.

AD-A080 367 AIR FORCE INST OF TECH WRIGHT-PATTERSON AFB OH SCHOO--ETC F/G 17/9
PREDICTED MICROWAVE ELECTRO-MAGNETIC BACKSCATTERING RETURNS FOR--ETC(U)
DEC 79 F DIBARTOLOMEO

UNCLASSIFIED AFIT/GE/EE/79D-11 NL

2 OF 2
AD
A080 367

END
DATE
FILMED
3-80
DDC

```
      PROGRAM SCATTER(INPUT,OUTPUT)
      COMPLEX A1,A2,B1,B2,H,P1,P2,P,U1,U2,X,Y,ESCAT,J
      REAL PI,THETA,A,B,D,E1,E2,F1,F2,G1,G2,C1,C2,KA,
     $S1,S2,Q,T1,T2,ARG,V,W,IER,MMBSJ0,MMBSJ1,MMBSJ2
      DIMENSION ESCATM(100),ANGLE(100),SIGMA(100)
      READ* THETA
      PI=3.141593
      THETA=(THETA/360.)*(2*PI)
      KA=0.
      A=1.414214
      B=-(PI/4)
      DO 20 I=1,25
      KA=KA+1.
      D=2*(((2*KA)/PI)**(1./2.))
      E1=COS((PI/4.) - (THETA/2.))
      E2=COS((PI/4.) + (THETA/2.))
      F1=ABS(E1)
      F2=ABS(E2)
      G1=D*F1
      G2=D*F2
      CALL FRESNEL(G1,C1,S1)
      CALL FRESNEL(G2,C2,S2)
      H=CMPLX(0.,B)
      H=CEXP(H)
      P1=CMPLX(C1,S1)
      P2=CMPLX(C2,S2)
      A1=A*H*P1
      A2=A*H*P2
      ARG=2*KA*(SIN(THETA))
      V=(1 + SIN(THETA))/(2*SIN(THETA))
      W=(1 - SIN(THETA))/(2*SIN(THETA))
      MMBSJ2=(2/ARG)*MMBSJ1(ARG,IER) - MMBSJ0(ARG,IER)
      X=((A1**2)*W + (A2**2)*V)*MMBSJ1(ARG,IER)
      Y=((A1**2)*W - (A2**2)*V)*MMBSJ2
      J=(0.,1.)
      Y=Y*J
      Y1=REAL(Y)
      Y2=AIMAG(Y)
      X1=REAL(X)
      X2=AIMAG(X)
      ESCAT1=X1-Y1
      ESCAT2=X2-Y2
      ESCAT=CMPLX(ESCAT1,ESCAT2)
      ESCAT=ESCAT*J
      ESCAT=-ESCAT
      ESCATR=REAL(ESCAT)
      ESCATI=AIMAG(ESCAT)
      ESCATM(I)=((ESCATR**2.) + (ESCATI**2.))**(1./2.)
      SIGMA(I)= (ESCATM(I)**2.)
      ANGLE=ATAN(ESCATI/ESCATR)
      ANGLE(I)=((ANGLE)/(2*PI))*360.
      IF((ESCATR.LT.0.).AND.(ESCATI.GT.0.)) ANGLE(I)=ANGLE(I) + 1
80.
      IF((ESCATR.LT.0.).AND.(ESCATI.LT.0.)) ANGLE(I)=ANGLE(I) - 1
80.
   20 CONTINUE
      KA=0.
      PRINT30
```

```
30    FORMAT(11X,//,8X,"KA",7X,"SIGMA/PI**2",14X,"ESCAT",/,
     $37X,"MAG",9X,"PHASE",/)
      DO 40 I=1,25
      KA=KA + 1.
      PRINT50,KA,SIGMA(I),ESCATM(I),ANGLE(I)
50    FORMAT(" ",3X,F7.2,5X,E10.3,7X,E10.3,5X,F7.2)
40    CONTINUE
      STOP
      END
      SUBROUTINE FRESNEL(AA,C,S)
      DIMENSION X(2000),Y(2000),ZX(2000),ZY(2000)
      INTEGER NDIM
      IF((AA.GT.-0.01).AND.(AA.LT.0.01))GO TO 6
      GO TO 11
6     C=0.0
      S=0.0
      GO TO 4
11    H=.01
      BB=ABS(AA)
      NDIM=BB/H + .1
      K=NDIM+1
      DO 10 I=1,K
      A=I*H - H
      X(I)=COS(1.57080*(A**2.))
      Y(I)=SIN(1.57080*(A**2.))
10    CONTINUE
      SUM2=0.
      SUM4=0.
1     HH=.5*H
C
C     INTEGRATION LOOP
      DO 2 I=1,NDIM
      SUM1=SUM2
      SUM3=SUM4
      SUM2=SUM2 + HH*(X(I)+X(I+1))
      SUM4=SUM4 + HH*(Y(I)+Y(I+1))
      ZX(I)=SUM1
2     ZY(I)=SUM3
3     ZX(NDIM)=SUM2
      ZY(NDIM)=SUM4
7     IF(AA.GE.0.1)GO TO 8
      C=(-1.)*ZX(NDIM)
      S=(-1.)*ZY(NDIM)
      GO TO 9
8     C=ZX(NDIM)
      S=ZY(NDIM)
9     CONTINUE
4     RETURN
      END
```

KA	SIGMA/PI**2	ESCAT MAG	ESCAT PHASE
1.00	.409E+00	.640E+00	-.09
2.00	.104E+01	.102E+01	-92.45
3.00	.370E+00	.608E+00	2.59
4.00	.700E+00	.837E+00	105.75
5.00	.297E+00	.545E+00	-165.44
6.00	.265E+00	.514E+00	-67.00
7.00	.848E-01	.291E+00	14.66
8.00	.714E-01	.267E+00	100.69
9.00	.226E-01	.150E+00	147.33
10.00	.240E-01	.155E+00	-120.14
11.00	.444E-01	.211E+00	-80.24
12.00	.340E-01	.184E+00	12.08
13.00	.980E-01	.313E+00	90.71
14.00	.652E-01	.255E+00	-178.69
15.00	.110E+00	.332E+00	-85.81
16.00	.563E-01	.237E+00	1.94
17.00	.676E-01	.260E+00	94.77
18.00	.253E-01	.159E+00	168.41
19.00	.275E-01	.166E+00	-99.14
20.00	.169E-01	.130E+00	-51.91
21.00	.138E-01	.117E+00	45.27
22.00	.294E-01	.171E+00	97.22
23.00	.199E-01	.141E+00	-174.10
24.00	.513E-01	.226E+00	-91.91
25.00	.330E-01	.182E+00	-5.07

```
      PROGRAM DISK25(INPUT,OUTPUT,TAPE5=INPUT,TAPE6=OUTPUT)
C     FAR FIELD SCATTERING BY A CIRCULAR METALLIC DISK
      DIMENSION LABEL(5),VAR(5)
      COMPLEX F4,PSI,W,YO,YETAO,U,X,Z,ZA,ZB,ZC,ZD
     1,IX,EPART,EPARP,EPERT,EPERP,ESNT,ESNP
      COMMON EIG(50),D(50,50),DNEG(50),P1(50),F4(50)
     1,SO(50),P(50),SETA(50),SETAO(50),PSI(50),W(50),YO(50)
     1,YETAO(50),U(50),X(50),CMPHI(50),SMPHI(50)
      DATA LABEL(1)/10H    KA    /
      DATA LABEL(2)/10H THETA I  /
      DATA LABEL(3)/10H   POL    /
      DATA LABEL(4)/10H THETA S  /
      DATA LABEL(5)/10H  PHI S   /
      IX=(0.,1.)
      WRITE(6,11)
 11   FORMAT(1X,///,1X,"SCATTERING BY A METALLIC CIRCULAR DISK
     1/,5X,"(HODGE -- VERSION 12/17/78)")
      WRITE(6,26)
 26   FORMAT(1X,///,1X,"(TYPE KA=0 TO STOP PROGRAM)",/,
     11X,"(TYPE KA=-1 FOR A DESRIPTION OF THE",
     1" PARAMETERS)",/,1X,"(NORMALIZATION:  ESCAT=A*EINC*ENORM
     1"/(2*R)*EXP(-J*K*R))",/,1X,"(ALL ANGLES IN DEGREES)")
 4    NOC=1
      INDEX=1
      WRITE(6,27)
 27   FORMAT(1X,///,1X,"1.  KA",14X,"= ")
      READ(5,*) VAR(1)
      IF(VAR(1).EQ.-1)GO TO 41
      IF(VAR(1).LE.0.)GO TO 5
      WRITE(6,28)
 28   FORMAT(1X,"2.  THETA INCIDENT  = ")
      READ(5,*) VAR(2)
      WRITE(6,29)
 29   FORMAT(1X,"3.  POLARIZATION    = ")
      READ(5,*) VAR(3)
      WRITE(6,30)
 30   FORMAT(1X,"4.  THETA SCATTERED = ")
      READ(5,*) VAR(4)
      WRITE(6,31)
 31   FORMAT(1X,"5.  PHI SCATTERED   = ")
      READ(5,*) VAR(5)
      WRITE(6,3)
 3    FORMAT(1X,//,1X,"WHICH VARIABLE IS TO BE INCREMENTED?")
      READ(5,*) NVAR
      IF((NVAR.LE.0).OR.(NVAR.GT.5))GO TO 23
      WRITE(6,21)
 21   FORMAT(1X,"TYPE NUMBER OF CASES:")
      READ(5,*) NOC
      WRITE(6,32)
 32   FORMAT(1X,"WHAT IS THE INCREMENT?")
      READ(5,*) VINCRE
 23   CONTINUE
      WRITE(6,24) LABEL(NVAR)
 24   FORMAT(1X,//,A10,4X,"CROSS SECTION",22X,"E NORM",/,
     113X,"SIGMA/(PI*A**2)",11X,"THETA",15X,"PHI",/,13X,
     1"THETA",7X,"PHI",8X,"MAG",5X,"PHASE",6X,"MAG",5X,
```

```
     1"PHASE",/)
 6    C=VAR(1)
      MMMAX=45
      NNMAX=45
      IRRMAX=45
      THED=VAR(2)*3.14159/180
      ETAD=COS(THED)
      THE=VAR(4)*3.14159/180
      ETA=COS(THE)
      PHI=VAR(5)*3.14159/180
      ALF=VAR(3)*3.14159/180
      CALF=COS(ALF)
      SALF=SIN(ALF)
 34   DO 10 MM=1,MMMAX
      M=MM-1
      IQ=0
      CALL SMND(M,NNMAX)
      CALL DBEIGN(C,M,NNMAX)
      CALL DBCDFN(C,M,MMMAX,NNMAX,IRRMAX)
      CALL DNEGN(C,M,NNMAX)
      CALL DBRAD(C,M,IQ,MMMAX,NNMAX,IRRMAX)
      IF(IQ.EQ.1)GO TO 10
      CALL FPSI(M,NNMAX)
      CALL POLYN(ETAD,M,IRRMAX)
      CALL DBANG(NNMAX,IRRMAX)
      DO 7 I=1,NNMAX
 7    SETAD(I)=SETA(I)
      CALL FW(M,NNMAX)
      CALL POLYN(ETA,M,IRRMAX)
      CALL DBANG(NNMAX,IRRMAX)
      CALL FY(M,NNMAX)
 10   CONTINUE
      DO 13 MM=1,MMMAX
      CALL FXU(MM,MMMAX)
      IF(MMMAX.LT.MM)GO TO 13
      CALL CSPHI(MM,PHI)
 13   CONTINUE
      CALL FZ(MMMAX,Z,ZA,ZB,ZC,ZD)
      EPART=ETA*(-2*Z*CMPHI(2)+ZA)
      EPARP=-2*Z*SMPHI(2)+ZB
      EPERT=ETA*(2*Z*SMPHI(2)-ZC)
      EPERP=-2*Z*CMPHI(2)+ZD
      IF(ETAD.EQ.0.)GO TO 2
      ESNT=2*IX*(CALF*EPART/ETAD+SALF*EPERT)/C
      ESNP=2*IX*(CALF*EPARP/ETAD+SALF*EPERP)/C
      GO TO 8
 2    ESNT=2*IX*SALF*EPERT/C
      ESNP=2*IX*SALF*EPERP/C
 8    EMAGT=CABS(ESNT)
      EMAGP=CABS(ESNP)
      SIGTHE=EMAGT*EMAGT
      SIGPHI=EMAGP*EMAGP
      E1=REAL(ESNT)
      E2=AIMAG(ESNT)
      IF(E1.EQ.0.)GO TO 16
```

```
      ARG=E2/E1
      EPHAT=180/3.14159*ATAN(ARG)
      IF((E1.LT.0.).AND.(E2.GT.0.))EPHAT=EPHAT+180
      IF((E1.LT.0.).AND.(E2.LT.0.))EPHAT=EPHAT-180
      GO TO 17
 16   EPHAT=90
      IF(E2.LT.0.)EPHAT=-90
 17   E1=REAL(ESNP)
      E2=AIMAG(ESNP)
      IF(E1.EQ.0.)GO TO 18
      ARG=E2/E1
      EPHAP=180/3.14159*ATAN(ARG)
      IF((E1.LT.0.).AND.(E2.GT.0.))EPHAP=EPHAP+180
      IF((E1.LT.0.).AND.(E2.LT.0.))EPHAP=EPHAP-180
      GO TO 19
 18   EPHAP=90
      IF(E2.LT.0.)EPHAP=-90
 19   IF(NVAR.EQ.0)NVAR=1
      IF(VAR(1).GT.15) GO TO 1000
      GO TO 2000
 1000 CALL SCATTER(VAR,EMAGT,EPHAT,SIGTHE)
 2000 CONTINUE
      WRITE(6,25) VAR(NVAR),SIGTHE,SIGPHI,EMAGT,EPHAT,
     1EMAGP,EPHAP
 25   FORMAT(1X,F7.2,2(1X,E10.3),2(1X,E10.3,1X,F7.2))
 37   IF(INDEX.EQ.NOC)GO TO 4
      INDEX=INDEX+1
      VAR(NVAR)=VAR(NVAR)+VINCRE
      GO TO 6
 5    CALL EXIT
 41   WRITE(6,40)
 40   FORMAT(1X,//,1X,"THE DISK OF RADIUS A LIES IN THE X-Y PLANE
",/,
     11X,"CENTERED AT THE ORIGIN.  THE CONVENTIONAL (R, THETA,",/
,1X,
     1"PHI) COORDINATE SYSTEM IS USED IN THE FAR FIELD.  ",/,1X,
     1"THE PLANE OF INCIDENCE OF THE PLANE WAVE IS THE",/,1X,
     1"X-Z (PHI=0) PLANE.  THE POLARIZATION ANGLE (POL)",/,1X,
     1"OF EINC IS MEASURED FROM THE PLANE OF INCIDENCE ",/,1X,
     1"IN THE PHI-DIRECTION. I.E., POL=0 IS THE PARALLEL",/,1X,
     1"(THETA) CASE AND POL=90 IS THE PERPENDICULAR (PHI)",/,1X,
     1"CASE.",2X,"THE RESULT IS A SOLUTION OF THE RIGOROUS",/,
     11X,"EIGENFUNCTION SCATTERING PROBLEM.")
      GO TO 4
 42   CONTINUE
      GO TO 4
      END
C
C     OBLATE SPHEROIDAL ANGULAR FUNCTION,S,OF ARGUMENT 0;
C     ORDERM,N; WITH N-M EVEN;UP TO ORDER N=M+2*NNMAX-2.
C     (EQUAL TO PMN(0))
C
      SUBROUTINE SMNO(M,NNMAX)
      COMPLEX F4
      COMMON EIG(50),D(50,50),DNEG(50),R1(50),F4(50)
     1,SO(50)
      SO(1)=1
```

```
      IF(M.EQ.0.)GO TO 1
      DO 2 MM=1,M
    2 SO(1)=(2*MM-1)*SO(1)
    1 DO 3 NN=1,NNMAX
      N=2*(NN-1)+M
    3 SO(NN+1)=-(N+M+1)*SO(NN)/(N-M+2)
      RETURN
      END
C
C     SIN AND COSINE FUNCTIONS OF PHI
C
      SUBROUTINE CSPHI(MM,PHI)
      COMPLEX F4,PSI,W,YO,YETAO,U,X
      COMMON EIG(50),D(50,50),DNEG(50),R1(50),F4(50)
     1,SO(50),P(50),SETA(50),SETAO(50),PSI(50),W(50),YO(50)
     1,YETAO(50),U(50),X(50),CMPHI(50),SMPHI(50)
      M=MM-1
      CMPHI(MM)=COS(M*PHI)
      SMPHI(MM)=SIN(M*PHI)
      RETURN
      END
C
C     OBLATE SPHEROIDAL EIGENVALUES OF ARGUMENT C, ORDER M,N
C     WITH N-M EVEN UP TO ORDER N=M+2*NNMAX-2
C
      SUBROUTINE OBEIGN(C,M,NNMAX)
      COMMON EIG(50)
      DIMENSION IP(50),ALPHA(50),BETA(50),P(50)
    4 CONTINUE
      M2=2*M
      C2=C*C
      ACC=1.0E-05
      NN2=NNMAX+2
      NI=NN2+1
      P(1)=1
      IP(1)=1
      DO 2 IOO=1,NN2
      IV=2*IOO-1
      IW=M2+2*IOO
      IX=M2+4*IOO-1
      ALPHA(IOO)=(C2*(M2*(2*IV-1)+2*IV*(IV-1)-1))/(IX*(IX-4))
     1-(M+IV-1)*(IV+M)
    2 BETA(IOO+1)=C2/IX*SQRT(IV*(IV+1)*IW*(IW-1)/(IX*IX-4.0))
      BETA(NN2+1)=0.
      BO=ABS(ALPHA(1))+ABS(BETA(2))
      DO 3 IOO=2,NN2
      AO=ABS(BETA(IOO))+ABS(ALPHA(IOO))+ABS(BETA(IOO+1))
      BETA(IOO)=BETA(IOO)*BETA(IOO)
      IF(AO.GT.BO) BO=AO
    3 CONTINUE
      AO=-BO
      BOI=BO
   13 CONTINUE
      BO=BOI
      DO 20 IOO=1,NNMAX
```

```
        N=2*IQQ-2+M
        A=AO
        B=BO
        IERR=-1
21      IIS=0
        CO=(A+B)/2
        IF(CO)50,22,50
50      ERR=(B-A)/ABS(CO)
        IERR=IERR+1
        IF(IERR-60)40,41,41
41      WRITE(6,42) N
42      FORMAT(2X,"ITERATIONS EXCEEDED FOR EIGENVALUE ",I3)
        GO TO 700
40      IF(ERR-ACC)24,24,22
22      P(2)=ALPHA(1)-CO
        DO 5 I=3,NI
        P(I)=(ALPHA(I-1)-CO-BETA(I-1)*(P(I-2)/P(I-1)))*P(I-1)
        PMAG=ABS(P(I))
        IF(PMAG.GT.1.0E+33) GO TO 7
5       CONTINUE
12      CONTINUE
        DO 6 I=2,NI
        IF(P(I))14,8,9
8       IF(P(I-1))9,9,14
14      IP(I)=-1
        GO TO 10
9       IP(I)=1
10      IF(IP(I)-IP(I-1))6,11,6
11      IIS=IIS+1
6       CONTINUE
        IF(IIS-IQQ)16,15,15
15      A=CO
        GO TO 21
16      B=CO
        GO TO 21
24      BO=CO
700     EIG(IQQ)=-CO
20      CONTINUE
        RETURN
7       NNMAX=I-4
        NI=NNMAX+3
        GO TO 4
        END
C
C       OBLATE SPHEROIDAL EIGENFUNCTION EXPANSION COEFFICIENTS
C       OF ARGUMENT C; ORDER M,N,R; WITH N-M EVEN, UP TO ORDER
C       N=M+2*NNMAX-2,R=2*IRRMAX+2
C
        SUBROUTINE OBCOFN(C,M,MMMAX,NNMAX,IRRMAX)
        COMMON EIG(50),D(50,50)
        DIMENSION DP(50)
        C2=C*C
        MM=M+1
        DO 1 NN=1,NNMAX
        N=M+2*NN-2
```

```
 4    DP(IRRMAX+3)=0
      DP(IRRMAX+2)=1.0E-30
      D(NN,1)=0
      D(NN,2)=1
      JJ=(N-M)/2+1
      DO 107 LL=1,IRRMAX
      L=LL-1
      IF(LL.GE.JJ) L=IRRMAX+JJ-LL
      IR=2*L
      IRM=M+IR
      AR=(M+IRM+2)*(M+IRM+1)*C2/((2*IRM+3)*(2*IRM+5))
      BR=(2*IRM*(IRM+1)-2*M*M-1)*C2/((2*IRM-1)*
     1  (2*IRM+3))-IRM*(IRM+1)
      CR=IR*(IR-1)*C2/((2*IRM-3)*(2*IRM-1))
      IF(LL-JJ)105,106,106
 105  D(NN,L+3)=-(CR*D(NN,L+1)+(BR+EIG(NN))*D(NN,L+2))/AR
      DMAG=ABS(D(NN,L+3))
      IF(DMAG.GT.1.0E+30) GO TO 3
      GO TO 107
 106  DP(L+1)=-(AR*DP(L+3)+(BR+EIG(NN))*DP(L+2))/CR
      DMAG=ABS(DP(L+1))
      IF(DMAG.GT.1.0E+30) GO TO 3
 107  CONTINUE
      DL=ABS(D(NN,JJ+1))
      DL=ALOG10(DL)
      DLP=ABS(DP(JJ+1))
      DLP=ALOG10(DLP)
      DL=ABS(DL)
      DLP=ABS(DLP)
      DL=DL+DLP
      IF(DL.GT.30.) GO TO 5
      CON=D(NN,JJ+1)/DP(JJ+1)
      ACON=ABS(CON)
      IF(ACON.GE.1.0E+32) GO TO 2
      DO 118 J=JJ,IRRMAX
 118  D(NN,J+2)=CON*DP(J+2)
      F=1
      IF(M)198,198,199
 199  DO 110 I=1,M
 110  F=F*(M+I)
 198  SUM=0
      MMX=IRRMAX+1
      DO 113 I=1,MMX
      IR=2*I
      SUM=SUM+F*D(NN,I+1)
      IF(I-JJ) 113,197,113
 197  FNM=F
 113  F=(-F*(IR+2*M-1))/IR
      ALF=FNM/SUM
      DO 114 I=1,MMX
      D(NN,I)=ALF*D(NN,I+1)
 114  CONTINUE
 1    CONTINUE
      RETURN
 3    IRRMAX=LL-1
```

```
      GO TO 4
    2 IRRMAX=IRRMAX-1
      GO TO4
    5 NNMAX=NN-1
      RETURN
      END
C
C     NEGATIVE D COEFFICIENT SUBROUTINE
C
      SUBROUTINE DNEGN(C,M,NNMAX)
      COMMON EIG(50),D(50,50),DNEG(50)
      DO 4 NN=1,NNMAX
      C2=C*C
      IF(M.GE.1) GO TO 2
      DO 5 II=1,NNMAX
    5 DNEG(II)=D(II,1)
      GO TO 3
    2 B1=1.0
      B2=0.0
      EI=EIG(NN)
      DO 1 IRR=1,M
      IR=2*IRR-2*M-2
      AR=(2*M+IR+2)*(2*M+IR+1)*C2/((2*M+2*IR+3)
     1*(2*M+2*IR+5))
      BR=(M+IR)*(M+IR+1)-EI-(2*(M+IR)*(M+IR+1)-2*M*M-1)
     1*C2/((2*M+2*IR-1)*(2*M+2*IR+3))
      CR=(IR)*(IR-1)*C2/((2*M+2*IR-3)*(2*M+2*IR-1))
      B3=B2
      B2=B1
    1 B1=(BR*B2-CR*B3)/AR
      A=D(NN,1)/B1
      DNEG(NN)=A
      DDM=ABS(DNEG(NN))
      IF(DDM.LT.1.0E-35) GO TO 6
    4 CONTINUE
    3 RETURN
    6 NNMAX=NN-1
      RETURN
      END
C
C     OBLATE SPHEROIDAL RADIAL FUNCTION R(4) OF ARGUMENT C:
C     ORDER M,N; WITH N-M EVEN; UP TO ORDER N=M+2*NNMAX-2.
C     ALSO NORMALIZATION FUNCTION, N.
C
      SUBROUTINE OBRAD(C,M,IQ,MMMAX,NNMAX,IRRMAX)
      COMMON EIG(50),D(50,50),DNEG(50),R1(50),F4(50)
      COMPLEX IX,R4,F4
      IX=(0.0,1.0)
      EEAC=1
      EAC=1
      EAC2=1
      GRO=1
      IF(M.EQ.0) GO TO 20
      MAXM=M+1
      DO 19 MM=2,MAXM
```

```
      IM=MM-1
      GRD=(2*IM-1)*(2*IM)*GRD
      EEAC=(2*IM-1)*EEAC
      EAC2=(2*IM-1)*(2*IM)*EAC2
19    EAC=IM*EAC
      IF(EEAC.GE.1.0E+17) GO TO 4
      IF(EAC2.GE.1.0E+30) GO TO 4
20    DO 17 NN=1,NNMAX
      N=2*(NN-1)+M
      SUM=0
      GR=GRD
      ENORM=0.
      DO 18 NR=1,IRRMAX
      IR=2*(NR-1)
      SUMP=GR*D(NN,NR)
      SUM=SUM+SUMP
      DMAG=ABS(D(NN,NR))
      IF(DMAG.LT.1.0E-30) GO TO 1
      ENORMP=2*GR*(D(NN,NR))**2/(2*IR+2*M+1)
2     ENORM=ENORM+ENORMP
      GRMAG=ABS(GR)
      IF(GRMAG.GT.1.0E+30) GO TO 5
      GR=(IR+2*M+1.)/(IR+1.)*(IR+2*M+2.)/(IR+2.)*GR
18    CONTINUE
      R1(NN)=(-1)**(NN-1)*2**M*EAC*C**M*D(NN,1)/((2*M+1)*SUM)
      R2=(-1)**(NN-1)*(2*M-1)*EAC*C**(M-1)/(2*EAC2)*3.14159
     1*(EEAC**2/SUM)*2**M/DNEG(NN)
      RR2=ABS(R2)
      IF(RR2.GE.1.0E+30) GO TO 4
      EEAC=(N+M+1)*EEAC/(N-M+2)
      IF(EEAC.GE.1.0E+17) NNMAX=NN
      R4=R1(NN)-IX*R2
      A5=ABS(ENORM)
      A1=ALOG10(A5)
      A4=ABS(R2)
      A2=ALOG10(A4)
      A3=A1+A2
      IF(A3.GT.30.) GO TO 3
      A5=ABS(R1(NN))
      A1=ALOG10(A5)
      A3=ABS(A1)+ABS(A2)
      IF(A3.GT.30.) GO TO 3
      F4(NN)=1/(ENORM*R4)
17    CONTINUE
      RETURN
1     ENORMP=0
      GO TO 2
3     F4(NN)=(0.,0.)
      GO TO 17
5     GR=0
      GO TO 18
4     MMMAX=M
      IQ=1
      RETURN
      END
```

```
C
C      PSI FUNCTION
C
       SUBROUTINE FPSI(M,NNMAX)
       COMPLEX IX,F4,PSI
       COMMON EIG(50),D(50,50),DNEG(50),R1(50),F4(50)
      1,SO(50),P(50),SETA(50),SETAO(50),PSI(50)
       IX=(0.,1.)
       MM=M+1
       PSI(MM)=(0.,0.)
       DO 1 NN=1,NNMAX
       N=M+2*NN-2
       PSI(MM)=PSI(MM)+IX**(N)*SO(NN)**2*F4(NN)
 1     CONTINUE
       RETURN
       END
C
C      ASSOCIATED LEGENDRE POLYOMIALS,OP,OF ARGUMENT ETAO;
C      ORDERPM,N; WITH N-M EVEN; OF TO ORDER N=M+2*NNMAX-2.
C
       SUBROUTINE POLYN(ETAO,M,NNMAX)
       DIMENSION PP(3)
       COMPLEX F4
       COMMON EIG(50),D(50,50),DNEG(50),R1(50),F4(50)
      1,SO(50),P(50)
       SQ=SQRT(1-ETAO*ETAO)
       PP(1)=0
       PP(2)=1
       IF(M.EQ.0) GO TO 1
       DO 2 L=1,M
 2     PP(2)=(2*L-1)*SQ*PP(2)
 1     P(1)=PP(2)
       DO 3 NN=2,NNMAX
       N=M+2*NN-3
       DO 4 L=1,2
       PP(3)=((2*N-1)*ETAO*PP(2)-(N+M-1)*PP(1))/(N-M)
       N=N+1
       PP(1)=PP(2)
 4     PP(2)=PP(3)
 3     P(NN)=PP(3)
       RETURN
       END
C
C      OBLATE SPHEROIDAL ANGULAR FUNCTIONS, S, OF ARGUMENTS
C      C AND ETAO; ORDER M,N; WITH N-M EVEN; UP TO ORDER
C      N=M+2*NNMAX-2.
C
       SUBROUTINE OBANG(NNMAX,IRRMAX)
       COMPLEX F4
       COMMON EIG(50),D(50,50),DNEG(50),R1(50),F4(50)
      1,SO(50),P(50),SETA(50),SETAO(50)
       DO 1 NN=1,NNMAX
       SETA(NN)=0
       DO 2 IRR=1,IRRMAX
 2     SETA(NN)=SETA(NN)+D(NN,IRR)*P(IRR)
```

```
1     CONTINUE
      RETURN
      END
C
C     W FUNCTION
C
      SUBROUTINE FW(M,NNMAX)
      COMPLEX IX,F4,W,PSI
      COMMON EIG(50),D(50,50),DNEG(50),R1(50),F4(50)
     1,SD(50),P(50),SETA(50),SETAD(50),PSI(50),W(50)
      IX=(0.,1.)
      MM=M+1
      W(MM)=(0.,0.)
      DO 1 NN=1,NNMAX
      N=M+2*NN-2
1     W(MM)=W(MM)+IX**N*SETAD(NN)*SD(NN)*F4(NN)
      RETURN
      END
C
C     Y FUNCTION
C
      SUBROUTINE FY(M,NNMAX)
      COMPLEX F4,YD,YETAD,PSI,W
      COMMON EIG(50),D(50,50),DNEG(50),R1(50),F4(50)
     1,SD(50),P(50),SETA(50),SETAD(50),PSI(50),W(50),YD(5
     1,YETAD(50)
      MM=M+1
      YD(MM)=(0.,0.)
      YETAD(MM)=(0.,0.)
      DO 1 NN=1,NNMAX
      N=M+2*NN-2
      YD(MM)=YD(MM)+(-1)**N*R1(NN)*SD(NN)*SETA(NN)*F4(NN)
1     YETAD(MM)=YETAD(MM)+(-1)**N*R1(NN)*SETAD(NN)*SETA(
)
      RETURN
      END
C
C     S AND U FUNCTIONS
C
      SUBROUTINE FXU(MM,MMMAX)
      COMPLEX IX,F4,PSI,W,YD,YETAD,U,X,PT
      COMMON EIG(50),D(50,50),DNEG(50),R1(50),F4(50)
     1,SD(50),P(50),SETA(50),SETAD(50),PSI(50),W(50),YD(5
     1,YETAD(50),U(50),X(50)
      IX=(0.,1.)
      IF(MM.EQ.1) GO TO 1
      IF(MM.EQ.MMMAX) GO TO 2
      PT=PSI(MM-1)*PSI(MM+1)
      PTT=CABS(PT)
      IF(PTT.EQ.0.) GO TO 3
      U(MM)=2*IX**(MM-2)*(W(MM-1)+W(MM+1))/(PSI(MM-1)+PSI(
      X(MM)=2*IX**(MM-2)*(W(MM-1)-W(MM+1))/(PSI(MM-1)+PSI(
      RETURN
1     U(1)=-IX*W(2)/PSI(2)
      X(1)=(0.,0.)
      RETURN
```

```
2     U(MM)=IX**(MM-2)*2*W(MM-1)/PSI(MM-1)
      X(MM)=U(MM)
      RETURN
3     MMMAX=MM-1
      RETURN
      END
C
C     Z FUNCTIONS
C
      SUBROUTINE FZ(MMMAX,Z,ZA,ZB,ZC,ZD)
      COMPLEX IX,IQ,Z,ZA,ZB,ZC,ZD,F4,PSI,W,YO,YETAO,U,X
      COMMON EIG(50),D(50,50),DNEG(50),R1(50),F4(50)
     1,SO(50),P(50),SETA(50),SETAO(50),PSI(50),W(50),YO(50)
     1,YETAO(50),U(50),X(50),CMPHI(50),SMPHI(50)
      IX=(0.,1.)
      Z=(0.,0.)
      ZA=Z
      ZB=Z
      ZC=Z
      ZD=Z
      MAXMM=MMMAX-1
      DO 3 MM=1,MAXMM
      M=MM-1
      A=2
      B=1
      C=1
      IF(MM.EQ.1) A=1
      IF(MM.EQ.2) B=2
      IF(MM.EQ.2) C=0
      IQ=IX**(-M)
      Z=Z+A*YETAO(MM)*CMPHI(MM)
      IF(MM.EQ.1) GO TO 2
      ZA=ZA+IQ*(U(MM+1)*CMPHI(MM+1)-B*U(MM-1)*CMPHI(MM-1))
     1*YO(MM)
      ZB=ZB+IQ*(U(MM+1)*SMPHI(MM+1)+U(MM-1)*SMPHI(MM-1))
     1*YO(MM)
      ZC=ZC+IQ*(X(MM+1)*SMPHI(MM+1)-X(MM-1)*SMPHI(MM-1))
     1*YO(MM)
      ZD=ZD+IQ*(X(MM+1)*CMPHI(MM+1)+C*X(MM-1)*CMPHI(MM-1))
     1*YO(MM)
      GO TO 1
2     ZA=ZA+U(2)*CMPHI(2)*YO(1)
      ZB=ZB+U(2)*SMPHI(2)*YO(1)
      ZC=ZC+X(2)*SMPHI(2)*YO(1)
      ZD=ZD+X(2)*CMPHI(2)*YO(1)
1     CONTINUE
3     CONTINUE
      RETURN
      END
      SUBROUTINE SCATTER(VAR,ESCATM,ANGLE,SIGMA)
      COMPLEX A1,A2,B1,B2,H,P1,P2,R,U1,U2,X,Y,ESCAT,J
      REAL PI,THETA,A,B,D,E1,E2,F1,F2,G1,G2,C1,C2,KA,
     $S1,S2,Q,T1,T2,ARG,V,W,IER,MMBSJ0,MMBSJ1,MMBSJ2
      DIMENSION VAR(1)
      PI=3.141593
```

```
      THETA=((VAR(2))/360.)*(2*PI)
      KA=VAR(1)
      A=1.414214
      B=-(PI/4)
      D=2*(((2*KA)/PI)**(1./2.))
      E1=COS((PI/4.) - (THETA/2.))
      E2=COS((PI/4.) + (THETA/2.))
      F1=ABS(E1)
      F2=ABS(E2)
      G1=D*F1
      G2=D*F2
      CALL FRESNEL(G1,C1,S1)
      CALL FRESNEL(G2,C2,S2)
      H=CMPLX(0.,B)
      H=CEXP(H)
      P1=CMPLX(C1,S1)
      P2=CMPLX(C2,S2)
      A1=A*H*P1
      A2=A*H*P2
      ARG=2*KA*(SIN(THETA))
      V=(1 + SIN(THETA))/(2*SIN(THETA))
      W=(1 - SIN(THETA))/(2*SIN(THETA))
      MMBSJ2=(2/ARG)*MMBSJ1(ARG,IER) - MMBSJ0(ARG,IER)
      X=((A1**2)*W + (A2**2)*V)*MMBSJ1(ARG,IER)
      Y=((A1**2)*W - (A2**2)*V)*MMBSJ2
      J=(0.,1.)
      Y=Y*J
      Y1=REAL(Y)
      Y2=AIMAG(Y)
      X1=REAL(X)
      X2=AIMAG(X)
      ESCAT1=X1-Y1
      ESCAT2=X2-Y2
      ESCAT=CMPLX(ESCAT1,ESCAT2)
      ESCAT=ESCAT*J
      ESCAT=-ESCAT
      ESCATR=REAL(ESCAT)
      ESCATI=AIMAG(ESCAT)
      ESCATM =((ESCATR**2.) + (ESCATI**2.))**(1./2.)
      SIGMA = (ESCATM **2.)
      ANGLE=ATAN(ESCATI/ESCATR)
      ANGLE =((ANGLE)/(2*PI))*360.
      IF((ESCATR.LT.0.).AND.(ESCATI.GT.0.)) ANGLE =ANGLE  + 180.
      IF((ESCATR.LT.0.).AND.(ESCATI.LT.0.)) ANGLE =ANGLE  - 180.
      RETURN
      END
      SUBROUTINE FRESNEL(AA,C,S)
      DIMENSION X(2000),Y(2000),ZX(2000),ZY(2000)
      INTEGER NDIM
      IF((AA.GT.-0.01).AND.(AA.LT.0.01))GO TO 6
      GO TO 11
 6    C=0.0
      S=0.0
      GO TO 4
 11   H=.01
```

```
      BB=ABS(AA)
      NDIM=BB/H + .1
      K=NDIM+1
      DO 10 I=1,K
      A=I*H - H
      X(I)=COS(1.57080*(A**2.))
      Y(I)=SIN(1.57080*(A**2.))
10    CONTINUE
      SUM2=0.
      SUM4=0.
1     HH=.5*H
C
C     INTEGRATION LOOP
      DO 2 I=1,NDIM
      SUM1=SUM2
      SUM3=SUM4
      SUM2=SUM2 + HH*(X(I)+X(I+1))
      SUM4=SUM4 + HH*(Y(I)+Y(I+1))
      ZX(I)=SUM1
2     ZY(I)=SUM3
3     ZX(NDIM)=SUM2
      ZY(NDIM)=SUM4
7     IF(AA.GE.0.1)GO TO 8
      C=(-1.)*ZX(NDIM)
      S=(-1.)*ZY(NDIM)
      GO TO 9
8     C=ZX(NDIM)
      S=ZY(NDIM)
9     CONTINUE
4     RETURN
      END
```

```
SCATTERING BY A METALLIC CIRCULAR DISK
     (HODGE -- VERSION 12/17/78)


(TYPE KA=0 TO STOP PROGRAM)
(TYPE KA=-1 FOR A DESRIPTION OF THE PARAMETERS)
(NORMALIZATION:  ESCAT=A*EINC*ENORM/(2*R)*EXP(-J*K*R))
(ALL ANGLES IN DEGREES)


1.   KA              =
   44000B    CM STORAGE USED
       2.168 CP SECONDS COMPILATION TIME1
2.   THETA INCIDENT  =45
3.   POLARIZATION    =0
4.   THETA SCATTERED =45
5.   PHI SCATTERED   =0


WHICH VARIABLE IS TO BE INCREMENTED?1
TYPE NUMBER OF CASES: 25
WHAT IS THE INCREMENT?1
```

KA	CROSS SECTION SIGMA/(PI*A**2)		E NORM			
			THETA		PHI	
	THETA	PHI	MAG	PHASE	MAG	PHASE
1.00	.351E+00	0.	.593E+00	-22.65	0.	90.00
2.00	.903E+00	0.	.950E+00	-110.86	0.	90.00
3.00	.263E+00	0.	.513E+00	148.85	0.	90.00
4.00	.353E+00	0.	.594E+00	85.18	0.	90.00
5.00	.334E+00	0.	.578E+00	-3.41	0.	90.00
6.00	.447E+00	0.	.669E+00	-105.68	0.	90.00
7.00	.149E+00	0.	.387E+00	148.80	0.	90.00
8.00	.738E-01	0.	.272E+00	58.53	0.	90.00
9.00	.659E-02	0.	.812E-01	43.29	0.	90.00
10.00	.194E-01	0.	.139E+00	-45.88	0.	90.00
11.00	.534E-01	0.	.231E+00	-95.93	0.	90.00
12.00	.456E-01	0.	.213E+00	167.71	0.	90.00
13.00	.102E+00	0.	.319E+00	87.48	0.	90.00
14.00	.627E-01	0.	.250E+00	-11.15	0.	90.00
15.00	.982E-01	0.	.313E+00	-103.23	0.	90.00
16.00	.563E-01	0.	.237E+00	1.94	0.	90.00
17.00	.676E-01	0.	.260E+00	94.77	0.	90.00
18.00	.253E-01	0.	.159E+00	168.41	0.	90.00
19.00	.275E-01	0.	.166E+00	-99.14	0.	90.00
20.00	.169E-01	0.	.130E+00	-51.91	0.	90.00
21.00	.138E-01	0.	.117E+00	45.27	0.	90.00
22.00	.294E-01	0.	.171E+00	97.22	0.	90.00
23.00	.199E-01	0.	.141E+00	-174.10	0.	90.00
24.00	.513E-01	0.	.226E+00	-91.91	0.	90.00
25.00	.330E-01	0.	.182E+00	-5.07	0.	90.00

Appendix C

Program Listing for the Fast Fourier Transform (FFT)

The following is a program listing of the Fast Fourier Transform which performs the Direct and Inverse Discrete Fourier Transforms (Ref 13:331).

In the FFT subroutine argument list, X represents the complex array to be transformed, M represents the power of the two of which is the length of the FFT, and XI indicates whether a direct FFT or inverse FFT is to be performed. If XI is a plus one, the direct FFT is performed. If XI is minus one, the inverse FFT is performed.

An example of calling the FFT subroutine from a main routine is:

```
CALL FFT (DOG,10,1.)
```

In this Call statement, "DOG" is the complex array to be transformed, "10" is the power of two of which is the length of the FFT and "1." indicates that a Direct FFT will be performed.

A few precautions in using the FFT subroutine shown should be stated. Using the above example, the precautions are:

(1) DOG must be a complex array with 2^{10} complex locations.

(2) The length of the FFT of DOG will have 2^{10} complex locations.

(3) The second parameter in the argument list, namely "10" must be a positive integer and must not have a decimal point.

(4) The third and last parameter in the list, namely "1." must have a decimal point.

(5) The length of the FFT must be confined to half the maximum number of real array locations that are possible with the computing machine used.

```
      SUBROUTINE FFT(X,M,XI)
      COMPLEX X(1),U,W,T
      N=2**M
      NV2=N/2
      NM1=N-1
      J=1
      DO 7 I=1,NM1
      IF(I.GE.J) GO TO 5
      T=X(J)
      X(J)=X(I)
      X(I)=T
 5    K=NV2
 6    IF(K.GE.J) GO TO 7
      J=J-K
      K=K/2
      GO TO 6
 7    J=J+K
      PI=3.14159265358979
      DO 20 L=1,M
      LE=2**L
      LE1=LE/2
      U=(1.0,0.0)
      W=CEXP(CMPLX(0.,-XI*PI/LE1))
      DO 20 J=1,LE1
      DO 10 I=J,N,LE
      IP=I+LE1
      T=X(IP)*U
      X(IP)=X(I)-T
 10   X(I)=X(I)+T
 20   U=U*W
      IF(XI.GT.0.) RETURN
      DO 30 I=1,N
 30   X(I)=X(I)/N
      RETURN
      END
```

Appendix D

Brief Review of the Selection of the FFT Parameters

The realization of the Discrete Fourier Transform on the modern digital computer in the form of the Fast Fourier Transform is a valuable tool in the field of linear systems. However, if the FFT parameters are not carefully picked according to certain rules, the results of performing an FFT on a sequence will provide erroneous results. So, it is wise to explore the relationships between FFT parameters in the time and frequency domains (Ref 15:282-284).

First of all, the parameters of interest are:

$T \triangleq$ increment between time samples (seconds).

$f_s \triangleq$ sampling rate (hertz) = $1/T$

$F \triangleq$ increment between frequency samples (hertz) = frequency resolution

$t_p \triangleq$ record length (seconds) = effective period of time signal = $1/F$

$f_0 \triangleq$ folding frequency = $f_s/2$ (hertz)

$f_h \triangleq$ highest possible frequency in spectrum (hertz)

$N \triangleq$ number of samples in record

In order to avoid aliasing,

$$f_s \geq 2f_h \qquad \text{(D-1)}$$

This implies that,

$$T \leq \frac{1}{2f_h} \tag{D-2}$$

For a desired frequency resolution

$$t_p = \frac{1}{F} \tag{D-3}$$

If f_h and F are both specified, N must satisfy

$$N \geq \frac{2f_h}{F} \tag{D-4}$$

The following is an example of using the FFT to obtain the DFT of the 10GHz pulse used in Chapter III and Chapter IV.

The pulse consists of five cycles of 10GHz R-f centered at the origin. The pulse is shown in Figure 11. Because of the periodic assumption of the time signal that the DFT makes, the negative half of the pulse is seen to be shifted up in time ending at t_p.

The first step is to estimate what the highest frequency component of the incident pulse is. From experiment it is obvious that the Fourier Transform of the pulse of R-F is a shifted sinc(x) frequency spectrum which never dies out as frequency increases. However, some criteria can be set where by if one of the minor lobes of the sinc(x) waveform goes below a certain percentage of the main lobe peak value, the frequency associated with that minor lobe would be considered the highest possible frequency in the spectrum of the pulse. The continuous Fourier Transform of the 10GHz R-f pulse is

$$S_{(f)} = 5 \times 10^{10} \frac{\sin [15.7 \times 10^{-10}(f-10^{10})]}{[15.7 \times 10^{-10}(f-10^{10})]} \tag{D-5}$$

At 13GHz up from the center frequency of 10GHz, or 23GHz, the magnitude of the sinc(x) function drops to 5 percent of its maximum value. This 23GHz will thus be taken as the highest possible frequency in the spectrum. The following relationships hold.

$$f_h = 23 \times 10^9 \text{Hz} \tag{D-6}$$

$$f_s \geq 2f_h = 46 \times 10^9 \text{Hz} \tag{D-7}$$

$$T \leq \frac{1}{f_s} = 0.0217 \text{ nsec}$$

If f_s is set at 100GHz

$$T = \frac{1}{f_s} = 0.01 \text{ nsec} \tag{D-9}$$

There will be ten samples per cycle of the incident pulse and thus 50 samples per full incident pulse. As was noted in Appendix C, to use the FFT subroutine shown there, the length of the FFT must be a power of 2. If N is picked at 1024:

$$t_p = 1024 \times T$$

$$= 10.24 \text{ nsec} \tag{D-10}$$

$$F = \frac{1}{t_p} = 97.656 \times 10^6 \text{Hz} \tag{D-11}$$

Therefore the highest possible frequency in the spectrum of the pulse will occur at

$$\text{Sample \#} = \frac{f_h}{F} \cong 236 \tag{D-12}$$

Therefore, the frequency response of the scattering from the object the incident pulse is impinging on, can be cut off at sample 250 to sample 1024-250=774 without great loss in accuracy. Thus, when the DFT of the pulse and the sampled frequency response are multiplied and inverse transformed, the reflected pulse will be obtained. Because of the way the points were picked, the process of multiplication of transforms and inverse transforming will perform linear convolution and not cyclical convolution. For more information on cylical convolution refer to the literature (Ref 15:p.284-295).

VITA

Frank DiBartolomeo, Jr. was born on 5 December 1956 in New York City, New York, the son of Mr. and Mrs. Frank DiBartolomeo, Sr. He graduated from Bergen County Vocational-Technical High School, Hackensack, New Jersey in 1974. He received the degree of Bachelor of Science in Electrical Engineering and graduated Cum Laude from the New Jersey Institute of Technology, Newark, New Jersey in May 1978. Upon graduation, he received a commission in the United States Air Force through the ROTC program of which he was designated a Distinguished Graduate. He entered the School of Engineering, Air Force Institute of Technology, in June 1978. He received the degree of Master of Science in Electrical Engineering in December 1979. He is married to the former Kathy Currie and they have no children.

Permanent Address: 27 Velock Drive
Little Ferry, New Jersey 07643

UNCLASSIFIED
SECURITY CLASSIFICATION OF THIS PAGE (When Data Entered)

REPORT DOCUMENTATION PAGE

READ INSTRUCTIONS BEFORE COMPLETING FORM

1. REPORT NUMBER
AFIT/GE/EE/79D-11

2. GOVT ACCESSION NO.

3. RECIPIENT'S CATALOG NUMBER

4. TITLE (and Subtitle)
PREDICTED MICROWAVE ELECTRO-MAGNETIC BACKSCATTERING RETURNS FOR SIMPLE REFLECTIVE TARGETS

5. TYPE OF REPORT & PERIOD COVERED
MS Thesis

6. PERFORMING ORG. REPORT NUMBER

7. AUTHOR(s)
Frank DiBartolomeo, Jr.
2 Lt USAF

8. CONTRACT OR GRANT NUMBER(s)

9. PERFORMING ORGANIZATION NAME AND ADDRESS
Air Force Institute of Technology (AFIT/EN)
Wright-Patterson AFB Ohio 45433

10. PROGRAM ELEMENT, PROJECT, TASK AREA & WORK UNIT NUMBERS

11. CONTROLLING OFFICE NAME AND ADDRESS
Rome Air Development Center (OCTM)
Griffiss AFB New York 13441

12. REPORT DATE
Dec 1979

13. NUMBER OF PAGES
121

14. MONITORING AGENCY NAME & ADDRESS (if different from Controlling Office)

15. SECURITY CLASS. (of this report)
UNCLASSIFIED

15a. DECLASSIFICATION/DOWNGRADING SCHEDULE

16. DISTRIBUTION STATEMENT (of this Report)

Approved for public release; distribution unlimited.

17. DISTRIBUTION STATEMENT (of the abstract entered in Block 20, if different from Report)

18. SUPPLEMENTARY NOTES
Approved for public release; IAW AFR 190-17

JOSEPH P. HIPPS, Maj, USAF
Director of Public Affairs

19. KEY WORDS (Continue on reverse side if necessary and identify by block number)

Circular Disk	Radar	Scattering
Fast Fourier Transform	Radar Images	Signatures
FFT	Radar Returns	Sphere
Images	Radar Scattering	Synthetic Aperture Radar
Linear Systems	Radar Signatures	

20. ABSTRACT (Continue on reverse side if necessary and identify by block number)

The problem of identifying the perfectly conducting sphere and the perfectly conducting, infinitely thin circular disk via the backscattered far field from the object with a known incident signal is examined. A method utilizing synthetic aperture radar principles to obtain slant range verses cross range image plots of the discrete point scatterers on an object is discussed. A computer program to calculate the far field backscattering from the sphere is developed. Another computer program, found in the literature, which —

DD FORM 1473, 1 JAN 73 EDITION OF 1 NOV 65 IS OBSOLETE

UNCLASSIFIED
SECURITY CLASSIFICATION OF THIS PAGE (When Data Entered)

(> or =)

calculates the far field backscattering from the infinitely thin circular disk, is extended for ka $\geq$ 15. In the above programs, the backscattering is obtained as a function of frequency and treated as the frequency response of a linear system. The input to this system is 5 cycles of 10 GHz R-F. The return signal is the output of the system and is obtained by using conventional linear system theory. Since a sphere is symmetric, the same return is obtained at all aspect angles. This return is examined. However, returns from the circular disk are different at different aspect angles. These returns from the disk are examined.